APPLICATION OF POLYANILINE COATED FIBER BRAGG GRATING OPTICAL SENSOR FOR CHLOROFORM DETECTION

IRMA ZULAYKA BINTI MOHAMAD AHAD

FACULTY OF SCIENCE
UNIVERSITY OF MALAYA
KUALA LUMPUR

2017

University of Malaya

APPLICATION OF POLYANILINE COATED FIBER BRAGG GRATING OPTICAL SENSOR FOR CHLOROFORM DETECTION

IRMA ZULAYKA BINTI MOHAMAD AHAD

DISSERTATION SUBMITTED IN FULFILMENT OF THE REQUIREMENTS FOR THE DEGREE OF MASTER IN RESEARCH

DEPARTMENT OF CHEMISTRY
FACULTY OF SCIENCE
UNIVERSITY OF MALAYA
KUALA LUMPUR

2017

University of Malaya

UNIVERSITY OF MALAYA
ORIGINAL LITERARY WORK DECLARATION

Name of Candidate: **IRMA ZULAYKA BINTI MOHAMAD AHAD**

Matric No: **SGR130077**

Name of Degree: **MASTER OF SCIENCE**

Title of Project Paper/Research Report/Dissertation/Thesis ("this Work"):
APPLICATION OF POLYANILINE COATED FIBER BRAGG GRATING OPTICAL SENSOR FOR CHLOROFORM DETECTION

Field of Study: **POLYMER CHEMISTRY**

I do solemnly and sincerely declare that:

(1) I am the sole author/writer of this Work;
(2) This Work is original;
(3) Any use of any work in which copyright exists was done by way of fair dealing and for permitted purposes and any excerpt or extract from, or reference to or reproduction of any copyright work has been disclosed expressly and sufficiently and the title of the Work and its authorship have been acknowledged in this Work;
(4) I do not have any actual knowledge nor do I ought reasonably to know that the making of this work constitutes an infringement of any copyright work;
(5) I hereby assign all and every rights in the copyright to this Work to the University of Malaya ("UM"), who henceforth shall be owner of the copyright in this Work and that any reproduction or use in any form or by any means whatsoever is prohibited without the written consent of UM having been first had and obtained;
(6) I am fully aware that if in the course of making this Work I have infringed any copyright whether intentionally or otherwise, I may be subject to legal action or any other action as may be determined by UM.

Candidate's Signature Date:

Subscribed and solemnly declared before,

Witness's Signature Date:

Name:
Designation:

University of Malaya

ABSTRACT

Fiber Bragg grating (FBG) optical sensor coated with polyaniline (PAni) was used for the detection of organic compounds. In this study, PAni was synthesized through chemical oxidation method by using aniline (Ani) as a monomer and ammonium persulfate (APS) as an initiator. Dioctyl sodium sulfosuccinate (AOT) was added as a dopant in order to increase the solubility and conductivity of PAni. The chemical structures of PAni were confirmed by Fourier transform infra-red (FTIR) and ultraviolet-visible (UV-Vis) spectra while the conductivity of PAni was determined using four-point probes measurement. In the preparation of optical sensor, FBG was first etched in the aqueous hydrofluoric acid solution (48 %) to remove the cladding layer and PAni was then coated on the FBG. Different organic compounds such as 1-propanol, 2-propanol, ethylenediamine, chloroform, dichloromethane, dimethyl sulphide (DMS) and dimethyl disulphide (DMDS) were detected by PAni coated FBG sensor using the optical sensor set up. The response of sensor was monitored based on the Bragg wavelength shift at ~1557 nm using optical spectrum analyzer (OSA). Among all organic compounds, the sensor possesses the highest Bragg wavelength shift (0.095 nm) in chloroform detection. Therefore, further studies in the optical sensor application are focused on chloroform detection. The sensitivity of sensor was manipulated by different synthesis parameters of PAni such as different AOT dopant ratios (Ani: AOT= 5: 3, 5: 5 and 5: 7) and different polymerization temperatures (25 °C, 0 °C and -5 °C). Among all PAnis, Ani:AOT = 5: 5 (0 °C) sensor was found to be the best in chloroform detection that showed good sensitivity (0.0015), good recyclability up to 10 times with fast response time (7 s) and recovery time (8 s), good linearity (0.9988) and lower detection limit of 9.22 ppm. The supporting data from FTIR, UV-vis

University of Malaya

and conductivity analysis suggested that the proposed mechanism for the interaction between PAni and chloroform is the dipole-dipole interaction (physical interaction) between the partial negative charge ($Cl^{\delta-}$) of chloroform and the partial positive charge ($NH^{\delta+}$) of PAni.

University of Malaya

ABSTRAK

Penderia optik jeriji gentian Bragg (FBG) bersalut dengan polianilina (PAni) telah digunakan sebagai penderia untuk mengesan sebatian organik. Dalam kajian ini, PAni telah disintesis melalui kaedah pengoksidaan kimia dengan menggunakan anilina (Ani) sebagai monomer dan ammonium persulfat (APS) sebagai bahan pemula. Dioctyl natrium sulfosusinat (AOT) telah ditambah sebagai dopan untuk meningkatkan kelarutan dan kekonduksian bagi PAni. Struktur kimia bagi PAni telah disahkan dengan spektra perubahan Fourier infra-merah (FTIR) dan ultraviolet-benderang (UV-Vis) manakala kekonduksian bagi PAni ditentukan dengan menggunakan pengukuran prob empat-titik. Dalam penyediaan penderia optik, FBG telah direndam dalam larutan akueus hidrofluorik asid (48%) untuk menyingkirkan lapisan luar FBG dan PAni kemudiannya telah disalutkan ke atas FBG. Pelbagai sebatian organik seperti 1-propanol, 2-propanol, etilenadiamine, kloroform, diklorometana, dimetil sulfida (DMS) dan dimetil disulfida (DMDS) telah dikesan dengan penderia PAni bersalut FBG menggunakan tetapan penderia optik. Tindak balas daripada penderia dipantau berdasarkan anjakan panjang gelombang Bragg pada ~ 1557 nm dengan menggunakan penganalisis spektrum optik (OSA). Antara semua sebatian organik, penderia menunjukan anjakan panjang gelombang Bragg yang tertinggi dalam larutan kloroform. Oleh itu, kajian bagi penderia seterusnya telah ditumpukan kepada pengesanan kloroform. Kepekaan bagi penderia telah dimanipulasi dengan menggunakan pelbagai sintesis parameter bagi PAni seperti nisbah AOT dopan yang berbeza (Ani: AOT = 5: 3, 5: 5 dan 5: 7) dan suhu pempolimeran yang berbeza (25 °C, 0 °C dan - 5 °C). Antara semua PAni, penderia Ani:AOT = 5: 5 (0 °C) telah didapati sebagai penderia optik yang terbaik dalam pengesanan kloroform dengan menunjukkan kepekaan yang terbaik (0.0015), keupayaan kitar semula yang baik sehingga 10 kitaran dengan masa tindak

University of Malaya

balas yang cepat (7 s) dan masa pemulihan yang baik (8 s), kelinearan yang baik (0.9988) dan had pengesanan yang rendah (9.22 ppm). Data sokongan daripada analisis FTIR, UV-vis dan kekonduksian mencadangkan bahawa mekanisma bagi interaksi antara PAni dan kloroform adalah interaksi dwikutub-dwikutub (interaksi fizikal) antara cas separa negatif ($Cl^{\delta-}$) pada kloroform dan cas separa positif ($NH^{\delta+}$) pada PAni.

University of Malaya

ACKNOWLEDGEMENTS

I would like to thank all those people who made this thesis possible and an enjoyable experience for me. First of all I wish to express my thanks to University of Malaya (PPP grant, PG013-2014A and UMRG grant, RG271-13AFR) for providing financial support in completing this research studies. Besides, I would like to thank the staff at Department of Chemistry, Faculty of Science University Malaya (UM) for giving help and guide in handling the instruments.

I wish to express my appreciation to my supervisor, Prof Dr Gan Seng Neon (University of Malaya) and my co-supervisor, Dr Phang Sook Wai (Tunku Abdul Rahman University College) for continuous guide and help me in my research study. Surely, my research cannot be completed without their effort, motivation, knowledge and encouragement. I would like also to give special thanks to Prof Dr Sulaiman Wadi Harun and Prof Dr Harith Ahmad from Department of Physics, Faculty of Science, University of Malaya (UM) for the opportunity to use certain facilities at their place.

I am grateful to my friends especially Kavirajaa Pandian, Nurrafiqah Mokhtar, Hazira Hussin, Nur Aziera Jumat, Mariam Fadzlina Ramli and Ninik Irawati for their encouragement and supports during my research study. Finally, I would like to deliver my sincere gratitude to my family; Mr Mohamad Ahad Hassan, Mrs Foziah Hussin, A'ainaa Fatin Mohamad Ahad and Zharith Sofhia Mohamad Ahad who kept constantly support, help and encourage me during this study.

University of Malaya

TABLE OF CONTENTS

University of Malaya

University of Malaya

University of Malaya

University of Malaya

University of Malaya

LIST OF FIGURES

University of Malaya

University of Malaya

University of Malaya

University of Malaya

LIST OF TABLES

University of Malaya

University of Malaya

LIST OF ABBREVIATIONS

Ag	:	Silver
Ani	:	Aniline
AOT	:	Dioctyl sodium sulfosuccinate
APS	:	Ammonium persulphate
AsF_5	:	Arsenic pentafluoride
ATR	:	Attenuated total reflection
Au	:	Gold
Cl	:	Chloride
CP	:	Conducting polymer
DMS	:	Dimethyl sulfide
DMDS	:	Dimethyl disulfide
DPPTP	:	1,2,4,5- tetraphenyl-1,4-dihydropyrrolo[3,2- b] pyrrole
EB	:	Emeraldine base
EDX	:	Energy- dispersive X-ray microscopy
E_{in}	:	Input wave
EIS	:	Electrochemical impedance spectroscopy
EMI	:	Electromagnetic interference
E_{out}	:	Output wave
ES	:	Emeraldine salt
FBG	:	Fiber Bragg Grating
FESEM	:	Field emission scanning electron microscopy
F-P	:	Fabry-pérot
FTIR	:	Fourier transform infrared
HCl	:	Hydrochloric acid
HF	:	Hydrofluoric acid
HOMO	:	Highest occupied molecular orbital
I_B	:	Intensity of quinoid
I_Q	:	Intensity of benzenoid
IR	:	Infra-red
LB	:	Leucoemeraldine base
LED	:	Light emitting diode
LiCl	:	Lithium chloride

University of Malaya

LOD	:	Limit of detection
LOQ	:	Limit of quantitation
LR	:	Linear range
LUMO	:	Lowest unoccupied molecular orbital
MMF	:	Multimode fiber
MWCNT	:	Multi- walled carbon nanotube
OSA	:	Optical spectrum analyzer
OSHA	:	Occupational Safety and Health Administration
PA	:	Polyacetylene
PAni	:	Polyaniline
Pd	:	Palladium
PEDOT	:	Poly(3,4-ethylenedioxythiophene)
PPy	:	Polypyrrole
PPV	:	Poly(phenyl viniene)
Pt	:	Platinum
PTh	:	Polythiophene
rGO	:	Reduced graphene oxide
RH	:	Relative humidity
RI	:	Refractive index
RSD	:	Relative standard deviation
SEM	:	Scanning electron microscopy
SMF	:	Single mode fiber
UV-Vis	:	Ultraviolet - visible
XRD	:	X-ray diffraction

University of Malaya

LIST OF SYMBOLS

Abs	:	Absorbance
cm	:	Centimeter
dBm	:	Decibel meter
g	:	gram
kHz	:	Kilohertz
n_{eff}	:	Effective index
nm	:	Nanometer
ppm	:	Part per million
rpm	:	Revolutions per mminute
s	:	Seconds
S/ cm	:	Conductivity unit in siemens per centimeter.
V	:	Voltages
w/w %	:	Weight percentage
μm	:	Micrometer
°C	:	Degree Celsius
Π	:	Pi
λ_B	:	Bragg wavelength
Λ	:	Period grating
% T	:	Percentage of transmission
σ	:	Conductivity
Ω	:	Ohm
%	:	Percentage
δ-	:	Partial negative charge
δ+	:	Partial positive charge

University of Malaya

LIST OF APPENDICES

University of Malaya

University of Malaya

University of Malaya

University of Malaya

CHAPTER 1: INTRODUCTION

1.1 Conducting Polymers (CPs)

For a long time, polymers are commonly used as insulating materials due to their non-conductive behaviour. In the year 1960, Alan Heeger, Alan MacDiarmid and Hideki Shirakawa have changed this perception with their new finding that certain polymers can be made conductive almost like a metal. These polymers are called as conducting polymers (CPs) (Okan & Qinguo, 2009). Due to the discovery of CPs, research works based on polyaniline (PAni), polypyrrole (PPy) and polythiophene (PTh) have been extensively studied due to their interesting properties that can be used in numerous applications. In the other words, CPs are also known as synthetic metal which refers to organic polymers that have the electrical properties of metal and retaining the mechanical properties and processibility of polymers.

The most important factor affecting the conductive behaviour of CPs is the present of conjugated structure along the polymer chain. In the conjugation system of CPs chain, the bonds between carbon atoms are connected by alternating single and double bond. Every bond contains localized sigma and pi bonds which form a strong and weaker chemical bond as shown in Figure 1.1. The continuous delocalization of electrons along the polymer chain can enhance the conductivity of CPs (El-Sherif et al., 2007). However, the conjugation is not enough to make the CPs become highly conductive. In fact, the conductivity of the pure CPs is quite low (10^{-10} to 10^{-5} S/cm). The conductivity of CPs can be improved from semiconductor to the metallic region (10^{4} S/cm) by a process that was known as “doping” (Bai & Shi, 2007).

University of Malaya

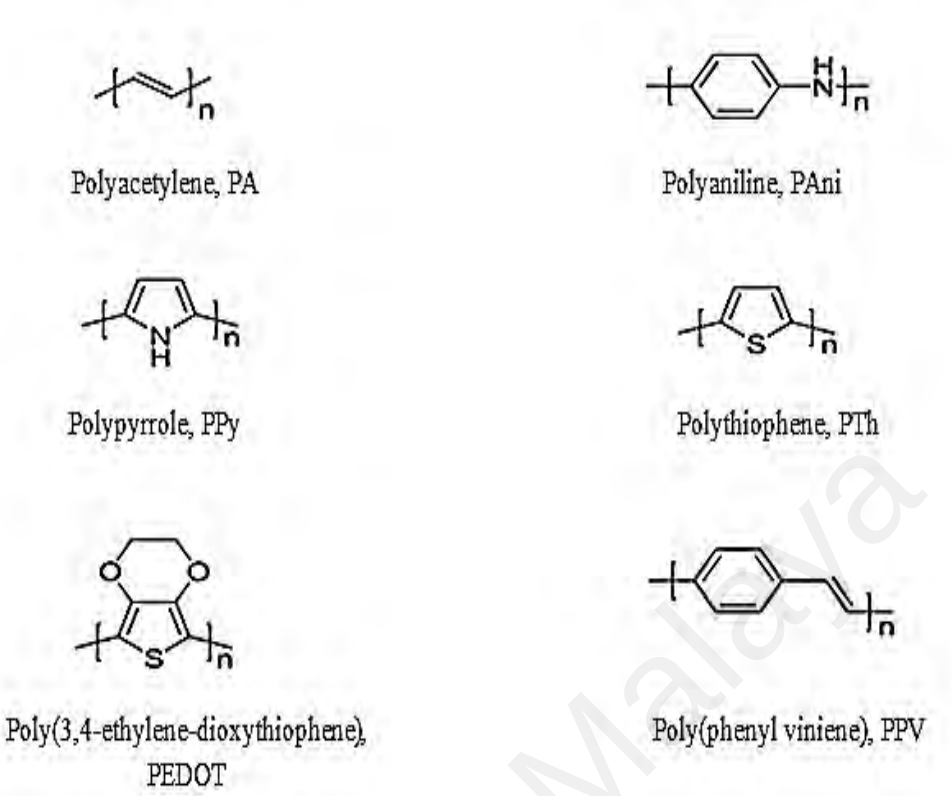

Figure 1.1: Chemical structures of CPs.

Doping is the unique process which could enhance the conductivity of a CP. During the doping process, charge carriers are introduced either in the form of "electrons" or "holes" into the CPs chain in order to improve their conductive properties. "Electrons" refer to the free electrons created during doping process, while "holes" refer to the locations of missing electrons. When a hole is filled by an electron jumping from the neighbouring position, a new hole (or carbocation) is created. The charge carriers (holes or electrons) are moving along the polymer chain as shown in Figure 1.2.

University of Malaya

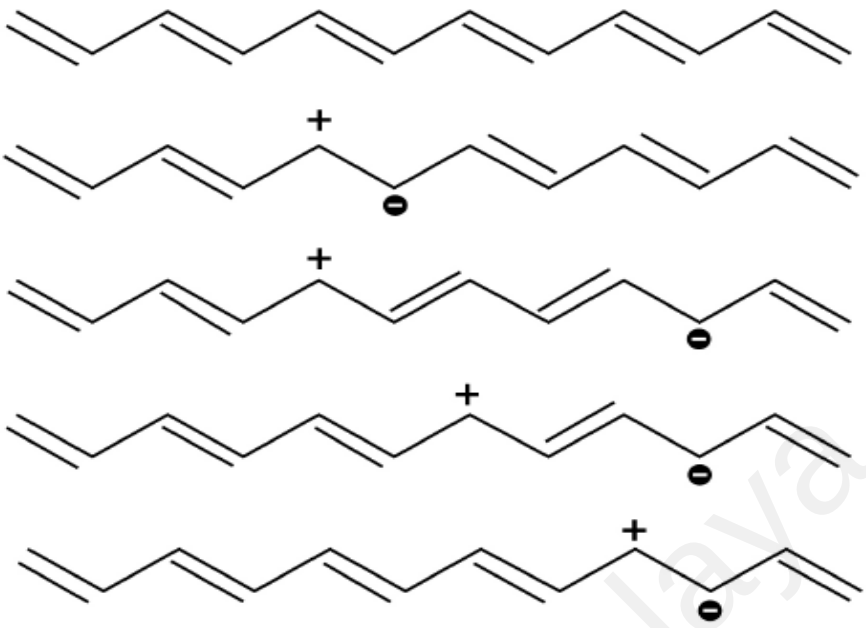

Figure 1.2: Mechanism of doping process in CPs chain.

There are two types of dopants, namely p-dopant and n-dopant. N-dopant is known as an electron donor (e.g. reducing agents) that loss its extra valence electrons to conduction band. It will provide more electrons to CP chain and making it become n-type semiconductor polymer (Dubey & Leclerc, 2011). In contrast, p-dopant is an electron acceptor (e.g. oxidizing agents) that would accept electron from valence band. It will create more holes in CPs chain and making it as p-type semiconductor polymer (Dubey & Leclerc, 2011). Furthermore, the amount of dopant used in polymerization significantly affects the electrical, magnetic and optical properties of CPs (Heeger, 2001). Thus, doping process is the most important factor that can enhance the conductivity of CPs.

Nowadays, many researchers have paid great attention to CPs because of their interesting properties such as low cost, lightweight, good flexibility, excellent ambient stability, and reversible absorption kinetics (Omastová et al., 1999). Besides, CPs are

University of Malaya

easy to prepare through chemical and electrochemical polymerization (Kinyanjui et al., 2006). The electrical, magnetic, and optical properties of CPs are able to adjust and modify through the synthesis parameters such as dopant ratio, oxidant ratio, polymerization temperatures and so on (Li et al., 2006). Based on its excellent properties, CPs are potentially applied in many fields such as anti-corrosion coating, super capacitors, antistatic coating, electromagnetic shielding, light emitting diode (LED), transistor, actuator, laser, biomedical devices, solar cell, sensors and batteries (Atesa et al., 2012).

1.2 Polyaniline (PAni)

Among all CPs, polyaniline (PAni) has been studied extensively by many researcher in numerous applications due to its promising properties such as simple and easy synthesis with low fabrication cost, low density, various morphologies, high catalytic activity, excellent environmental stability and high electrical conductivity. Besides, PAni also possesses a unique structural characteristic where the conductivity can be manipulated through the protonation and doping process (Arsat et al., 2009).

In general, PAni can exist in four different distinct colors due to their different oxidation states which are fully reduced leucoemeraldine base (LB; yellow), half oxidized emeraldine base (EB; blue), doped emeraldine salt (ES; green) and fully oxidized pernigraniline (purple) (Figure 1.3). PAni can easily convert from one to another state in which others CP do not possess this ability. Herewith, it can be easy to identify the changes in oxidation state of PAni by observing its color changes (Malapo et al., 2012).

University of Malaya

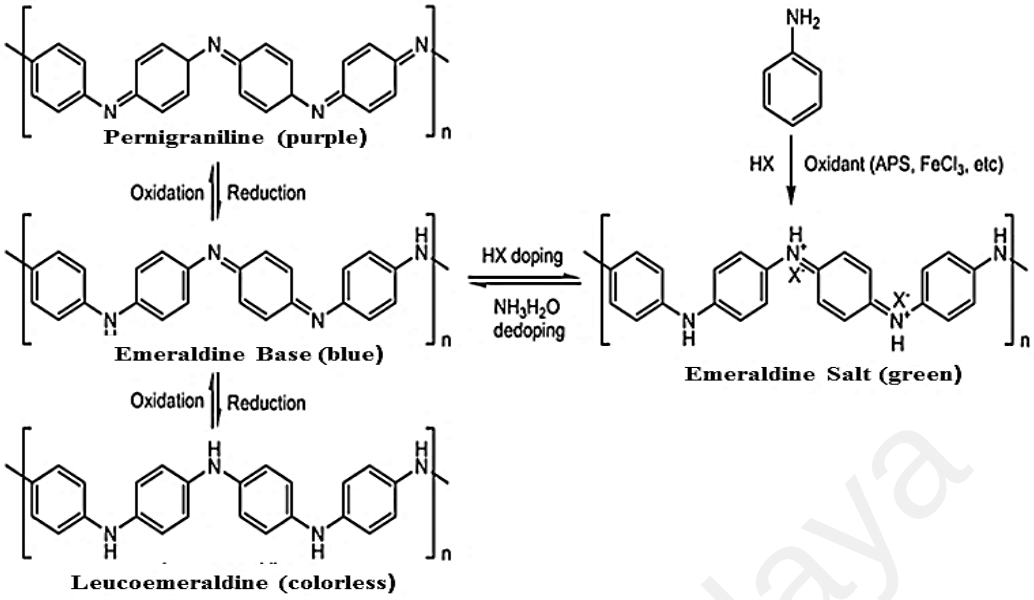

Figure 1.3: The reversible reaction of PAni in different oxidation states.

PAni can undergo a fast and reversible redox reaction which it can be reversibly switched to other oxidation states by acid-doping process. For example, when non-conducting PAni-EB (~10^{-10} Ω/ cm) was doped with acid solution, it can be switched to conducting PAni-ES (10^{-2} Ω/ cm to 10^{1} Ω/ cm) as shown in Figure 1.3 (Song & Choi, 2013). The conducting PAni-ES consists of benzenoid and quinoid units with amine (-NH) and imine (=N-) site in its chain. The amount of benzenoid and quinoid structures on PAni chain can be adjusted by controlling the pH of acid solution and the addition of desired quantity of dopants. During acid-doping process, benzenoid structure can be transformed to quinoid structure by introducing charge carrier to PAni chain. The delocalization of charge carrier is actually contributes to the formation of cation (polaron) and dication (bipolaron) that significantly improve the conductivity of PAni (Molapo et al., 2012).

University of Malaya

Thus, PAni is considered as promising material that can undergo numerous applications due to its unique properties. PAni has been designed for electromagnetic absorber technologies in microwave study where it contains high conductivity with excellent dielectric permeability and magnetic permeability (Luo et al., 2016). Besides, PAni also was implemented in solar cell technologies due to its high electro catalytic activity (Ramachandran et al., 2015). In the last two decades, PAni is applied as optical and chemical sensor due to its excellent sensing properties such as good flexibility, excellent environmental stability and ability to make physical and chemical interaction during exposure to analyte solutions (Razak et al., 2015).

1.3 Optic Sensor

Recently, many researchers attempt to develop the sensing devices from the optical fiber due to its advantages such as electrical immunity, small size that allows the remote real-time sensing, tolerant of harsh environment (not easy to corrode) and long term stability. The optical fiber sensor is a device that has ability to convert a physical and chemical magnitude into a detectable signal such as current, absorbance, acoustic variable and so on. In general, the physical property of optical sensor shows significant changes after the interaction with analyte. The important factor needs to be considered in order to produce a successful sensor design is the efficiency of the combination of sensing material and sensing system. Besides, the successful sensor design must have several unique features such as fast response time, good sensitivity and excellent repeatability (Ahuja & Parande, 2012).

In general, optical fibers are manufactured from glass which consists of core, cladding and buffer layers as showed in Figure 1.4. The center part of the optical fiber is

University of Malaya

known as core. Light from the source is travel along the fiber's core. This part is covered by the cladding layer. Cladding layer is commonly made from glass or plastic which used to protect light in the core from leaking out into the surrounding, reducing the scattering loss at the surface of the core and to protect the fiber from exposed to contaminant. The fiber is surrounded by additional layer which is buffer layer as extra protection (Kawase et al., 1988).

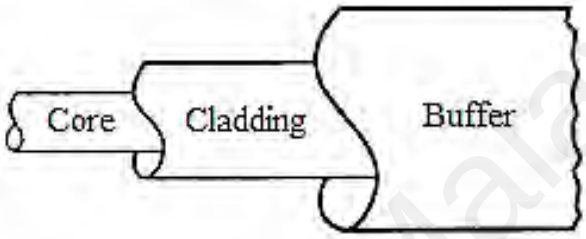

Figure 1.4: The significant components in optical fiber.

The optic fiber sensor can be divided into two classes, namely extrinsic and intrinsic sensor. In the extrinsic sensing, the optical fiber has been used to transmit the light from or to the sensing region where the signal modulation take place outside of the fiber. Besides, the extrinsic sensor commonly applied in low level measurement due to its disadvantages such as low resolution, less sensitive and high connection problems. In contrast, the intrinsic sensor e.g. Fiber Bragg Grating is more expensive due to its unique properties like high sensitivity, reduces connection problems and excellent performance in high level measurement. In the intrinsic sensing, the optical fiber is used as the sensing element where it directly interacts with the external perturbation and modulates the light signal in the fiber. There are many measurements carried out using the intrinsic sensor such as vibration, displacement, velocity, acceleration, strain, temperature and pressure (Ghetia et al., 2013).

University of Malaya

Basically, there are two types of optical fiber which are single mode fiber (SMF) and multi-mode fiber (MMF). The structure and light transmission of SMF and MMF is shown in Figure 1.5. The SMF is used to carry single mode of light over the longer distances while the MMF is commonly used over short distances communication. SMF has smaller core (~8 - 10 μm) than MMF (~50 - 100 μm). The SMF has many advantages such as able to avoid overlapping of light transmission, fast transmission speed, lower loss of signal and etc. This is due to its small diameter of core and single light ray on SMF. Thus, SMF is the best optical fiber used in sensor application (Teja et al., 2012).

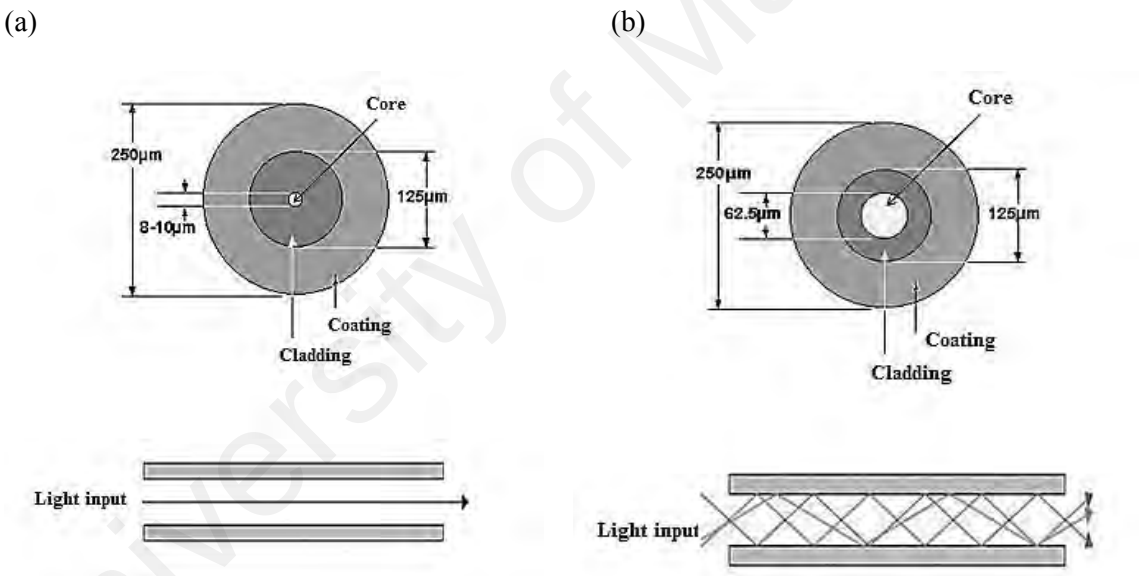

Figure 1.5: The light transmission in (a) SMF and (b) MMF.

In the last three decades, one of the most popular SMF used in sensor application is fiber Bragg grating (FBG). FBG is manufactured from a glass fiber. In FBG, refractive index of the core (~1.48) is higher than the refractive index of the cladding layer (~1.46). Generally, this refractive index significant creates the fixed

index modulation according to the exposure pattern. The fixed modulation is known as a grating (Ghosh et al., 2015). There are many advantages of FBG such as inexpensive, light weight, immune to electromagnetic interference (EMI) and have ability to measure any parameters (Chen et al., 2011).

Besides, FBG is also used as an optical filtering device that can reflect light of a specific wavelength which the normal fibers do not possess this ability. In fact, the normal fiber has a uniform refractive index where significantly produces many noises in its optical result. While in FBG structure, the refractive index of core periodically changed. Refer to Figure 1.6, when light with various wavelengths are introduced into the FBG core, one particular wavelength that in phase with the grating period is reflected back to the input end. Other wavelengths that are not in phase with a grating period are transmitted through the fiber (Yang et al., 2016).

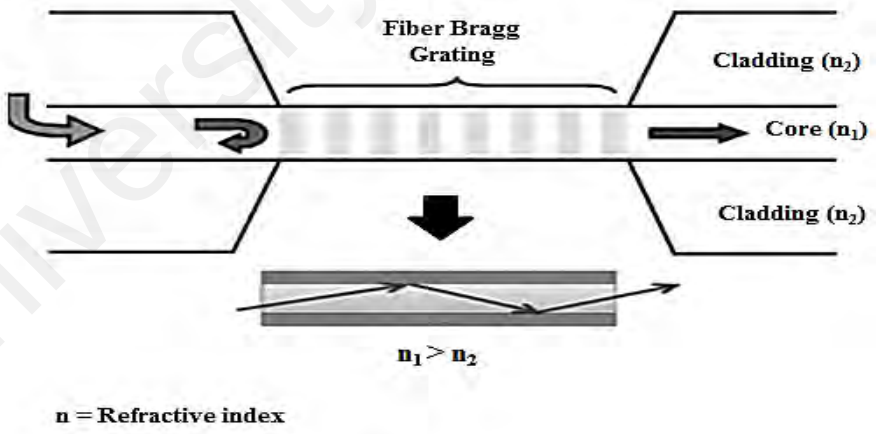

Figure 1.6: Reflection and transmission of light along of the core of FBG.

University of Malaya

1.4 Problem Statement

One of the major contaminants in environment is organic. In general, organic compounds are carbon-based organic pollutants that can easily evaporate into atmosphere due to its high vapour pressures. It was originated from chemical industries like solvent in paint and thinner, degreasers, cleaning agent, lubricant and petrochemical fuel (Ying & Krishnan, 2010). Excess amount of organic compounds can give negative effects on environment, plant growth, and human health (e.g. irritation, nerve damage and cancer).

Among all organic compounds, chloroform is the biggest challenge for analytical researcher due to its weak interaction with other chemical compounds. Chloroform as depicted in Figure 1.7 is introduced into environment by the anthropogenic sources such as transportation, adhesives, degreaser, solvent in paint, colour remover and others. According to the Occupational Safety and Health Administration (OSHA), the permissible exposure limit of chloroform is ~50 ppm. Continuous exposure of chloroform can cause numerous health effects such as irritation, digestive disorder, headache, lung congestion, kidney damage, liver damage convulsion, cancer and most seriously death (Pradip & Arup, 2013). Thus, it is necessary to develop an effective sensor device for organic compounds especially chloroform in order to maintain the environmental cleanness as well to decrease the risk of a health problem cause by this pollutant.

University of Malaya

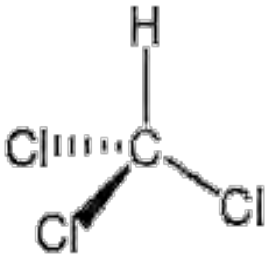

Figure 1.7: Chemical structure of chloroform.

The aim of this study is to design the simple PAni coated FBG sensor as a new optical device for chloroform detection with good environmental stability, good reversibility and reproducibility, and shows excellent performance at room temperature.

1.5 Application of PAni as Optical Sensor in Chloroform Detection

During the last decades, the most widely used techniques in chloroform detection involve the spectrophotometer (e.g. Fourier transform infrared (FTIR) and ultraviolet-visible (UV-Vis)) and metal oxide. These methods are not suitable for on-line monitoring because they are easily affected by the environmental factors such as surrounding temperature and air humidity (Mekki et al., 2013; Wolfrum et al., 2006). FBG has recently become the most popular optical materials used in sensor application. There are many advantages of FBG such as inexpensive, light weight, immune to EMI, high sensitivity, remote sensing, high repeatability, and the most important is excellent environmental stability (Ashish et al., 2015). On the other hand, PAni is commonly applied as optical and chemical sensor due to its excellent sensing properties such as good flexibility, excellent environmental stability and ability to make physical and

University of Malaya

chemical interaction during exposure to analyte solutions (Ayad et al., 2008; Xiaolin et al., 2013).

Based on our knowledge, the smart chloroform sensor based on the combination of PAni and FBG is firstly studied. The passive cladding layer of FBG sensor is removed due to the lower refractive index of cladding which can affect the sensor performance. This passive cladding layer is replaced by PAni thin film in order to improve the sensitivity of FBG sensor. The optical sensor response of PAni coated FBG before and after immersed in chloroform solution will be monitored based on the Bragg wavelength shift (~1557 nm) by using optical spectrum analyser (OSA). The chemical interaction between PAni thin film and chloroform will be confirmed by FTIR, UV-Vis and conductivity analysis.

1.6 Research Objectives

The research objectives in this study are listed below:

1. To synthesis and characterize PAni through chemical oxidation method by using different synthesis parameters (different dopant ratio and different polymerization temperature).
2. To apply PAni as optical sensor in detection of organic compounds (especially chloroform).
3. To optimize parameters for PAni coated FBG in chloroform detection.
4. To investigate the mechanism for the interaction between chloroform and PAni by using FTIR, UV-Vis and conductivity analysis.

University of Malaya

CHAPTER 2: LITERATURE REVIEW

2.1 Background of CPs

In year 1920, Hermann Staudinger discovered the concept of macromolecule in polymer chemistry. Macromolecule is the larger molecule consisting of a number of repeating units that connecting each other by the covalent bonds. In year 1950, this finding was continued by Karl Ziegler and Guilio-Natta; they developed the modern plastic industries by introducing catalyst in the polymer synthesis (Murkherjee, 2014). In year 1953, Paul Flory discovered more deeply about the experimental and theoretical study in the physical chemistry of macromolecule (Flory, 1974). However, polymers designed from Staudinger, Ziegler, Natta and Flory studies are saturated polymers which have great insulating property but cannot conduct electricity. These disadvantages of traditional polymers have limited the application of the polymers.

The disadvantages of traditional polymer makes Alan Heeger, Alan MacDiarmid and Hideki Shirakawa bring forward their attention to discover about the electrical CPs that possess the ability to conduct electricity like metals (Heeger et al., 2002). In early 1970, the first CP, polyacetylene (PA) was synthesized by Shirakawa and co-worker using the Ziegler-Natta catalyst. During the synthesis of PA, they accidentally added more Ziegler-Natta catalyst and found that PA film showed silvery appearance instead of black precipitate. However, the silvery PA film still not highly conductive likes metals (Heeger, 2001).

In years 1977, Shirakawa, MacDiarmid and Heeger tried to improve the conductivity of PA by doping halogen (e.g. chlorine, bromine and iodine) and arsenic

University of Malaya

pentafluoride (AsF_5). This process named as a doping process. During this process, iodine gas was introduced to PA chain and created a hole along the polymer chain. The respective hole is then filled by an electron jumping from the neighbouring position, a new hole (or carbocation) is created. The movement of carbocation along the polymer chain significantly increased the conductivity about 10^9 times where more conductive than the original PA (before treated with dopant) (Heeger et al., 2002).

The finding about the increasing conductivity of the doped PA by Shirakawa and co-workers have attracted the great attention from many researchers due to the high conductivity level of CPs as shown in Figure 2.1. Based on the discovery of PA, research studies on other CPs families such as polyaniline (PAni), polypyrrole (PPy), polythiophene (PTh), poly (3, 4-ethylenedioxythiophene) (PEDOT) and etc. were developed rapidly due to their interesting properties in numerous applications. The organic polymer that possesses the electrical, magnetic and optical properties of a metal while retaining the mechanical properties and processibility of a traditional polymer, is known as "synthetic metal" (Kinyanjui et al., 2006).

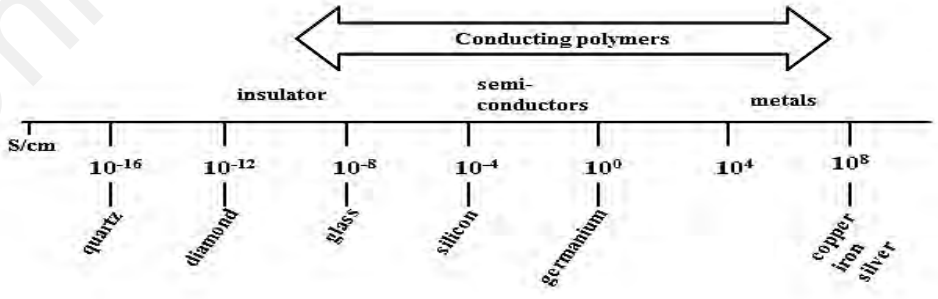

Figure 2.1: Conductivity range for CP and other materials.

University of Malaya

2.2 Previous Study of PAni

Among all CPs, PAni had attracted great attention from many researchers like Runge, Letheby, Green and Woodhead to investigate more deeply about the unique characteristic of PAni. PAni also becomes notable choice of raw material for various applications due to its unique properties such as high conductivity, light, excellent corrosion resistance and facile processibility. In general, PAni can be easily prepared by electrochemical and chemical methods (Gospodinova & Terlemezyan, 1998). The molecular structure of PAni can be modified through different polymerization parameter such as different temperature, different dopant ratio, different oxidant ratio and etc (Sapurina & Stejskal, 2008; Tran et al., 2011).

A key property that distinguishes PAni from other CPs is it can exist in different oxidation states that attributes to different colour changes. There are four oxidation states of PAni namely fully reduced leucoemeraldine base (LB), half oxidized emeraldine base (EB), doped emeraldine salt (ES) and fully oxidized form of pernigraniline that exist in yellow, blue, green and purple, respectively. PAni can be reversibly switched to all of these different oxidation states through the acid-doping and the oxidation-reduction reaction. The changes in oxidation state of PAni can be identified by observing its colour changes (Malapo et al., 2012). This unique property of PAni makes it potentially applied in multidisciplinary areas such as sensors, electromagnetic shielding, solar cells and others.

In year 2007, Nagagouda and Varma prepared the PAni-LB through the chemical oxidation method in aqueous acetic acid solution for the supercapacitor application. The morphology of PAni-LB nanofibers is affected by the concentration of acetic acid with

University of Malaya

diameter range of 20 nm to 50 nm. Besides, PAni-LB nanofiber can undergo a spontaneous redox reaction with metal ions like silver (Ag), palladium (Pd), gold (Au) and platinum (Pt) and resulting deposition in various shapes e.g. leaf, particulate, nanowires and cauliflower, respectively. Thus, PAni-LB nanofibers synthesized in this study shows a good capacitor property that possesses higher decomposition temperature (up to ~120°C) and higher dielectric constant ~3500 at high frequency (Nagagouda & Varma, 2007).

In year 2012, Zaarei and co-workers proposed the new preparation method of anti-corrosion epoxy coating by the addition of PAni-EB. These coating solution was prepared from the dispersion of PAni-EB in 3-(aminomethyl)-3,5,5-trimethylcyclohexan-1-amine by using sonication, separation and submicron filtration methods. These coating solutions (at different stages of preparation) were characterized by optical microscopy and scanning electron microscopy (SEM). The efficiency of anti-corrosion of these coating materials were measured by electrochemical impedance spectroscopy (EIS) and salt spray method. In this study, the addition of 0.5% EB in initial mixture of epoxy hardener produces the better anti-corrosion property compared with pure epoxy coating. At the end of this study, they found that the addition of 2.5% EB in epoxy hardener using their proposed method significantly produces the superior anti-corrosion property of epoxy coating (Zaarei et al., 2012).

In year 2014, Sun and co-worker proposed the graphene/pernigraniline composite as good promising material for anti-corrosion of copper. In this study, graphene/pernigraniline composite was synthesized through insitu polymerization and reduction/dedoping process. These resultant composites have a flake-like structure and possess low conductivity as 2.3×10^{-7} S/cm. On the other hand, it also possesses both

University of Malaya

excellent impenetrable and insulating properties from the combination of reduced graphene oxide (rGO) and pernigraniline. At the end of their study, they found that the performance of anti-corrosion was achieved by the growing of pernigraniline on the rGO surface that avoid the increasing of electrical resistance for graphene–graphene/metal coating. Besides, the graphene/pernigraniline composites are less flexible and commonly unfold during the coating process which can prolong the diffusion pathway of corrosive media in the coating matrix (Sun et al., 2014).

Among all oxidation states, PAni in ES form is commonly applied as promising materials in numerous applications due to its excellent conductive and electrochemically active properties compared with others PAni. Luo and co-worker have carried out the research by using PAni-ES that posssess high conductivity, excellent dielectric permeability and magnetic permeability for microwave absorption study (Luo et al., 2016). PAni-ES also was implemented in solar cell technologies due to its high electro catalytic activity (Ramachandran et al., 2015). Furthermore, the most popular application of PAni-ES is optical and chemical sensor due to its excellent sensing properties such as good flexibility, excellent environmental stability and ability to make physical and chemical interaction during exposure to chemical solutions.

Sambasevam and co-workers have designed a simple chemical sensor for hydrazine detection using PAni-ES thin film. The PAni-ES was synthesized through chemical oxidation method in the present of sodium bis(2-ethyl hexyl) sulfosuccinate (AOT) dopant. The presence of 2-ethylhexyl groups on AOT would reduce the interaction between PAni chain and increase its affinity and solubility in non-polar organic solvent. While, the presence of oxygen atom on ester and sulfonate group on AOT would increase the solubility of PAni in polar organic solvent. In their study, PAni

University of Malaya

with highest concentration of AOT possessed high conductivity (0.4-0.8 S/cm), good sensitivity with fast respond time (7 seconds) and good reusability up to 10 cycles during hydrazine detection. Thus, the addition of AOT dopant does not only improve the solubility but also enhance the conductivity and processability of PAni thin film as a chemical sensor in hydrazine detection (Sambasevam et al., 2015).

Research conducted by Chiam and co-workers have showed that the PAni-ES could be potentially applied in optical sensor for alcohol detection. In this study, a simple microfiber sensor coated with PAni-ES has been designed by drop coating technique. The PAni-ES coated microfiber exhibits wavelength shift from 1540 nm to 1539.87 nm. The response of Pani-ES coated microfiber sensor is significantly affected by the refractive index of alcohol solution and number of alkyl substituent of alcohol. In this study, PAni-ES coated microfiber sensor was successfully designed for alcohol detection that exhibits high sensitivity and good recyclability up to 10 times (Chiam et al., 2014). Moreover, in year 2016, the PAni-ES coated FBG sensor for pH detection with high sensitivity, good reusability (10 times) and fast respond time of 10s was also successfully developed by Chiam and co-workers (Chiam et al., 2016).

2.3 Literature of Optical Fiber Sensor

During 19th century, Daniel Colladon introduced the practical guided light in optical communication. In mid 20th century, a copper wire was used as a waveguide for telecommunication field. This copper wire is expensive and has limitation on signal performance due to the specific amount of frequencies. Thus, in year 1950, Kao and Hockam had developed the alternative waveguide in order to overcome the disadvantages of copper wires. They introduced the laser as a new waveguide with

University of Malaya

many advantages such as lightweight, low fabrication cost, high operational bandwidth, faster and wide transmission capacity (Kao & Hockman, 1966).

Research conducted by Kao had found that the optical fiber can reduce the attenuation loss less than 20 dB/km. This finding are supported by Keck and co-workers; they also obtained the attenuation of optical fiber of 20 dB/km. Revolution of optical fiber in communications has widely developed into the sensor application over the last six decades. In fact, the fiber optic sensor contains many advantages compared to traditional electrical sensor such as compact, lightweight, immune to electromagnetic interference, large dynamic range and good environmental stability (Li & Nolan, 2008).

As mentioned in Chapter 1, optical fiber sensor is capable to be used either in intrinsic or extrinsic sensing modulation. The physical property of the intrinsic optical sensor was changed by an environmental signal where the sensing interaction was only occurred inside the fiber. Harun and co-workers proposed the fabrication of microfiber loop resonator (intrinsic optical sensor) by flame heating technique. They found that the transmission spectrum of the microfiber was unchanged while the extinction ratio was decreased with temperature. This is due to the change in the material's refractive index (Harun et al., 2011).

In contrast, extrinsic optical fiber normally acts as a medium in order to generate light to sensing location and does not involved any interaction between light and sample. Rao and co-workers introduced the fabrication of micro extrinsic Fabry-perot (F-P) interferometric sensor using the micro-explosion mechanism of near-infrared femtosecond laser pulses at 1 kHz. The micro extrinsic fiber can be applied in many

University of Malaya

applications due to its advantages such as high degree of integration, easy fabrication, and low cost (Rao et al., 2002).

2.4 Development of FBG as an Optical Sensor

Due to the development of optical fiber sensor, many researchers try to develop sensing devices based on optical fiber materials likes fiber Bragg grating (FBG). In year 1978, the first fiber grating had been demonstrated by Hill and co-workers at the Canadian Research Center in Ottawa. They successfully altered the refractive index of core of single mode fiber when it was irradiated by UV light. The fiber grating also known as Hill grating where refers to the self-induced grating. In fact, the fiber grating was commonly used as an effective wavelength filters for multiplexing signal. However, it still has some limitation in its performance such as it only works at the internal writing Argon laser wavelength (488 nm) (Hill & Meltz, 1997).

In year 1989, the discovery and refinement of fiber grating through external writing "holographic method" was introduced by Meltz and co-workers. From their experiment, they found that the fiber gratings filter with holographic method can works at different wavelength. Moreover, the effectiveness of fiber grating as a wavelength filter in multiplexing signal was influenced by several parameters such as grating period, length and refractive index modulation. The changes in these parameters can be used to determine the reflectivity and wavelength change of the fiber grating (Purchase et al., 1999).

University of Malaya

Correia and co-workers proposed the organo-silica di-ureasil hybrid coated on FBG for relative humidity (RH) detection. The organo-silica di-ureasil hybrid was prepared by sol-gel method and deposited on FBG through deep coating method. The presence of siliceous-based network on di-ureasil layer can enhance the sensor performance such as strong adhesion, durability and compatibility. Thus, the proposed di-ureasil based optical sensors provide a good response for the RH detection (Correia et al., 2012).

2.5 Summary of Literature Review

Based on the literature studies, CPs is an interesting novel polymer materials used in many applications. Among all CP, PAni is the best candidate for sensing devices due to its excellent advantages such as simple synthesis, possess low fabrication cost, ease of deposition, low density and etc. In principal, the suitable combination of the sensing material and sensing systems is the most important thing needs to be considered to produce a successful sensor design. Thus, FBG sensor is the new sensor system that can overcome the disadvantages of traditional sensors (e.g. spectrophotometer and metal oxide) that these methods are not suitable for on-line monitoring and easily affected by the environmental factors.

This present research work had combined both the advantages of FBG and PAni in order to build the smart optical sensor for organic compounds (especially chloroform) detection. The sensor developed in this study was used PAni film as the modified cladding in FBG sensor. The sensor works on the principle of wavelength (~1557 nm) shift modulation induced by the FBG. The Bragg wavelength of PAni coated FBG sensor at ~1557 nm was shifted either to higher or lower wavelength due to the

University of Malaya

interaction between the sensitive regions of sensor (PAni) and organic compound analytes.

Among all organic compounds, PAni coated FBG sensor possesses the highest Bragg wavelength shift in chloroform solution. Therefore, further studies in the optical sensor application are focusing on chloroform detection. The effect of synthesis parameters of PAni such as different molar ratios of AOT dopant (3, 5 and 7) and different polymerization temperatures (25 °C, 0 °C and -5 °C) on the sensitivity of PAni coated FBG sensor in chloroform detection will be investigated in this study.

Based on our knowledge, the novel PAni coated FBG sensor for chloroform detection is firstly reported here. Besides the sensor performance of PAni coated FBG sensor, the chemical interaction between PAni film and chloroform will also be investigated through FTIR, UV-vis and conductivity analysis. Moreover, the sensor performance for PAni coated FBG sensor includes limit of detection, interference study, real sample analysis, recovery and reusability is also investigated in this study.

University of Malaya

CHAPTER 3: METHODOLOGY

3.1 Chemicals and Materials

All chemicals used in the synthesis of PAni such as aniline (Ani), dioctyl sodium sulfosuccinate (AOT), ammonium persulphate (APS), toluene (99.8 %) and lithium chloride (LiCl, 96.5 %) were purchased from Sigma-Aldrich, USA while hydrochloric acid (HCl, 37 %) was purchased from RCl Labscan, Thailand. Organic compound analytes used in the sensor application part such as chloroform (99 %), dichloromethane (99.9 %), 1-propanol (99 %), 2-propanol (99.7 %), ethylenediamine (99 %), dimethylsulfide (DMS, 99 %) and dimethyl disulfide (DMDS, 99 %) were procured from MERCK, Germany. Hydrofluoric acid (HF, 48 %) that used in the etching process also was purchased from MERCK, Germany. Acetone (99.5 %, Sigma-Aldrich, USA) was used as a solvent in the preparation of chloroform solution and it also was used for cleaning laboratory glass wares. Distilled water was purified using water purification system.

Another material used in this study is a single mode fiber Bragg grating (FBG) with reflectivity of > 90 %, bandwidth of < 0.3 nm and center wavelength of 1557 nm. This single mode FBG was purchased from Kumpulan Abex. Sdn. Bhd., Malaysia.

3.2 Apparatus

Apparatus such as beaker, dropping funnel, dropper, measuring cylinder, separating funnel, spatula, weighing paper, petri dish, magnetic stirrer, retort stand and ice box were used during synthesis of PAni film. While other apparatuses such as

University of Malaya

volumetric flask, pipette, pre-clean microscope glass slide, sample vials, ultraviolet-visible (UV-Vis) cuvette cell were used during the sensor application part.

3.3 Instruments

Instruments such as hot plate stirrer, rotary vapor and analytical balance were used for PAni synthesis. Spin coater (SPS, SPIN 150-NPP) was used to coat PAni film on the glass slide for characterization study. Fourier transform infrared (FTIR, Perkin Elmer RX1 model) spectrometer, ultraviolet- visible (UV-Vis, UV-1650 PC model) spectrometer and resistivity meter were used for the characterization of PAni while the optical trinocular microscope with digital camera (Optika, B193) was used to measure the diameter of FBG during the etching process and thickness of PAni coated FBG. Optical spectrum analyzer (OSA, Anritsu MS9710B) and laser source (1550 nm) were used in optical sensor set-up for organic compounds (especially chloroform) detection.

3.4 Experimental

3.4.1 Synthesis of PAni

PAni was synthesized through chemical oxidation method using Ani as a monomer, AOT as a dopant and APS as an oxidant. In this study, PAni was synthesized using different synthesis parameters such as different dopant ratios, different polymerization temperatures and etc.

Firstly, AOT dopant (6.6684 g, molar ratio: 5) was dissolved in 1 M of HCl solution. Then, Ani monomer (1.3970 g, molar ratio: 5) was slowly added into AOT

University of Malaya

solution and stirred for two hours in order to obtain a homogenous Ani/AOT mixture. It was followed by the slow addition of APS (3.423 g, molar ratio: 5) solution into the mixture in order to initiate the polymerization. Polymerization reaction was carried out at 0 °C for 24 hours. The polymerization process was terminated by adding excess amount of toluene. After that, pure PAni was extracted into toluene solution using separating funnel in order to separate the unreacted Ani monomer, AOT and APS in the aqueous phase. The organic phase was then washed with distilled water in order to remove the left over water soluble impurities. The desired concentration of PAni solution (3 %) was obtained by extraction using rotary vapor. Concentration of PAni solution was obtained by calculating its weight percentage (w/w %).

The synthesis route was repeated for different molar ratios of AOT which are 3 and 7 as shown in Table 3.1. Besides, the similar synthesis routes were also repeated for different polymerization temperatures such as 25 °C, 0 °C and -5 °C. Lastly, the PAni film was coated on glass slide using spin coater (model: SPS, Spin 150-NPP) with 3000 rpm for further characterizations such as FTIR, UV-vis and conductivity analysis.

Table 3.1: Synthesis parameter of PAni film (0 °C, 24 h) with different AOT dopant ratios.

Samples	Ani ratio (Weight, g)	APS ratio (Weight, g)	AOT ratio (Weight, g)
PAni (5: 3)	5 (1.3970)	5 (3.423)	3 (4.0010)
PAni (5: 5)	5 (1.3970)	5 (3.423)	5 (6.6684)
PAni (5: 7)	5 (1.3970)	5 (3.423)	7 (9.3358)

University of Malaya

3.4.2 Characterization of PAni

3.4.2.1 FTIR spectroscopy

FTIR spectrometer is frequently used in organic and polymer synthesis, petrochemical engineering, pharmaceutical industry and food analysis to investigate the chemical structure of the chemical compounds (Jawad et al., 2016). FTIR analysis can be run either by transmission or reflection techniques (Madejová, 2003).

However, during the last five decades, FTIR based on reflection becomes the most flexible and popular analytical instrument for research application due to its technique is simpler than transmission IR. Reflectance IR analysis is classified into three types which are internal reflection spectroscopy – Attenuated Total Reflection (ATR), external reflection spectroscopy – Specular Reflection (smooth surfaces) and combination of internal and external reflection- Diffuse Reflection (DRIFT – rough surface) (Madejová, 2003).

Nowadays, FTIR-ATR gets wide attention from many researchers due to its advantages such as versatile that enables measuring all types of samples (e.g. solids, liquids and gases), non-destructive technologies, provide excellent reproducibility and etc. (Kumirska et al., 2010). FTIR-ATR involves the concept of total internal reflection where reflection of a light beam occurs at the angle that exceeds the critical angle as shown in Figure 3.1. There are many factors that affecting the ATR analysis such as the wavelength of internal reflection radiation, angle of incidence of internal reflection radiation, efficiency of sample and internal reflection element and so on.

University of Malaya

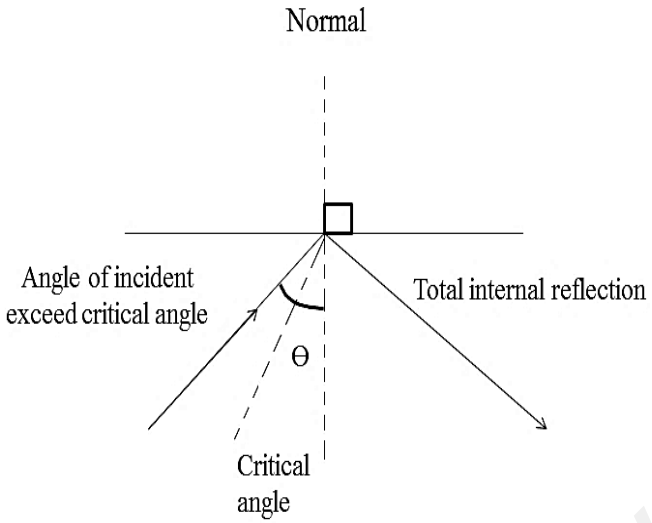

Figure 3.1: Illustration of total internal reflection of light occurs in the FTIR-ATR spectrometer.

In this study, FTIR-ATR spectrometer (Perkin Elmer RX1 model) was used to investigate the chemical structure of PAni film. FTIR spectrum of PAni thin film was recorded in the wavenumber range of 400 to 4000 cm^{-1}. During the FTIR analysis, PAni thin film that coated on the glass slide was located closely with ATR crystal (Figure 3.2). The incident IR beam that produced from a light source passed through the ATR crystal via total internal reflection. The evanescent wave that produced from this internal reflectance located at the reflecting surface on which the PAni sample held in contact with ATR crystal. This evanescent wave is attenuated when the sample absorb energy in the IR spectrum region. The attenuated IR beam exist the ATR crystal and directed to detector. The attenuated IR beam was collected from the reflecting surface, then recorded by the detector and produced the IR spectrum. The chemical structures of the PAni thin films that synthesized by different polymerization parameters were confirmed by FTIR-ATR analysis.

University of Malaya

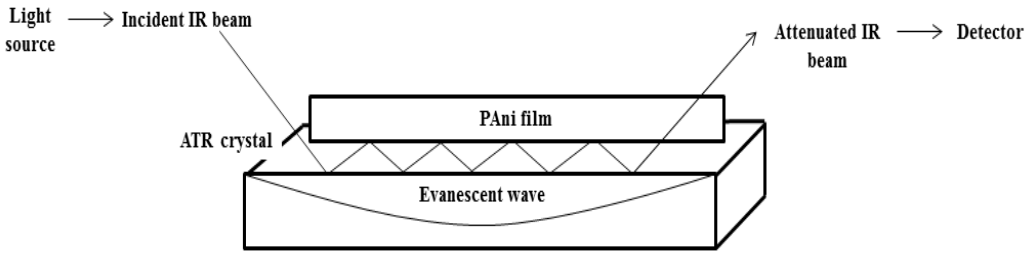

Figure 3.2: Penetration of the incident IR beam into PAni film sample during FTIR-ATR analysis.

3.4.2.2 UV-Vis spectroscopy

In the last three decades, UV-Vis spectroscopy becomes the most popular analytical technique in the research world due to its numerous advantages such as simple, versatile, fast and cost effective. Moreover, operation of UV-Vis spectrometer is straightforward and commonly used to identify some functional groups and chemical behaviour of some substances. Basically, absorption occurs in the UV-Vis spectrometer involves the excitation of electrons in the molecule. When a molecule absorbs energy, outer electron is promoted from the highest occupied molecular orbital (HOMO) to the lowest unoccupied molecular orbital (LUMO). UV-Vis spectrometer would record the particular wavelength that absorbed by the analyte (Bahera et al., 2012; Bhawani et al., 2015).

In this study, conducting behaviour of PAni was investigated using UV-Vis spectrometer (UV-1650 PC model) in the wavelength range of 300 to 900 nm. The components of UV-Vis spectrometer are including the light source, diffraction grating, sample and reference cells, monochromator and detector (Figure 3.3). The UV-Vis

University of Malaya

beam that produced from light source (tungsten and deuterium lamp) was isolated into the specific wavelength of light via the monochromator. The monochromatic wavelength was split into two equal intensities when it was passing through the mirror devices. One intensity beam was penetrated to a sample cell (PAni coated glass slide, I) while another intensity beam was penetrated to the reference cell (blank solution, I_o). Photodiode is a detector that commonly used in UV-Vis analysis. It works together with monochromator to filter and penetrates light of a single wavelength to detector. The UV-vis absorbance of compounds obeys the Beer-Lambert law (Equation 3.1).

$$\log_{10} I_o/I = \varepsilon lc \qquad \text{Equation 3.1}$$

where; I_o = intensity of light passes through the sample cell

I = intensity of light passes through the reference cell

ε = molar absorption coefficient

l = path length of the absorbing solution (cm)

c = concentration of the absorbing species in $mol.dm^{-3}$

University of Malaya

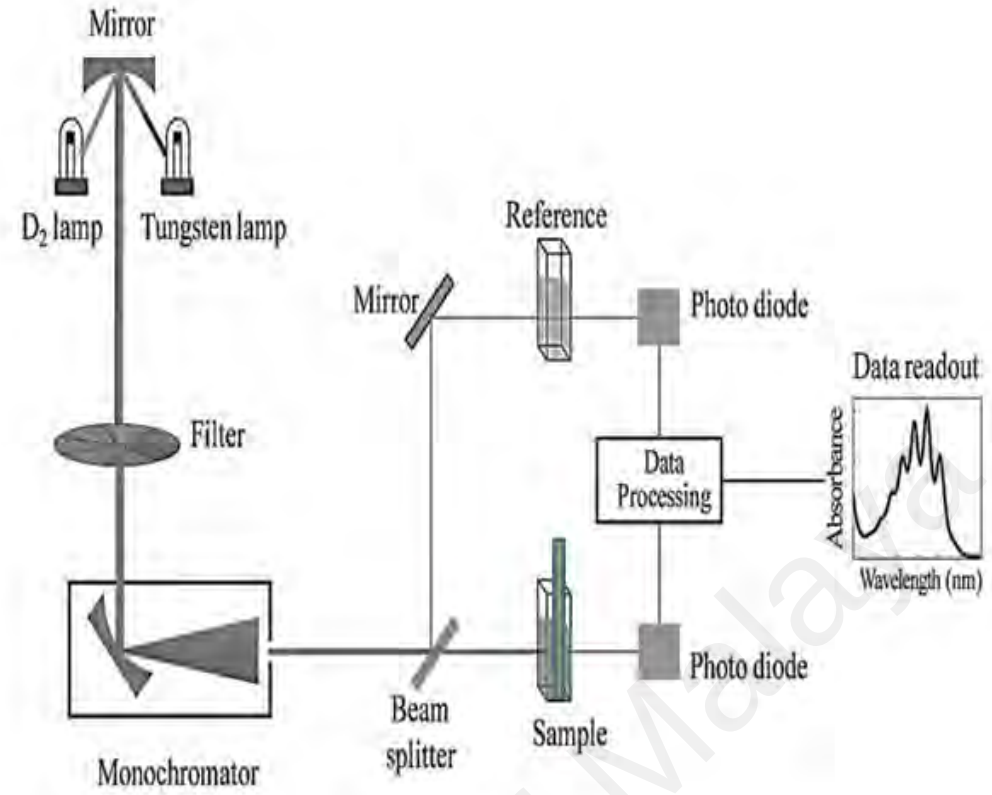

Figure 3.3: Schematic diagram of UV-vis spectrometer for PAni characterization (Zamani, 2013).

3.4.2.3 Conductivity measurement

Four-point probe is the most widespread method for resistivity measurement of semiconductor materials. It also is named as a Kelvin probe method. One of the advantages of using the four-point probe is its lower measurement error compared with two probe resistivity meter. This is attributable to its resistance, the spreading resistance under each probe and the interaction between the resistances of each probe with the semiconductor materials (Singh et al., 2015; Miccoli et al., 2015).

In this study, four-point probe resistivity meter (Loresta GP, MCP-T610) was used to measure the electrical conductivity of the PAni sample. The resistivity meter

allows the measurement of electrical conductivity in the range of 10^{-7} to 10^{7} S/cm. PSP probe with interspin distance of 1.5 mm was used in this study. During measurement, the PSP probe was placed in contact with PAni film as shown in Figure 3.4. The conductivity of PAni thin film was measured at different positions under room temperature. The conductivity of PAni thin film was directly obtained from the resistivity meter in the unit of S/cm. The final electrical conductivity data of the PAni film was obtained from the average of electrical conductivity at different positions

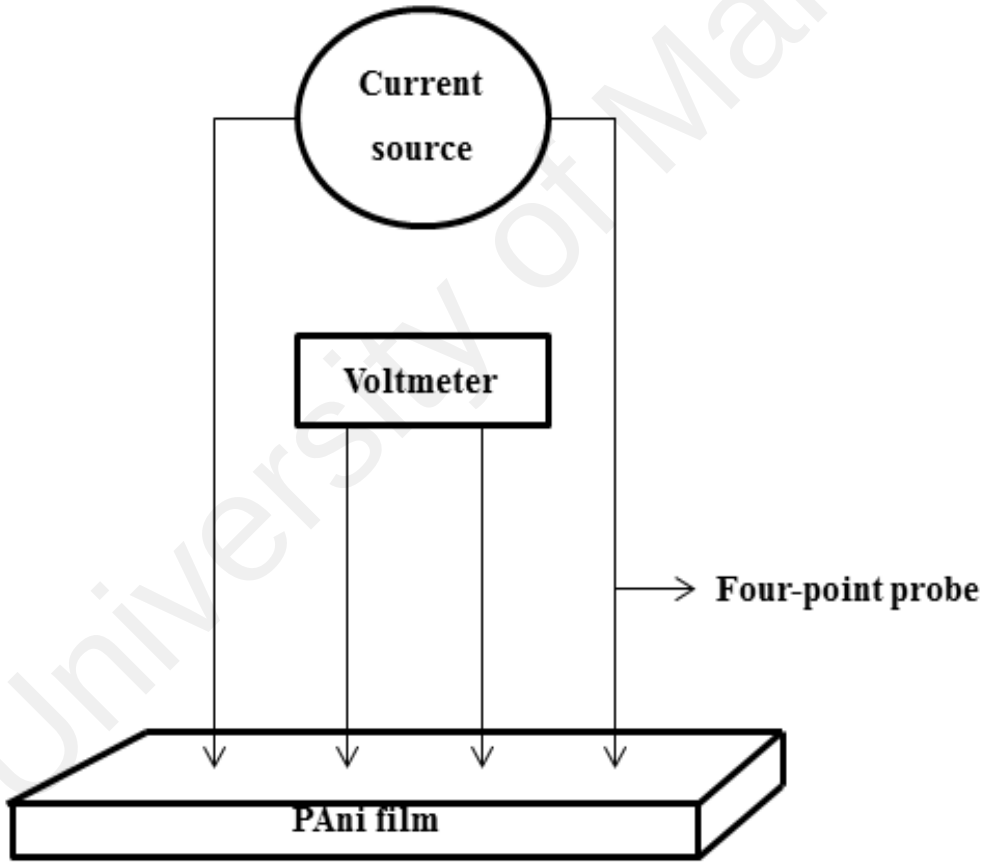

Figure 3.4: Illustration of the conductivity measurement of PAni film using four-point probe resistivity method.

University of Malaya

3.4.3 Preparation of PAni Coated FBG Sensor

In this study, the SMF-FBG has been chosen instead of MMF because the small diameter of core and single light ray on SMF can avoid any overlapping of light transmission, fast transmission speed, lower loss of signal and etc. FBG is manufactured with different RI as mentioned in Section 1.3. RI in the core part of FBG is higher than RI in the cladding part and this will significantly affect the FBG sensor performance (e.g. lower the sensitivity of the FBG sensor). Thus, in this study, cladding part of the FBG is removed by using hydrofluoric acid (HF, 46 %) solution and washed by distilled water to remove the remaining HF solution on the FBG (Figure 3.5). This process is named as "etching process". Microscope (Optika, Italy) is used to observe and measure the diameter of both cladding and core part of FBG. This routine was repeated until the diameter of core part for FBG becomes ~18 μm. After that, PAni solution was deposited onto the core part of FBG using the drop coating technique. Finally, the PAni coated FBG sensor is dried ~30 minutes at room temperature. In this study, the thickness of PAni coated on FBG sensor for chloroform detection is fixed (~30 μm).

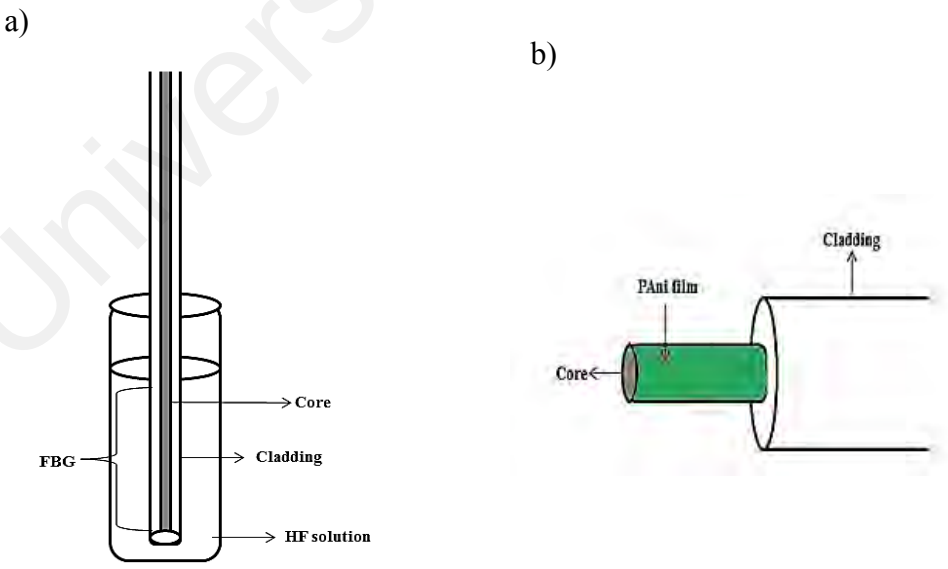

Figure 3.5: Preparation of PAni coated FBG: a) etching process of FBG in HF solution and b) coating process of PAni film on FBG.

University of Malaya

3.4.4 Application of PAni Coated FBG Sensor in Organic Compounds Detection

PAni coated FBG was applied as an optical sensor for organic compounds detection. The set-up of PAni coated FBG sensor which contains the SMF-FBG, light source, 3-directional coupler and OSA is shown in Figure 3.6. In this study, laser with wavelength of 1550 nm was used as a light source because its wavelength is suited with the Bragg wavelength of FBG (~1557 nm). Principally, FBG acts as an optical filter where one particular wavelength that obeys the Bragg condition was reflected and all other wavelength was transmitted along the fiber length. OSA detector was used to analyse the electrical signal as a function of the power, wavelength or frequency. The OSA detector was set-up using the parameters as shown in Table 3.2.

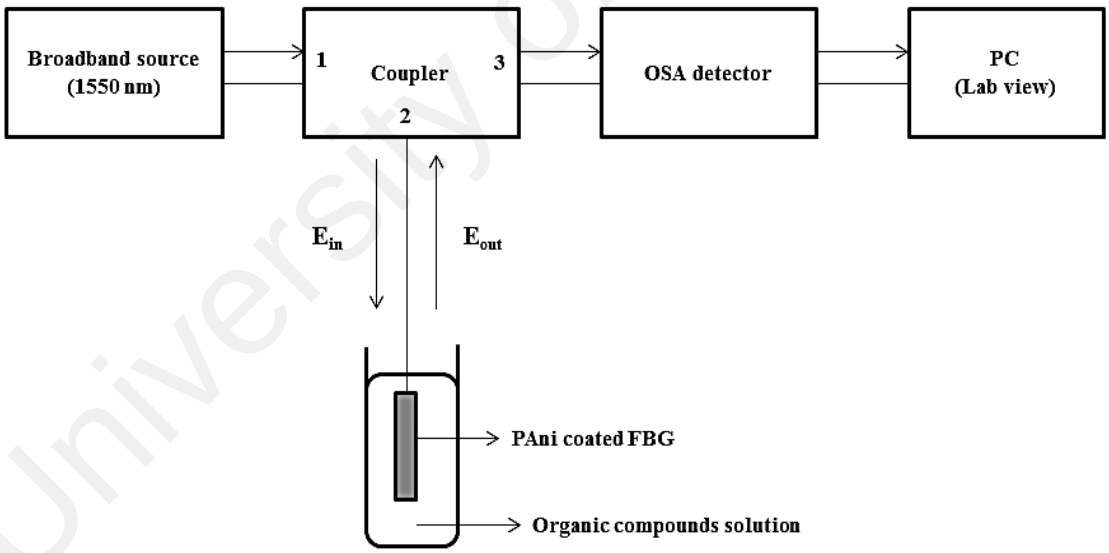

Figure 3.6: PAni coated FBG sensor set up for organic compounds detection.

University of Malaya

Table 3.2: Parameters for OSA detector set up during organic compounds detection.

Parameter	Value
Span	50
Log	10
Sampling point	2001
Wavelength (full range)	1520-1570 nm
Wavelength (specific range)	1552-1562 nm

As shown in Figure 3.6, PAni coated FBG sensor was connected to the three-directional coupler. The incident wave (E_{in}) from laser entered into port 1 and exited by passing through the port 2 before it entered into the PAni coated FBG sensor. The output wave (E_{out}) was produced when light passing through the FBG device. Then the light exited from FBG device through port 3 on the coupler and it was analysed and recorded by OSA detector. Data obtained from optical sensor analysis were interpreted using "Lab View" software.

During organic compounds detection, PAni coated FBG sensor was immersed into different types of organic compound solutions (3 %). These organic compound solutions have been chosen from different functional groups such as hydroxyl group (1-propanol and 2-propanol), amine group (ethylenediamine), chlorinated aliphatic hydrocarbon group (chloroform and dichloromethane) and sulfide group (dimethyl sulphide and dimethyl disulphide). Before organic compounds detection, the initial Bragg wavelength of PAni coated FBG sensor was recorded as λ_o. After immersion in organic compound solutions for 10 seconds, the final Bragg wavelength of PAni coated FBG sensor in organic compound solutions was recorded as λ. Then, PAni coated FBG

University of Malaya

sensor was immersed into distilled water and dried at room temperature in order to recover the sensor back to its initial state. Thus, the Bragg wavelength shift of this sensor (λ_B) was calculated using Equation 3.2.

$$\lambda_B = \lambda - \lambda_o \qquad \text{Equation 3.2}$$

where, λ_B = Bragg wavelength shift

λ = final Bragg wavelength of PAni coated FBG sensor after organic compounds detection

λ_o = initial Bragg wavelength of PAni coated FBG sensor before organic compounds detection

3.4.5 Application of PAni coated FBG Sensor in Chloroform Detection.

Based on the result obtained from part 3.4.4, PAni coated FBG sensor possesses the highest Bragg wavelength shift (~1557 nm) in chloroform detection among all organic compounds. Thus, for further study, the application of PAni coated FBG sensor is focused on chloroform detection in concentration range of 10 ppm to 100 ppm. The sensitivity of PAni coated FBG sensor was manipulated using different synthesis parameters of PAni film such as different AOT dopant ratios (Ani: AOT= 5: 3, 5: 5 and 5: 7) and different polymerization temperatures (25 °C, 0 °C and -5 °C). The response of PAni coated FBG sensor was monitored based on the different of Bragg wavelength shift at ~1557 nm using OSA detector.

University of Malaya

Moreover, the chemical interaction between PAnis and chloroform during chloroform detection by PAni coated FBG sensor was investigated using the supporting data from FTIR, UV-vis and conductivity analysis. Based on our knowledge, none of the research investigated the detailed proposed mechanism between the analyte and optical sensor during chemical detection. Thus, the detailed proposed mechanism between PAni and chloroform molecules is firstly reported in this study.

Besides, the performance of PAni coated FBG sensor in chloroform detection was studied in more details in terms of the recyclability, selectivity, sensitivity, accurancy, limit of detection (LOD) and limit of quantitation (LOQ). Furthermore, PAni coated FBG sensor was applied in real water samples analysis for chloroform detection. These real water samples were collected from the chemistry laboratory (Department of Chemistry, University of Malaya), the residential area (Vista Angkasa Apartment, Kuala Lumpur) and the drinking water by reverse osmosis treatment (model: Jantzen). The known concentration of chloroform was spiked into the real water samples for further investigation. The recovery and relative standard deviation (RSD) value of PAni coated FBG sensor was obtained at the end of this study.

University of Malaya

CHAPTER 4: RESULTS AND DISCUSSION

4.1 PAni Coated on FBG for Organic Compounds Detection

4.1.1 Characterization of PAni

4.1.1.1 FTIR Analysis

The FTIR spectrum of doped PAni with Ani: AOT ratio of 5: 5 named as PAni 5: 5 was obtained in the wavenumber range of 400-4000 cm^{-1} as showed in Figure 4.1. The bands observed at 3246 cm^{-1} and 2960 cm^{-1} are attributed to the secondary N-H and the aromatic C-H stretching vibrations of PAni, respectively. The bands at 1613 cm^{-1} and 1470 cm^{-1} were assigned to the C=C stretching vibration mode of quinoid and benzenoid ring, respectively. In addition, the band at 1298 cm^{-1} represents the C-N stretching vibration in benzenoid ring while the vibration band at 1206 cm^{-1} is attributed to the C=O symmetric and asymmetric stretching from AOT dopant. On the other hand, the vibration band at 767 cm^{-1} was associated with C-H bending out of plane for the aromatic ring (Sambasevam et al., 2015).

University of Malaya

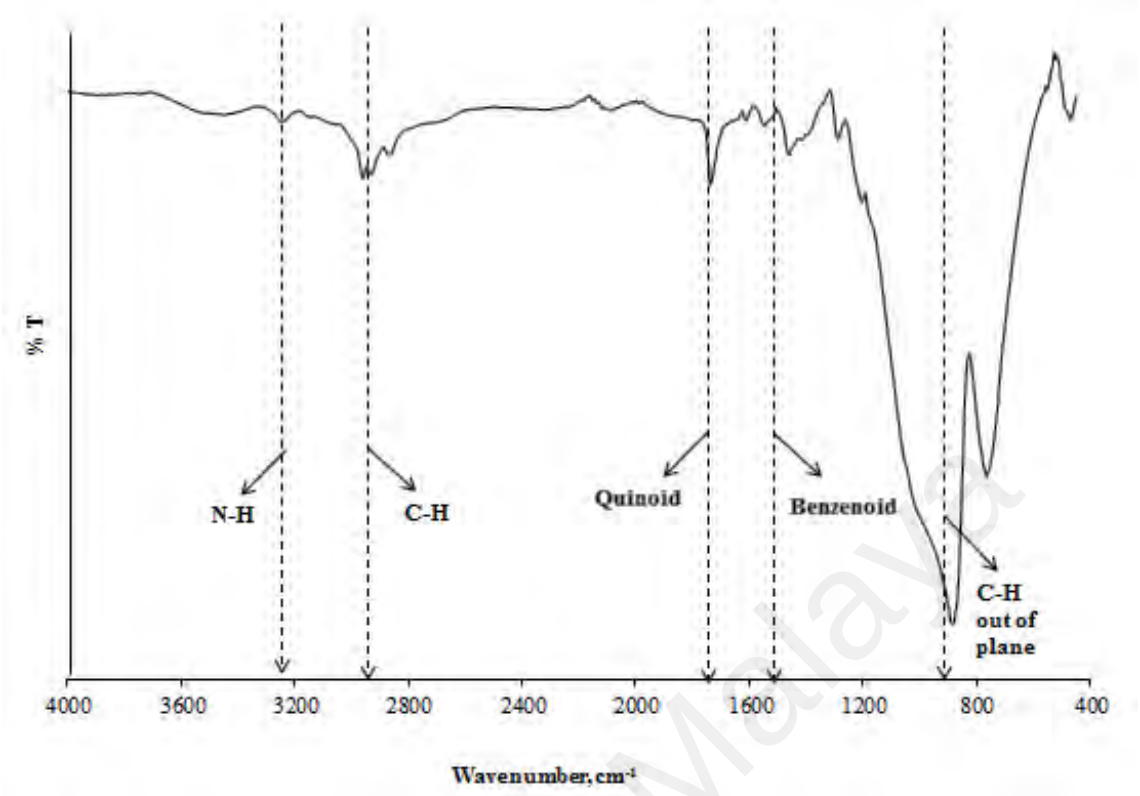

Figure 4.1: FTIR spectrum of PAni 5: 5 synthesized at 0 °C.

4.1.1.2 UV-Vis Analysis

The UV-Vis absorption spectrum of PAni 5: 5 was recorded by UV-Vis spectrophotometer in the wavelength range 300- 900 nm as shown in Figure 4.2. PAni 5: 5 shows three characterization peaks at ~350 nm, ~420 nm and ~765 nm. The absorption peak at ~350 nm refers to π-π^* transition of benzenoid rings while the shoulder peak at ~420 nm indicates the polaron to π^* transition which showed the characteristics of protonated PAni. The strong absorption peak at ~765 nm confirmed that the resulted PAni 5: 5 is in ES state, which is in the conductive form (Hawaldar et al., 2009). Thus, both characterizations from FTIR and UV-Vis analysis significantly confirmed the chemical structure of the resulted PAni.

University of Malaya

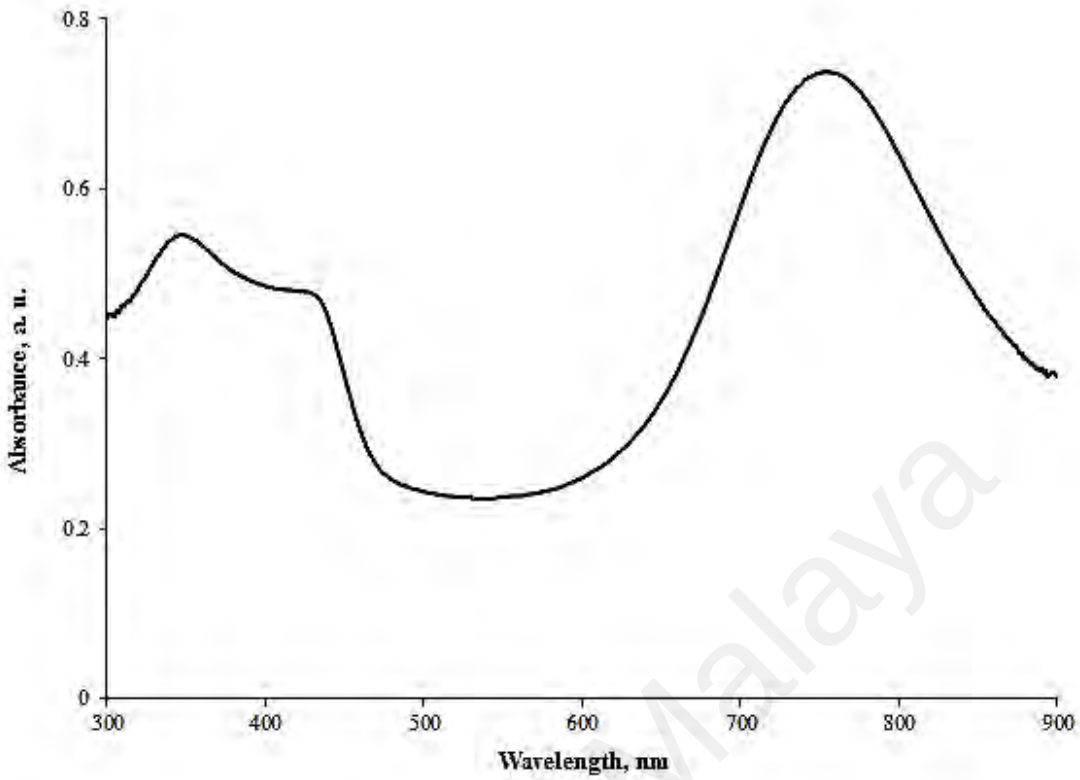

Figure 4.2: UV-Vis spectrum of PAni 5: 5 synthesized at 0 °C.

4.1.1.3 Conductivity Measurement

The conducting behaviour of PAni 5: 5 film was measured using four-point probe method at room temperature. The conductivity of PAni 5: 5 film is $1.468 \times 10^{-2} \pm 0.001$ S/cm. The higher conductivity value of the PAni 5: 5 film significantly proved that the resulted PAni is in the conductive ES form (UV-Vis absorption peak: ~765 nm) as shown in Figure 4.2.

University of Malaya

4.1.2 Application of PAni Coated FBG Sensor for Organic Compounds Detection

The sensor response for PAni 5: 5 coated FBG sensor in different organic compounds solution (3 %) such as 1-propanol, 2-propanol, ethylenediamine, chloroform, dichloromethane, dimethyl sulphide (DMS) and dimethyl disulphide (DMDS) are shown in Figure 4.3. The sensor response for PAni 5: 5 coated FBG sensor was monitored based on the Bragg wavelength shift at ~1557 nm. In this study, the sensor respond of PAni 5: 5 coated FBG sensor was not monitored based on the intensity at ~1557 nm due to the fluctuation of intensity. This is because the intensity of wavelength (~1557 nm) is easily affected by the environmental factor such as temperature and humidity of the surrounding. The aim of this section is to investigate the most sensitive organic compounds analyte that can be potentially detected by PAni coated FBG sensor.

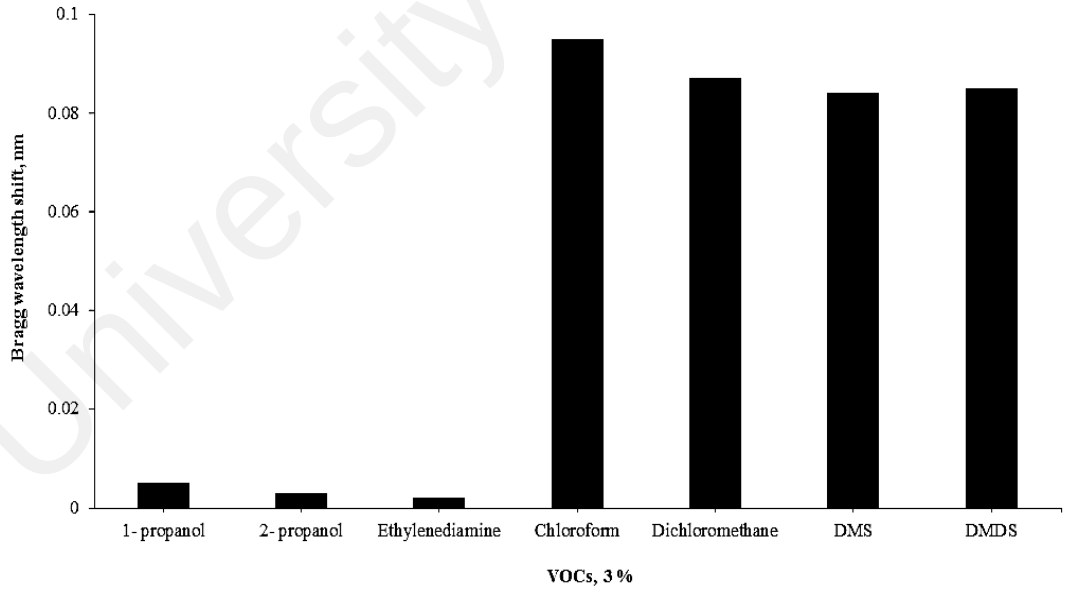

Figure 4.3: Bragg wavelength shift (~1557 nm) of PAni 5:5 coated FBG sensor in different organic compounds solution (3 %).

University of Malaya

In general, PAni 5: 5 coated FBG sensor showed the lowest Bragg wavelength shift (0.002 nm) in basic character organic compound analyte (ethylenediamine) while higher Bragg wavelength shift (0.003 - 0.098 nm) in acid character organic compound analytes (1-propanol, 2-propanol, chloroform, dichloromethane, DMS and DMDS) as shown in Figure 4.4.

For those with higher Bragg wavelength shift, acid character organic compound analytes showed increment in Bragg wavelength shift follow the sequence of –OH group, -S group and -Cl group due to the increasing of electronegativity from –OH group (1.4), -S group (2.5) and -Cl group (3.0). For the –OH group organic compound analytes, the Bragg wavelength shift of PAni 5: 5 coated FBG sensor in 1-propanol (0.005 nm) is higher than 2-propanol (0.003 nm). This is due to the strong effect of steric hindrance on 2-propanol that significantly disturbed the interaction between PAni 5: 5 and 2-propanol, thus has lower the Bragg wavelength shift towards PAni 5: 5 coated FBG. Among all organic compound analytes, chloroform showed the highest Bragg wavelength (0.098 nm) in PAni 5: 5 coated FBG due to its highest electronegativity and the acid character.

Based on the result obtained, PAni 5: 5 coated FBG showed short response time of 10 s and potentially applied as an efficient optical sensor in different types of organic compounds detection. During the sensor response, the chemical interaction between organic compound analytes and PAni 5: 5 was investigated in this study using the FTIR, UV-Vis and conductivity analysis as supporting data (Section 4.1.3).

University of Malaya

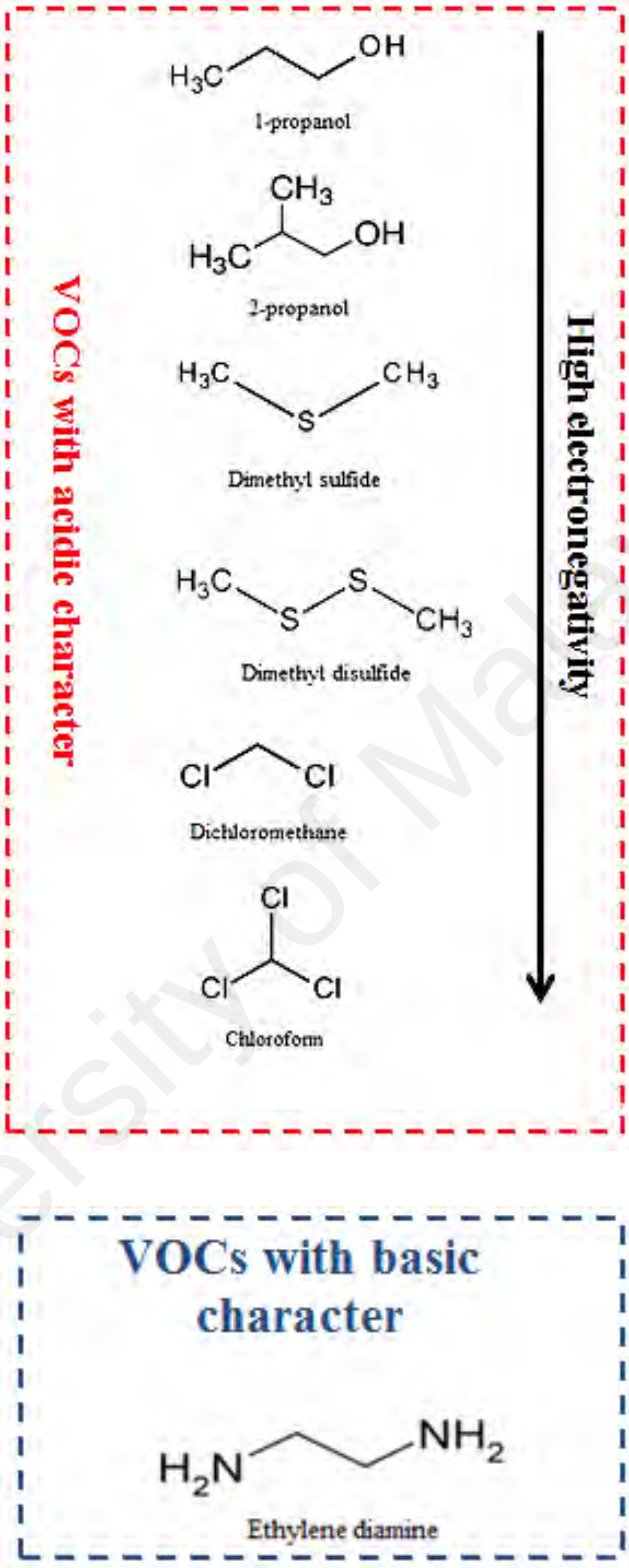

Figure 4.4: The chemical structures of different types of organic compounds.

University of Malaya

4.1.3 Supporting Data

4.1.3.1 UV-Vis Analysis

The UV-Vis spectra of PAni 5: 5 before and after immersion in different organic compounds solution (3 %) are shown in Figure 4.5 (acid character organic compound analytes) and Figure 4.6 (basic character organic compound analyte). The UV-Vis response for PAni 5: 5 coated FBG sensor was monitored based on the polaron peak at ~750 nm. Refer to Figure 4.5, the interaction between PAni 5: 5 and 1-propanol (acid character organic compound analytes) caused the polaron peak shifted to higher wavelength (~750 nm to ~780 nm). While, the interaction between PAni 5: 5 and ethylenediamine (basic character organic compound analyte) caused the polaron peak shifted to lower wavelength (~750 nm to ~590 nm) as shown in Figure 4.6.

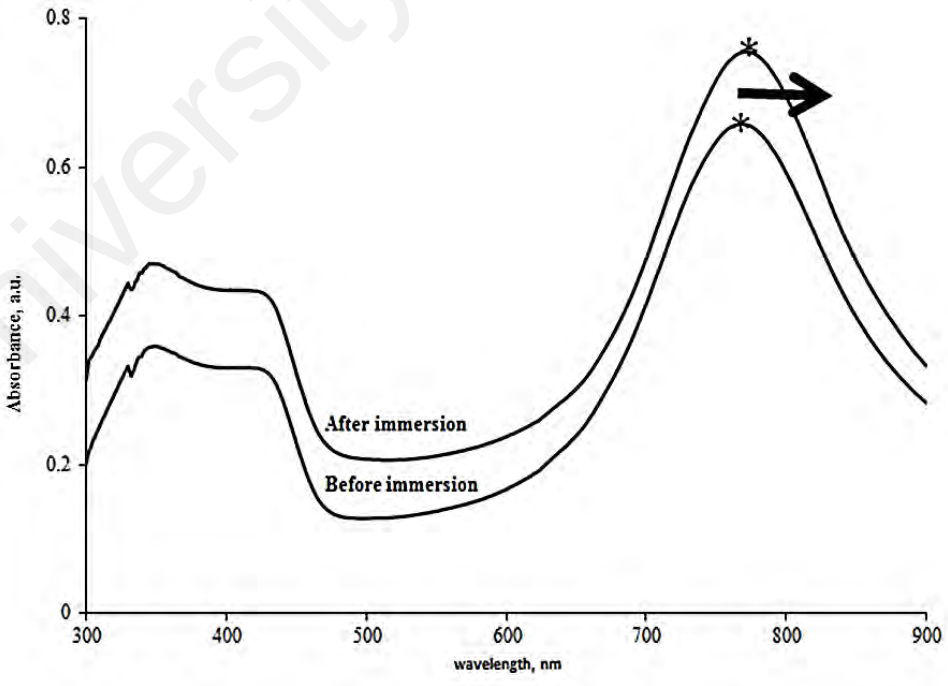

Figure 4.5: UV-Vis spectra that indicate the polaron shift of PAni 5: 5 before and after immersion in 1-propanol solution.

University of Malaya

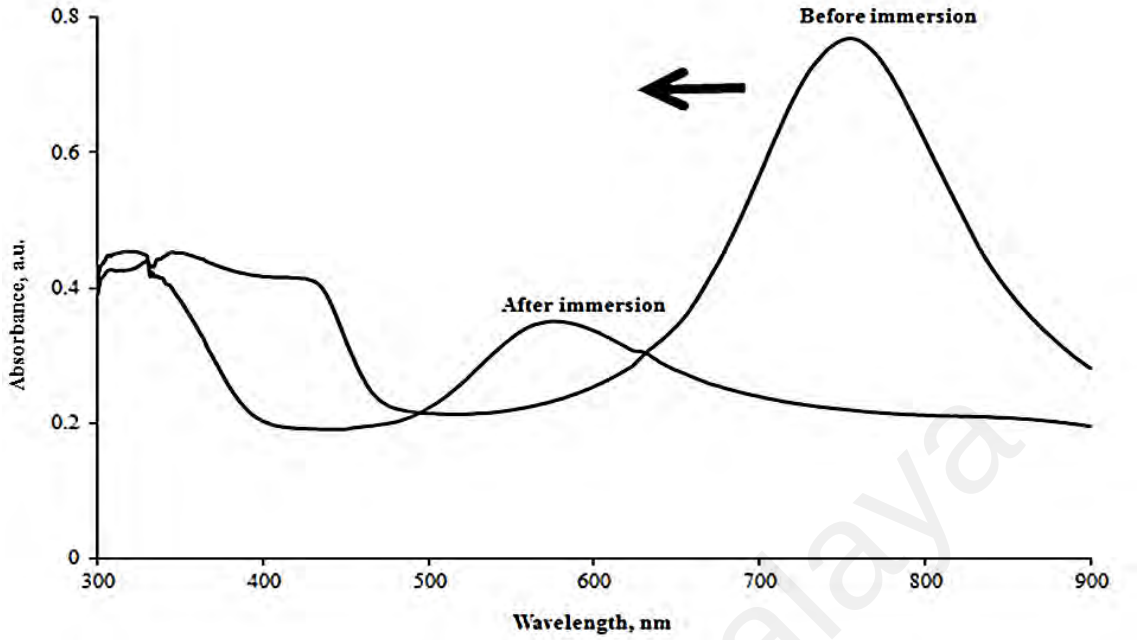

Figure 4.6: UV-Vis spectra that indicate the polaron shift of PAni 5: 5 before and after immersion in ethylenediamine solution.

In general, the wavelength shift of organic compound analytes in UV-Vis spectra is named as "solvatochromic shift". The solvatochromic shift can be classified as red shift and blue shift. The movement of the polaron peak to higher wavelength is known as red shift while the movement of the polaron peak to lower wavelength is known as blue shift (Bhadra et al., 2017). The interaction between PAni 5: 5 and all acid character organic compound analytes showed similar pattern (Appendix A1-A5) as 1-propanol as shown in Figure 4.5 that indicate a red shift in UV-Vis spectra. However, the interaction between PAni 5: 5 and basic character organic compound analyte (ethylenediamine) indicating a blue shift in UV-Vis spectra.

The UV-Vis respond between organic compound analytes and PAni 5: 5 can be determined by using the normalized UV-Vis (polaron) wavelength shift (P_f / P_i) as

University of Malaya

stated in Equation 4.1. The normalized UV-Vis (polaron) wavelength shift of PAni 5: 5 in different type of organic compound solutions are notable in Table 4.1. In this study, interaction between PAni 5: 5 with all acid character organic compound analytes (1-propanol, 2-propanol, chloroform, dichloromethane, DMS and DMDS) showed a higher P_f / P_i ratio ($\geq$ 1.0) at the polaron peak (red shift). It is due to the strong interaction between acid character organic compound analytes and protonated NH^+ site from PAni chain that may facilitate the delocalization of electrons to produce more polaronic structure along the PAni chain. The red shift of polaron peak indicates the transition of electrons from benzenoind ring to quinoid ring along the PAni chain. Besides, the P_f/ P_i ratio of PAni 5: 5 in acid character organic compounds was affected by their electronegativity. The increasing in electronegativity of acid character organic compound analytes will significantly increase the P_f/ P_i ratio after interaction with PAni 5: 5 (Chiam et al., 2014).

Normalized UV-Vis (polaron) wavelength shift = P_f/ P_i Equation 4. 1

where; P_f = Wavelength for polaron peak of PAni 5: 5 after immersion

P_i = Wavelength for polaron peak of PAni 5: 5 before immersion

In addition, the important factors that affect the solvatochromic shift in UV-Vis spectra are the dipole moments of solvent and solute molecules in the excited and ground state, respectively. In this study, the dipole moment of acid character organic compound analytes in excited state is greater than the dipole moment in ground state. Thus, it will lead to the higher stabilization of excited state in acid character organic

University of Malaya

compound analytes and cause a red shift in UV-Vis spectra after interaction with PAni 5: 5 (Bhadra et al., 2017).

In contrast, ethylenediamine with basic character shows lower P_f / P_i ratio (≤ 1.0) which indicates a blue shift at polaron peak. The dipole moment of basic character organic compound analyte (ethylenediamine) in excited state is lower than the dipole moment in ground state. This condition causes the ground state of ethylenediamine become more stable than the excited state and thus causing a blue shift at polaron peak (shift to lower wavelength) (Bhadra et al., 2017). In addition, the basic character of ethylenediamine may reduce the delocalization of electrons and decrease the polaronic structure along PAni 5: 5 chain. This condition would enhance the electron shift from quinoid to benzenoid structure along PAni 5: 5 chain (Zeghioud et al., 2015).

Table 4.1: The P_f / P_i ratio of PAni 5: 5 in different types of organic compounds solution.

Analytes	P_i (nm)	P_f (nm)	P_f / P_i
1-propanol	772	776	1.0065
2-propanol	779	785	1.0052
Chloroform	754	760	1.0080
Dichloromethane	758	763	1.0077
DMS	769	774	1.0067
DMDS	743	753	1.0068
Ethylenediamine	757	576	0.7609

University of Malaya

4.1.3.2 FTIR Analysis

The FTIR spectra of PAni 5: 5 before and after immersion in acid character organic compound analytes (e.g. 1-propanol) and basic character organic compound analyte (e.g ethylenediamine) are demonstrated in Figure 4.7 and Figure 4.8. After immersion in 1-propanol and ethylenediamine solution, PAni showed different intensity shift of FTIR at benzenoid (~1500 cm^{-1}) and quinoid (~1600 cm^{-1}) peaks that represent the interaction between the organic compound analytes with both benzenoid and quinoid ring along the PAni 5: 5 chains.

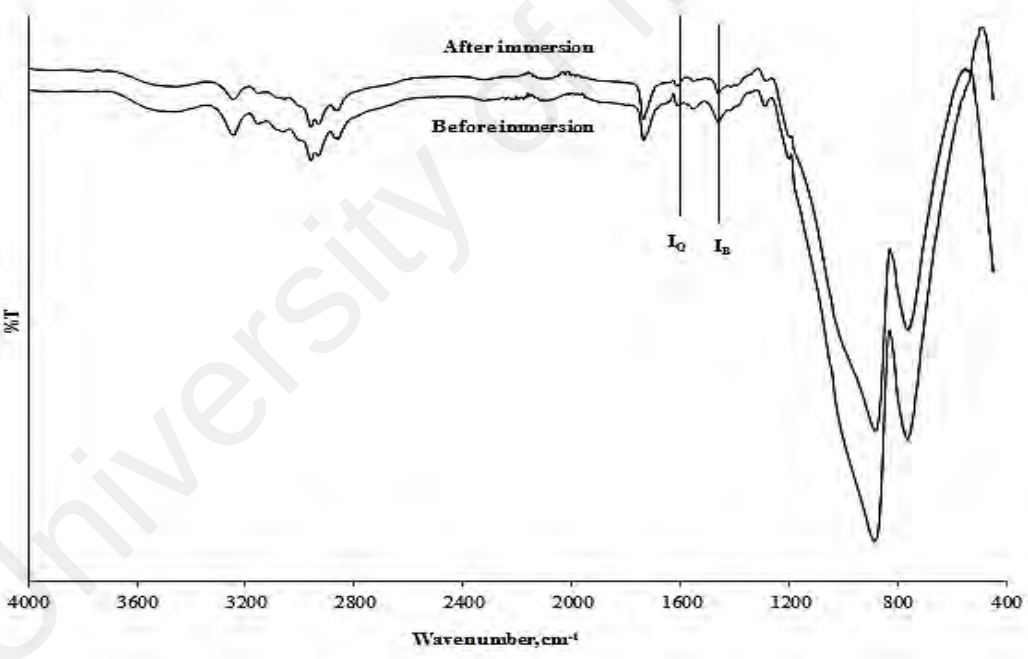

Figure 4.7: FTIR spectra of PAni 5: 5 before and after immersion in 1-propanol solution.

University of Malaya

Figure 4.8: FTIR spectra of PAni 5: 5 before and after immersion in ethylenediamine solution.

The FTIR respond between organic compound analytes and PAni 5: 5 can be determined based on the oxidation level and structural changes of PAni 5: 5 using the intensity ratio (I_Q/ I_B) as stated in Equation 4. 2 (Shao et al., 2012). The interaction between PAni 5: 5 and all acid character organic compound analytes showed similar pattern (Appendix A6-A10) as 1-propanol in FTIR spectra as shown in Figure 4.7. The I_Q/ I_B ratio of PAni 5: 5 after immersion in different types of organic compounds solution are tabulated in Table 4.2.

Intensity ratio = I_Q / I_B Equation 4. 2

where; I_Q = Intensity of quinoid after immersion

I_B = Intensity of benzenoid after immersion

University of Malaya

From the FTIR analysis, the I_Q/ I_B ratio of PAni 5: 5 showed an increment from 1.01 to 1.03 after immersion in acid character organic compound analytes. This is due to the dipole-dipole interaction between the partial positive charge of –NH- site on PAni 5: 5 and the partial negative charge of acid character organic compounds analytes. Thus, the acidity of PAni-ES (before immersion) significantly increased after immersion in acid character organic compound analytes. This phenomenon significantly increased the protonation along the PAni backbone and enhances the oxidation level of PAni (I_Q/ I_B increased) (Magnuson et al., 1999).

However, the I_Q/ I_B ratio of PAni 5: 5 showed a decrement from 1.00 to 0.79 after immersion in basic character organic compound analyte (ethylenediamine). Since, ethylenediamine is a weak base, the acidity of PAni-ES (before immersion) is significantly decreased after immersion in basic character organic compound analyte. This condition might be due to the decrease in the protonation along the PAni backbone that reduces the oxidation level of PAni (I_Q/ I_B decreased) (Focke et al., 1987).

Table 4.2: The I_Q/ I_B ratio of PAni 5: 5 after immersion in different types of organic compounds solution.

Analytes	I_Q/ I_B ratio
1-propanol	1.0198
2-propanol	1.0155
Chloroform	1.0375
Dichloromethane	1.0280
DMS	1.0250
DMDS	1.0250
Ethylenediamine	0.7850

University of Malaya

4.1.3.3 Conductivity Measurement

The conductivity respond of PAni 5: 5 toward different types of organic compound solutions (Figure 4.9) can be determined by the normalized conductivity (σ_f/σ_i) ratio as shown in Equation 4.3. As depicted in Figure 4.9, the interaction between PAni 5: 5 with basic character organic compound analyte (ethylenediamine) possessed a lower σ_f/σ_i ratio while the interaction between PAni 5: 5 with acid character organic compound analytes (1-propanol, 2-propanol, chloroform, dichloromethane, DMS and DMDS) possessed the higher σ_f/σ_i ratio.

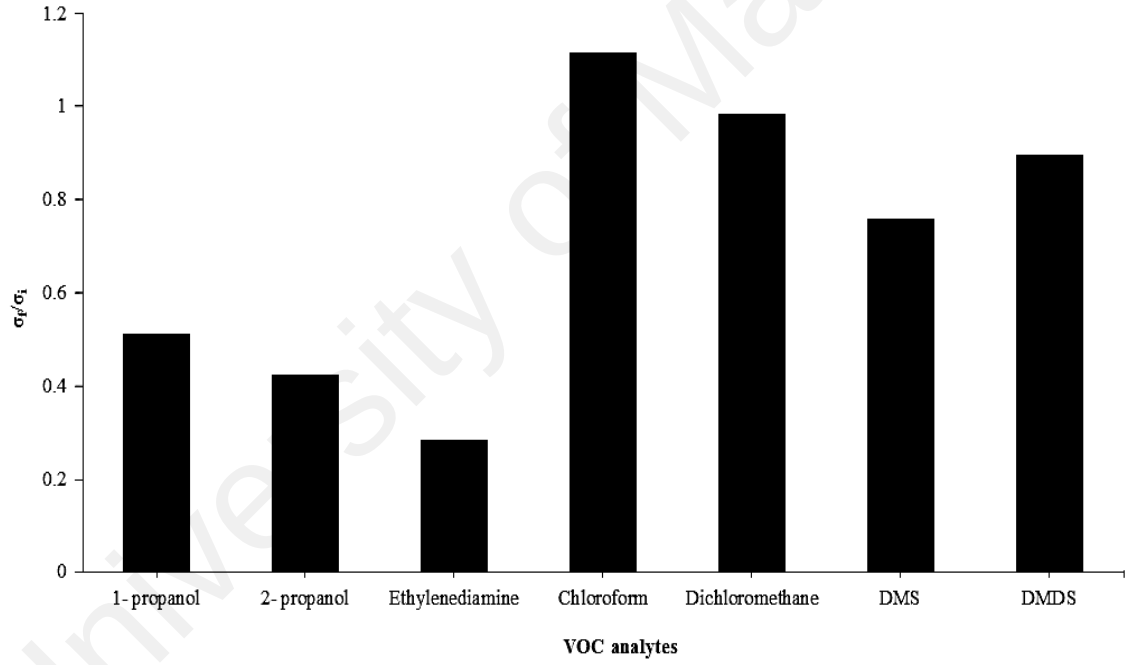

Figure 4.9: Conductivity responses of PAni 5: 5 toward different type of organic compound solutions.

Among all acid character organic compound analytes, chlorinated hydrocarbon group possessed the highest σ_f/σ_i ratio (0.9853-1.1162) due to its highest electronegativity and the acid character of chloroform and dichloromethane. For hydroxyl (-OH) group, the interaction of PAni 5: 5 with 1-propanol (0.5116) shows

University of Malaya

higher σ_f/σ_i than 2-propanol (0.4244). This due to the strong steric hindrance on 2-propanol that weaken the electrostatic interaction with the NH^+ sites along the PAni chain, thus significantly reduced the conductivity (Chiam et al., 2014).

Normalized conductivity = σ_f / σ_i Equation 4. 3

where; σ_f = Conductivity of PAni after immersion

σ_i = Conductivity of PAni before immersion

For sulfide group (acid character organic compound analytes), the interaction between PAni and DMDS (0.8975) shows higher σ_f/σ_i ratio than DMS (0.7600). This is because the high amount of sulfur atom in DMDS possessed higher dipole-dipole interaction with PAni 5: 5, thus improve the conductivity of PAni 5: 5. However, the lower amount of sulfur atom in DMS significantly reduces the dipole-dipole interactions that cause swelling of PAni 5: 5, thus decreased the conductivity of PAni 5: 5. (Li et al., 2009; Hannon et al., 2016).

For basic character organic compound analyte, ethylenediamine show the lowest σ_f/σ_i ratio (0.2839) because the basic character of ethylenediamine significantly reduces the acidity of PAni-ES, thus lower the conductivity of PAni 5: 5 (Focke et al., 1987). As conclusion, the supporting data that obtained from conductivity, UV-Vis and FTIR analysis clearly indicates the physical interaction between the PAni 5: 5 with different types of organic compound analytes during sensor detection.

University of Malaya

Among all organic compound analytes, PAni 5: 5 coated FBG sensor show the highest efficiency (highest Bragg wavelength shift) towards chloroform with the supporting data from conductivity, UV-Vis and FTIR analysis. Thus, in the later discussion, the application of PAni coated FBG sensor with different synthesis parameters (different AOT ratios and different polymerization temperatures) will be focused on the chloroform detection.

4.2 PAni (Different Dopant Ratios) Coated on FBG for Chloroform Detection

4.2.1 Characterization of PAni

4.2.1.1 FTIR Analysis

The FTIR spectra of PAni (different dopant ratios) that synthesized at 0 °C are shown in Figure 4.10. Typically, all PAni exhibit similar characteristic band in wavenumber range of 400-4000 cm^{-1}. The vibration bands at 879-894 cm^{-1} and 1189-1206 cm^{-1} correspond to the C-H bending out of plane of the aromatic ring and the C=O symmetric and asymmetric stretching from AOT dopant, respectively. The band at 1286-1298 cm^{-1} represents the C-N stretching vibration in the benzenoid ring. The presence of two vibration bands at 1613-1619 cm^{-1} and 1466-1470 cm^{-1} are assigned to the C=C stretching vibration mode of quinoid and benzenoid ring, respectively. The bands at 2954-2960 cm^{-1} and 3242-3246 cm^{-1} are attributed to the C-H and N-H stretching, respectively (Arasi et al., 2009).

University of Malaya

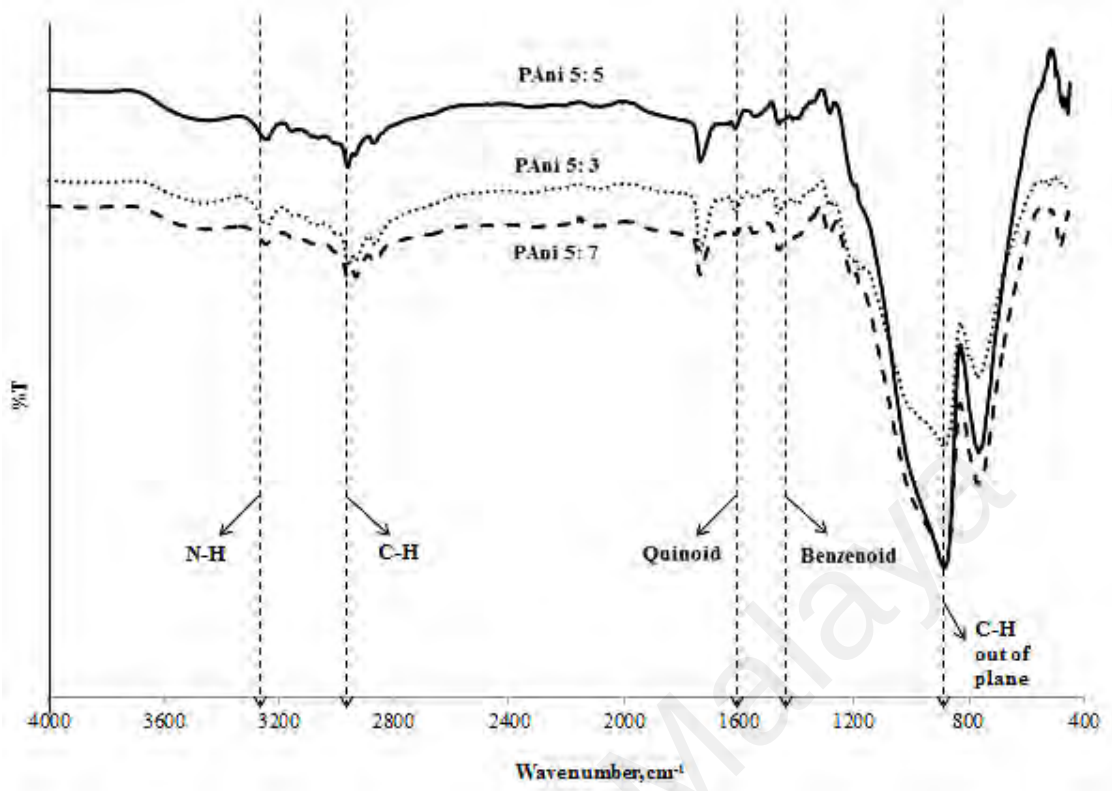

Figure 4.10: FTIR spectra of PAni (different dopant ratios) that synthesized at 0°C.

4.2.1.2 UV-Vis Analysis

The UV-Vis absorption spectra of PAni (different dopant ratios) that synthesized at 0°C shows similar absorption pattern in wavelength range of 300-900 nm (Figure 4.11). All PAnis show three characterization peaks at ~350 nm, ~420 nm and ~765 nm. The absorption peak at ~350 nm refers to the π-π* transition of benzenoid rings, while the peak at ~420 nm indicates the polaron to π* transition and localized polaron bands of protonated imines C=N. In addition, the strong absorption peak at ~765 nm significant proves all the resulted PAnis are in the form of ES state (conductive form) (Zulkhairi et al., 2015).

University of Malaya

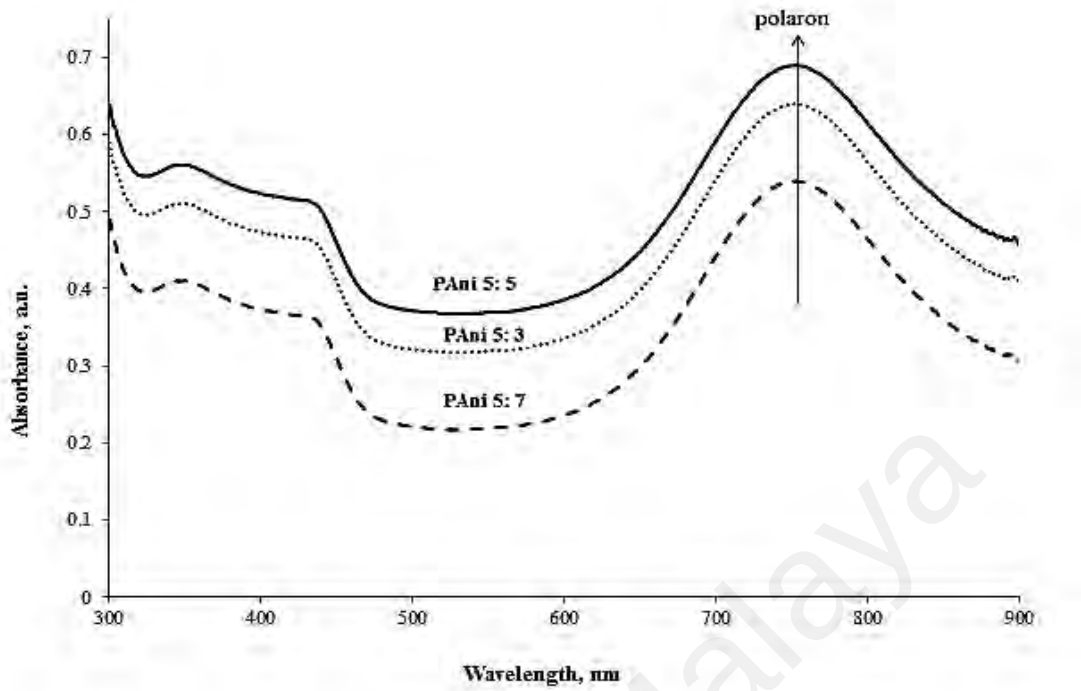

Figure 4.11: UV-Vis spectra of PAni (different dopant ratios) that synthesized at 0°C.

The absorbance peak at ~765 nm represents the doping level in the doped-PAni. In general, high doping level of PAni will significantly improve the electrical conductivity of PAni. Based on the UV-Vis spectra obtained, PAni 5: 5 shows the highest absorbance peak (~765 nm) that possesses a higher doping level followed by PAni 5:3 and PAni 5: 7 (Sambasevam et al., 2015). Thus, among all PAni obtained, PAni 5:5 possess the highest electrical conductivity due to its highest doping level at ~765 nm (polaron peak).

University of Malaya

4.2.1.3 Conductivity Measurement

The conductivity of PAni (different dopant ratios) that synthesized at 0°C are shown in Figure 4.12. Increasing AOT dopant ratio from 3 to 5 will significantly increase the conductivity of PAni film from 1.157 x 10^{-2} ± 0.001 S/cm to 1.627 x 10^{-2} ± 0.001 S/cm. However, the conductivity of PAni at dopant ratio of 7 was decreased to 0.978 x 10^{-2} ± 0.001 S/cm. In general, the conductivity of PAni depends on the amount of AOT dopant used in the polymerization of Ani (Kim et al., 2001). As shown in Figure 4.13, the presence of 2-ethyl hexyl groups on AOT would significantly reduce the interaction between PAni chains and increase the solubility in non-polar organic solvent while the presence of oxygen atoms on ester and sulfonate group would significantly increase solubility of PAni in a polar organic solvent (Kotlarchyk et al., 1985).

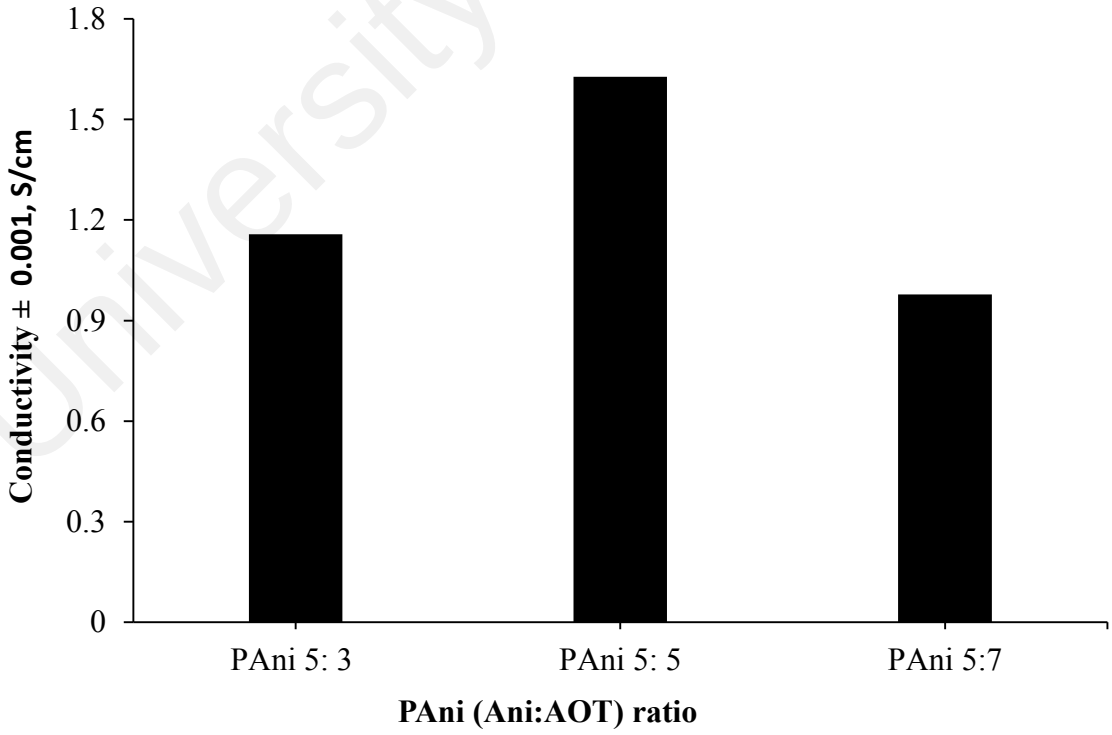

Figure 4.12: Conductivity of PAni (different dopant ratios) that synthesized at 0°C.

University of Malaya

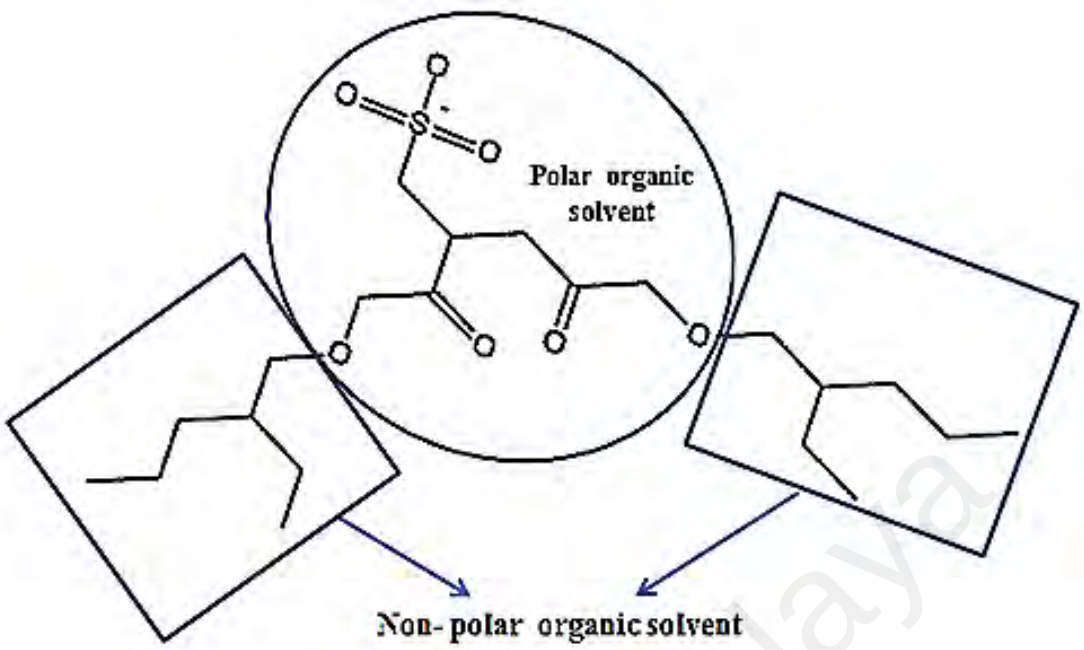

Figure 4.13: Chemical structure of AOT dopant.

The increasing of AOT dopant ratio from 3 to 5 provides more sulfonate group along the PAni chain that significant increased not only the solubility of PAni but also enhanced the electrical conductivity of PAni due to the increment of cation charge carrier (NH^+ reactive site) along the PAni chain. The higher amount of sulfonate group by further increase of AOT up to 7 would produce barriers that would reduce the amount cation charge carrier (NH^+) along PAni chain and causing the decrease in conductivity of PAni film (Zulkhairi et al., 2015). Thus, PAni 5: 5 is the optimum amount of AOT dopant ratio that possessed the highest conductivity ($1.627 \times 10^{-2} \pm 0.001$ S/cm).

In summary, both characterizations of FTIR and UV-Vis analysis significantly confirmed the chemical structure of the resulted PAni. Besides, the polaron peak at ~765 nm in UV-Vis spectrum and the conductivity data from four point probe

University of Malaya

significantly proved that the obtained PAni is in ES state that showed highest conductivity (0.978×10^{-2}- $1.627 \times 10^{-2} \pm 0.001$ S/cm).

4.2.2 Application of PAni (Different Dopant Ratios) Coated on FBG Sensor for Chloroform Detection

Figure 4.14 shows the response of PAni (different dopant ratios) coated FBG sensor in different concentrations of chloroform that monitored based on the Bragg wavelength shift at ~1557 nm using OSA detector. The response time of PAni (different dopant ratios) coated FBG sensor in different concentrations of chloroform is 7 s. Principally, the sensitivity of PAni (different dopant ratios) coated FBG sensor can be determined from the gradient of the slope for the Bragg wavelength shift of PAni (different dopant ratios) coated FBG. The linear regression analyses as shown in Appendix B1- B7 have been calculated in order to check the accuracy of the data.

University of Malaya

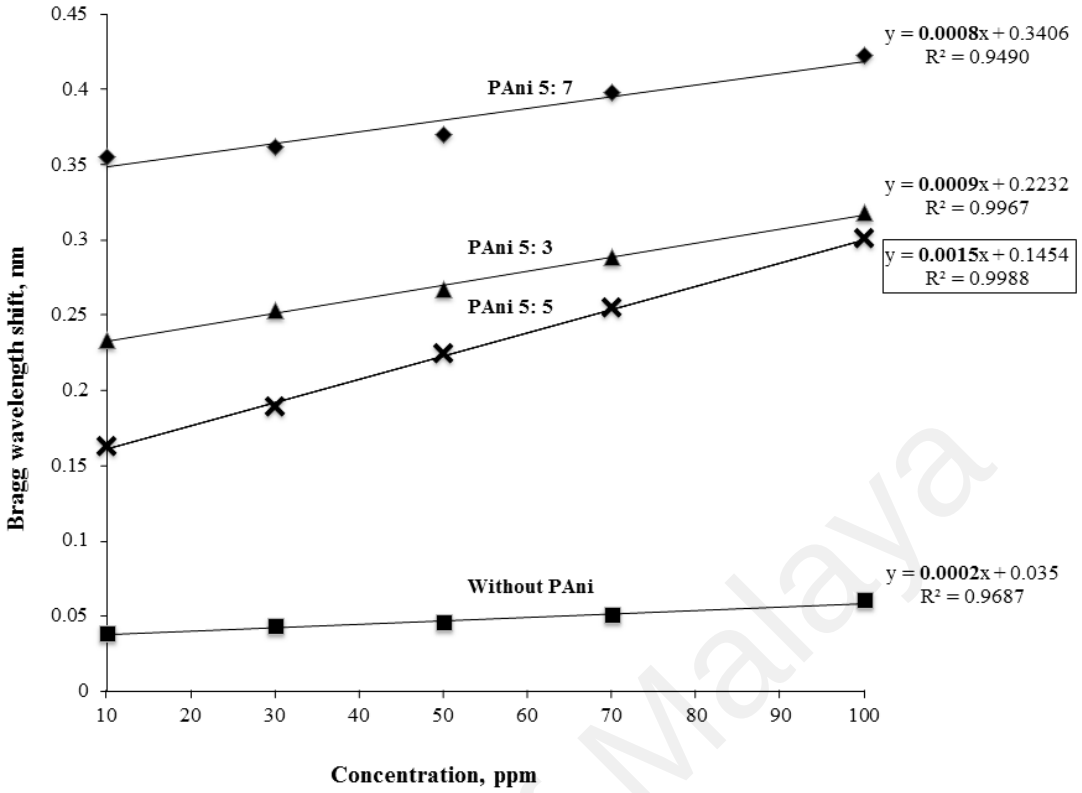

Figure 4.14: Bragg wavelength shift of PAni (different dopant ratios) coated FBG sensor in chloroform detection.

Based on the result obtained, PAni (different dopant ratios) coated FBG sensor showed higher sensitivity (from 0.0008 to 0.0015) compared to the FBG without PAni coating (0.0002). It is clearly demonstrated that the PAni acts as an active and sensitive layer (NH^+ reactive site along the PAni backbone) that can significantly interact with chloroform, thus improve the sensitivity of the sensor. However, the core part of the FBG acts as a passive and insensitive layer that is unable to interact with chloroform, thus reduce the sensitivity of the sensor (Park et al., 2010).

Based on these plots, FBG coated with PAni 5: 5 showed the highest sensitivity of 0.0015 compared to FBG coated with PAni 5: 3 (0.0009) and 5: 7 (0.0008). The

University of Malaya

difference in the sensitivity of PAni coated FBG sensor is attributed to the differences in both solubility and structure of PAni with different amount of AOT dopant. The increasing amount of AOT from 3 to 5 will produce more NH^+ reactive site along the PAni chain. Thus, the increment in both solubility and NH^+ reactive site (due to the increasing AOT amount from 3 to 5) will significantly enhance the interaction between PAni chain and chloroform.

However, further increment of AOT amount up to 7 significantly reduces the sensitivity of PAni 5: 7 coated FBG sensor. PAni 5: 5 consists of sufficient AOT amount in order to produce the maximum NH^+ reactive sites along the PAni chain. However, extra AOT amount (AOT 7) would significantly form some barrier (without formation of NH^+ reactive sites) that can block the interaction between PAni and chloroform, thus reduce the sensitivity (Kint et al., 2003).

Another important factor that affects the Bragg wavelength shift of PAni (different dopant ratios) coated FBG sensor is the concentration of chloroform solutions. Increasing concentration of chloroform (10-100 ppm) will significantly increase the Bragg wavelength shift of PAni (different dopant ratio) coated FBG sensor. This is because increasing of the chloroform concentration would provide more chloroform molecules that can readily react with NH^+ reactive site along the PAni chain, thus causing the increment in Bragg wavelength shift (Yin & Ruckenstein, 2000). Besides, the interaction between PAni and chloroform molecules significantly increased the refractive index (RI) of PAni and thus enhances the Bragg wavelength shift (Kim et al., 2012).

University of Malaya

Moreover, the chemical interaction between chloroform and PAni (different dopant ratios) were investigated in the following section (Section 4.2.3) using the UV-Vis, FTIR and conductivity analysis as supporting data.

4.2.3 Supporting Data

4.2.3.1 UV-Vis Analysis

The polaron shift (~750 nm) of PAni 5: 5 before and after immersion in 50 ppm of chloroform solution is shown in Figure 4.15. The interaction between chloroform (50 ppm) and PAni with different dopant ratios (PAni 5: 3 and PAni 5: 7) showed similar pattern (Appendix C1-C2) as PAni 5: 5 in UV-Vis spectra as shown in Figure 4.15. The P_f/ P_i ratio (based on equation 4.1) of PAni (different dopant ratios) after immersion in chloroform solution (50 ppm) are shown in Figure 4.16.

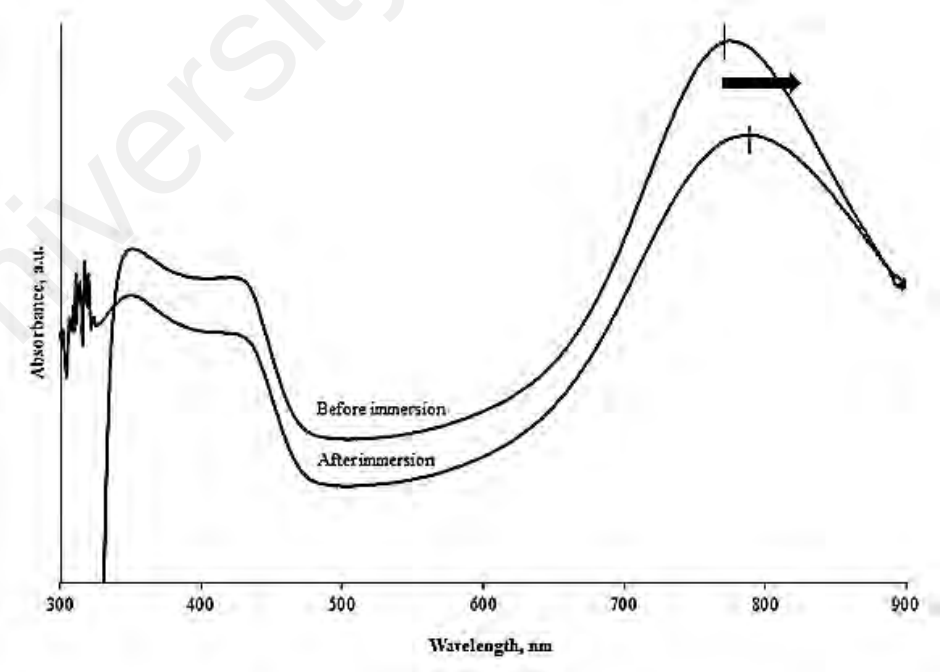

Figure 4.15: UV-Vis spectra that indicate polaron shift of PAni 5: 5 before and after immersion in chloroform (50 ppm) solution.

University of Malaya

Based on the result obtained (Figure 4.15), the polaron peak of PAni 5: 5 shifted to higher wavelength from ~750 nm (before immersion) to ~780 nm (after immersion) that indicates a red shift. It is because the dipole moment of chloroform in the excited state is greater than the dipole moment in the ground state after interaction with PAni 5: 5. Thus, it will lead to a higher stabilization of the excited state of chloroform and causing a red shift in the UV-Vis spectra (Bhadra et al., 2017).

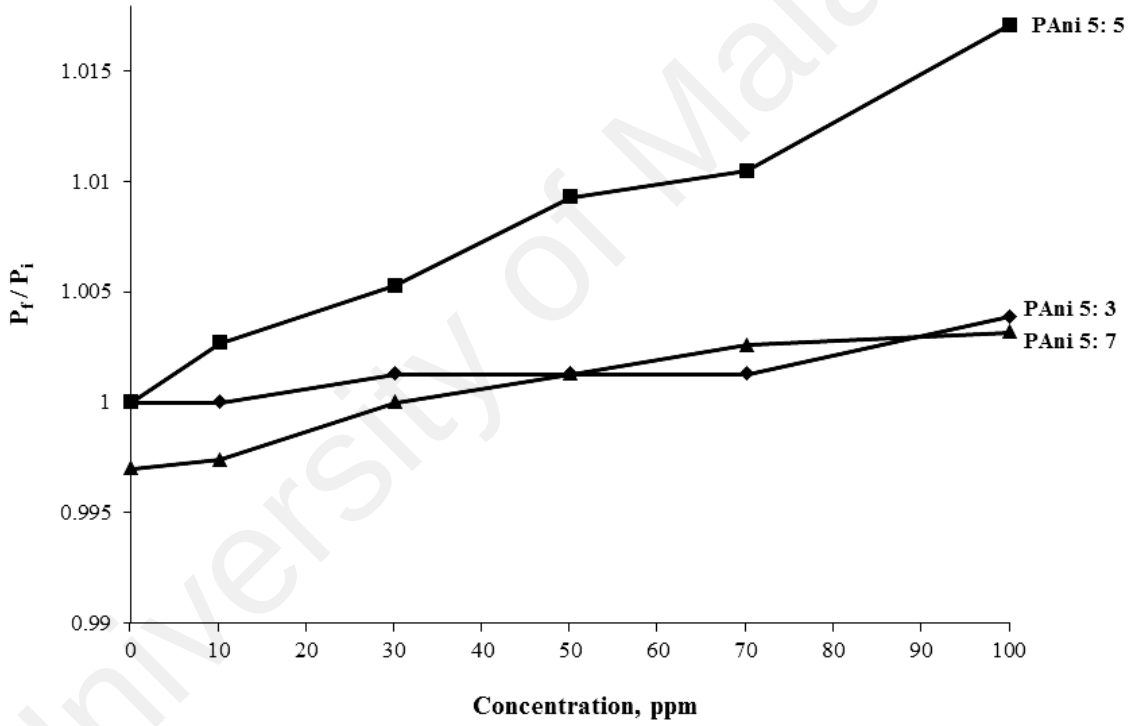

Figure 4.16: The P_f / P_i ratio for PAni (different dopant ratios) after immersed in different concentration of chloroform.

As shown in Figure 4.16, PAni 5: 5 showed the highest P_f / P_i ratio compared to PAni 5: 3 and PAni 5: 7. This is because the formation of more NH^+ reactive site along the PAni 5: 5 chain (as discussed earlier in "Section 4.2.1.3 Conductivity Study")

University of Malaya

eventually enhances the interaction between chloroform molecules and PAni, thus increased the P_f/P_i ratio of PAni 5: 5. However, PAni 5: 7 showed the lowest P_f / P_i ratio due to the formation of barriers that reduced the interaction between chloroform molecules and PAni, thus decreased the P_f/P_i ratio of PAni 5: 5.

As shown in Figure 4.16, as the concentration of chloroform increases from 0 ppm to 100 ppm, the P_f/P_i ratio increases. This implies to all PAni with difference dopant ratio. It is because the increasing of chloroform concentration would produce more chloroform molecules to interact with PAni 5: 5, thus enhance the polaron shift to higher wavelength with a greater P_f/P_i ratio (Bai & Shi, 2007).

4.2.3.2 FTIR Analysis

The FTIR responses of PAni 5: 5 before and after immersion in chloroform (50 ppm) solution is depicted in Figure 4.17. The interaction between chloroform (50 ppm) and PAni with different dopant ratio (PAni 5: 3 and PAni 5: 7) showed similar pattern (Appendix C3-C4) as PAni 5: 5 in FTIR spectra as shown in Figure 4.17. The I_Q/ I_B ratio of PAni (different dopant ratios) before and after immersion in chloroform solution (based on Equation 4.2) are tabulated in Table 4.3.

University of Malaya

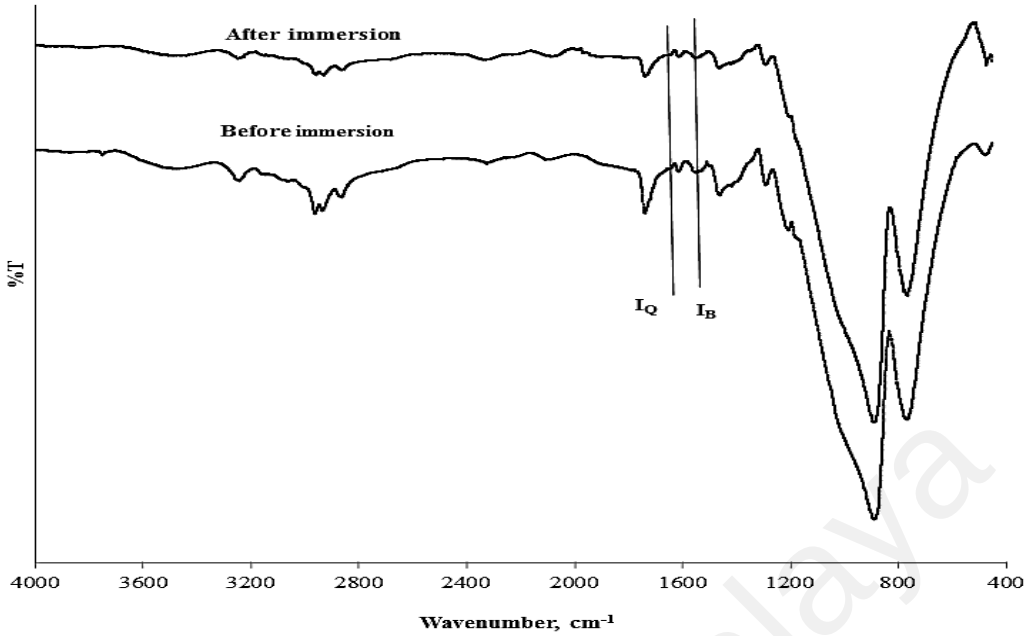

Figure 4.17: FTIR spectra of PAni 5: 5 before and after immersion in 50 ppm of chloroform solution.

As shown in Table 4.3, all PAni (different dopant ratios) showed almost similar I_Q/ I_B ratio (1.0020- 1.0084) before and after immersion in chloroform solution. The amount of benzenoid and quinoid structures along the PAni chain (different dopant ratios) are remain unchanged before and after immersion in chloroform due to the absence of the electron shifting between both quinoid and benzenoid structures. This clearly demonstrated that only the physical interaction (dipole-dipole moment) involved between the chloroform and PAni (different dopant ratios) during sensor detection (Li et al., 2009).

Referring to Table 4.3, increasing concentration of chloroform from 0 ppm to 100 ppm did not affect the I_Q/ I_B ratio for all PAni (different dopant ratios) during sensor detection. Thus, it significantly proved that the Bragg wavelength shift of PAni coated

University of Malaya

FBG sensor is contributed by the physical interaction between PAni thin film and chloroform (without any chemical interaction).

Table 4.3: The I_Q/I_B ratio of PAni (different dopant ratios) after immersion in different concentration of chloroform.

Concentration (ppm)	I_Q/I_B ratio					
	PAni 5: 3		PAni 5: 5		PAni 5: 7	
	Before	After	Before	After	Before	After
0	1.0040	1.0040	1.0049	1.0049	1.0020	1.0020
10	1.0040	1.0041	1.0052	1.0053	1.0028	1.0028
30	1.0045	1.0045	1.0062	1.0062	1.0033	1.0034
50	1.0045	1.0045	1.0062	1.0062	1.0038	1.0038
70	1.0049	1.0049	1.0077	1.0078	1.0045	1.0045
100	1.0049	1.0050	1.0084	1.0084	1.0047	1.0048

4.2.3.3 Conductivity Study

The conductivity respond of PAni (different dopant ratios) towards different concentration of chloroform can be determined by the σ_f/σ_i ratio (Figure 4.18) based on Equation 4.3. Theoretically, the σ_f/σ_i ratio of PAni would be increased by further increasing in the concentration of chloroform from 0 ppm to 100 ppm. However, in this study, the σ_f/σ_i ratio of PAni is contradicted with the UV-Vis analysis (Figure 4.15) and FTIR analysis (Figure 4.17). Refer to Figure 4.18, the σ_f/σ_i ratio of PAni (different dopant ratios) showed an increment from 0 ppm to 10 ppm of chloroform solution with

University of Malaya

a maximum value of 1.2720-1.4083. However, the σ_f/σ_i ratio of PAni (different dopant ratios) showed a significant decrease from 10 ppm to 30 ppm of chloroform solution.

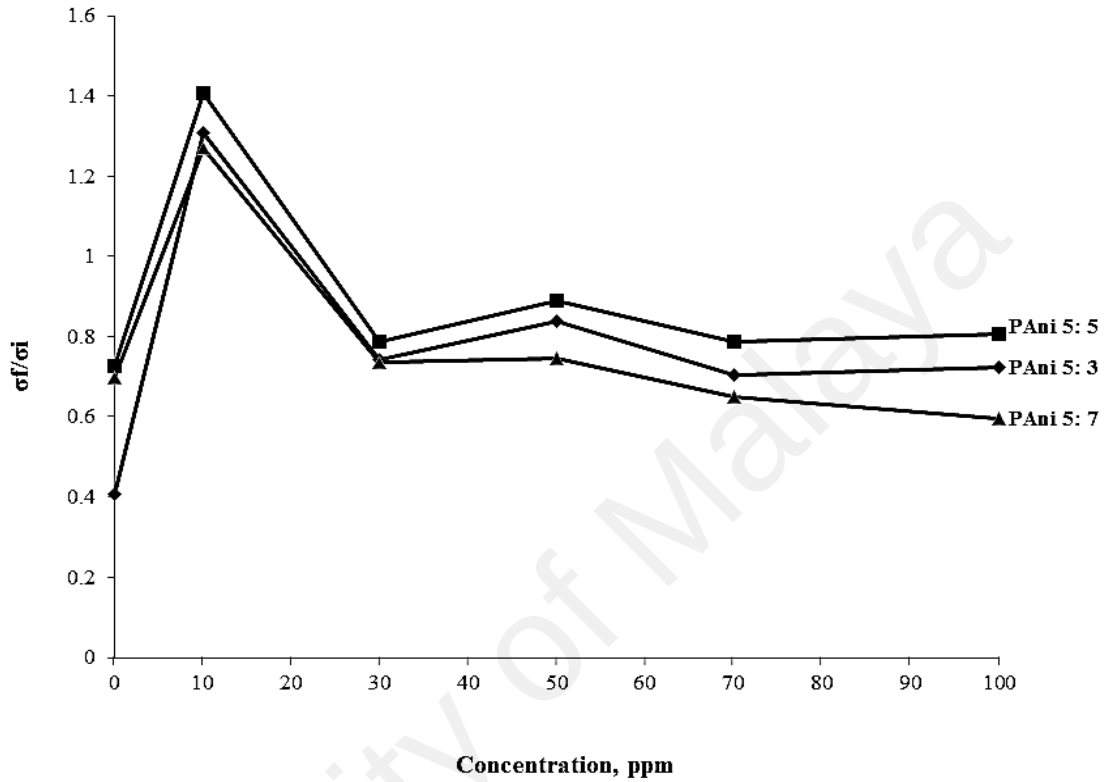

Figure 4.18: The σ_f/σ_i ratio of PAni (different dopant ratios) after immersion in different concentration of chloroform.

At the initial state (0-10 ppm), the increase in σ_f/σ_i ratio of PAni (different dopant ratios) is due to the increasing acidity of PAni in ES state when it interacts with chloroform solution (weak acid). The increasing in acidity will produce more charge carrier and protonation of imine group along PAni backbone, thus increase the σ_f/σ_i ratio of PAni. At 10 ppm of chloroform solution, the NH^+ reactive sites on PAni chain are saturated with chloroform molecules that indicated the highest σ_f/σ_i ratio of PAni. However, increasing concentration of chloroform above 10 ppm showed a significant decrease in σ_f/σ_i ratio due to the swelling effect from the overlapping layer of

University of Malaya

chloroform molecules (above the NH^+ reactive sites and first layer of chloroform) that would increase the hopping distance of the charge carrier on PAni chain, thus significantly reduced the $\sigma_f/\ \sigma_i$ ratio (Arenas et al., 2012).

Among all PAni, PAni 5: 5 showed the highest $\sigma_f/\ \sigma_i$ ratio compared to PAni 5:3 and PAni 5: 7 as showed in Figure 4.18. This is because PAni 5: 5 provides more NH^+ reactive sites along the PAni chains that eventually enhance the interaction of PAni with chloroform molecules, thus causing an increase in the $\sigma_f/\ \sigma_i$ ratio (Zulkhairi et al., 2015). However, PAni 5: 7 showed the lowest $\sigma_f/\ \sigma_i$ ratio due to the formation of barriers that significantly block the interaction between chloroform molecules and PAni, thus decreased the $\sigma_f/\ \sigma_i$ ratio.

4.2.3.4 Proposed Mechanism for the Interaction between Chloroform and PAni (Different Dopant Ratios)

PAni is potentially applied as a promising sensing material due to its ability to exist in the different oxidation state when interact with different types of chemical compounds like base, reducing agent and oxidizing agent. In this study, chloroform has been used as an analyte that act as a reducing agent due to its weak acid character. The possible interaction between PAni and chloroform molecules is proposed based on the FTIR, UV-Vis and conductivity analysis as the supporting data. In this study, the effect of different dopant ratios plays important role in the sensitivity of PAni coated FBG sensor.

University of Malaya

The increment in both solubility and NH^+ reactive sites (due to the increasing amount of AOT from 3 to 5) significantly enhanced the interaction between PAni chain and chloroform. However, further increment of AOT amount up to 7 significantly reduced the sensitivity of PAni 5: 7 coated FBG sensor. This has clearly demonstrated that PAni 5: 5 consists of sufficient AOT amount in order to produce the maximum NH^+ reactive sites along the PAni chain. However, extra AOT amount (AOT 7) would significantly formed some barrier (without formation of NH^+ reactive sites) that can block the interaction between PAni and chloroform, thus reduce the sensitivity.

From the FTIR analysis, the amount of benzenoid and quinoid structure on PAni chain before and after immersion in chloroform solution is almost similar due to the absence of the electron shifting between both quinoid and benzenoid structures. The UV-vis analysis shows that the polaron peak of PAni was shifted to higher wavelength after immersion in chloroform solution due to the dipole moment of chloroform in the excited state is greater than the dipole moment in the ground state after interaction with PAni. Thus, it will lead to a higher stabilization of the excited state of chloroform and causing a red shift in the UV-Vis spectra. Thus, the result from the supporting data significantly suggested that the mechanism for the interaction between PAni and chloroform is the physical interaction between the partial negative charge ($Cl^{\delta-}$) of chloroform molecules and the partial positive charge ($NH^{\delta+}$) on PAni chain as shown in Figure 4.19.

Among all PAni with different dopant ratios, PAni 5: 5 coated FBG sensor shows the highest efficiency (highest Bragg wavelength shift) towards chloroform with the supporting data from conductivity, UV-Vis and FTIR analysis. Thus, in the later

University of Malaya

discussion, the application of PAni coated FBG sensor with different polymerization temperatures will be focused on the PAni 5: 5.

a) PAni 5: 3

b) PAni 5: 5

c) PAni 5: 7

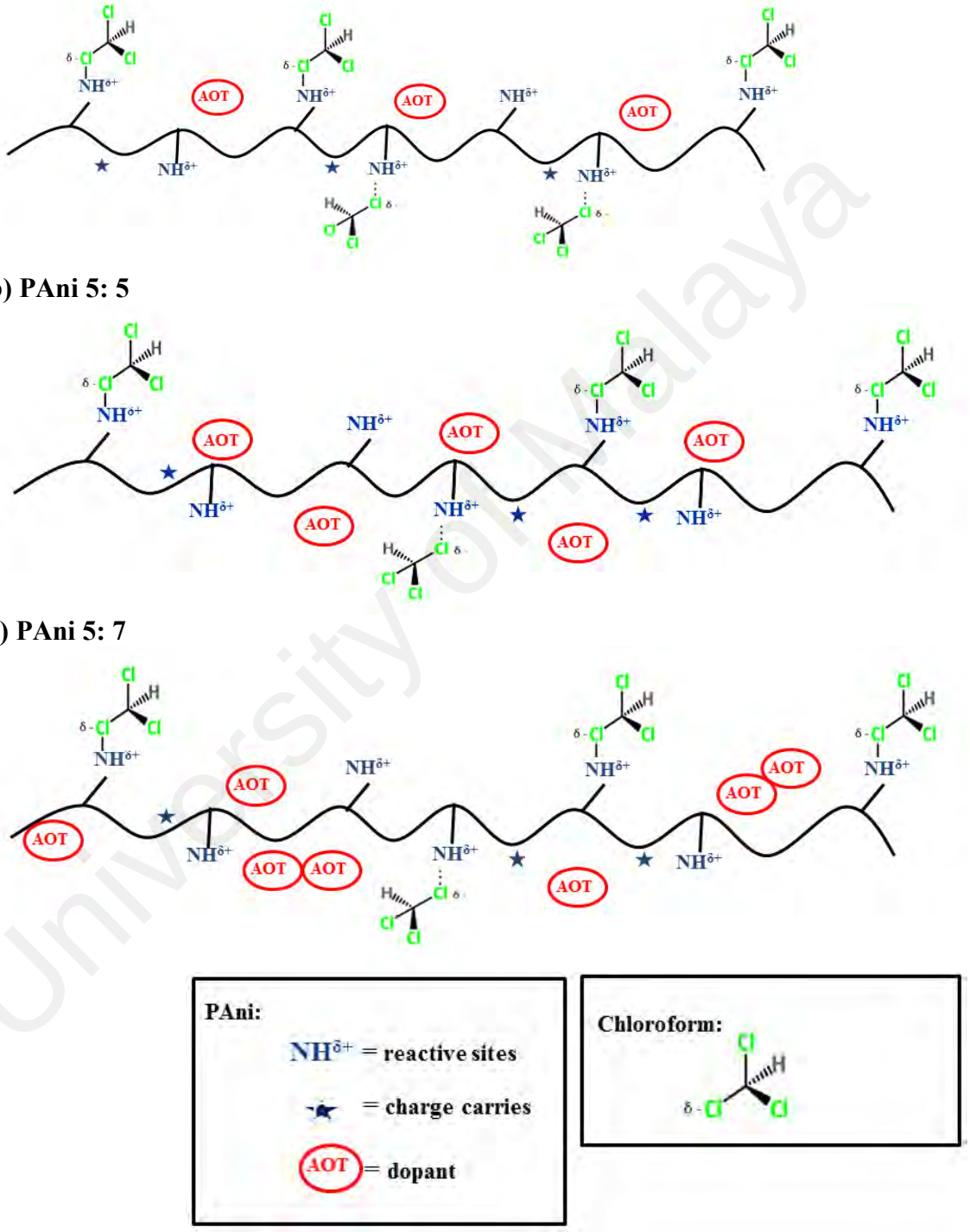

Figure 4.19: Proposed mechanisms for the interaction between PAni (different dopant ratios) during sensor detection.

University of Malaya

4.3 PAni (different polymerization temperatures) coated on FBG for chloroform detection

4.3.1 Characterization of PAni

4.3.1.1 FTIR Analysis

Figure 4.20 shows the FTIR spectra of PAni 5: 5 synthesized at different polymerization temperatures (-5 °C, 0 °C and 25 °C). All PAni exhibited similar characteristic band in wavenumber range of 400- 4000 cm^{-1}. The bands observed at 3242- 3246 cm^{-1} and 2954- 2960 cm^{-1} are corresponding to the N-H and C-H stretching vibration, respectively. Besides, the bands at 1466-1470 cm^{-1} and 1613-1619 cm^{-1} indicated the C=C stretching of benzenoid and quinoid ring vibration, respectively. The band at 1286- 1298 cm^{-1} represented the C-N stretching vibration in the benzenoid ring. Finally, the vibration bands at 879- 894 cm^{-1} and 1189- 1206 cm^{-1} corresponded to the C-H bending out of plane of the aromatic ring and the C=O symmetric and asymmetric stretching from AOT dopant, respectively (Devi et al., 2014).

University of Malaya

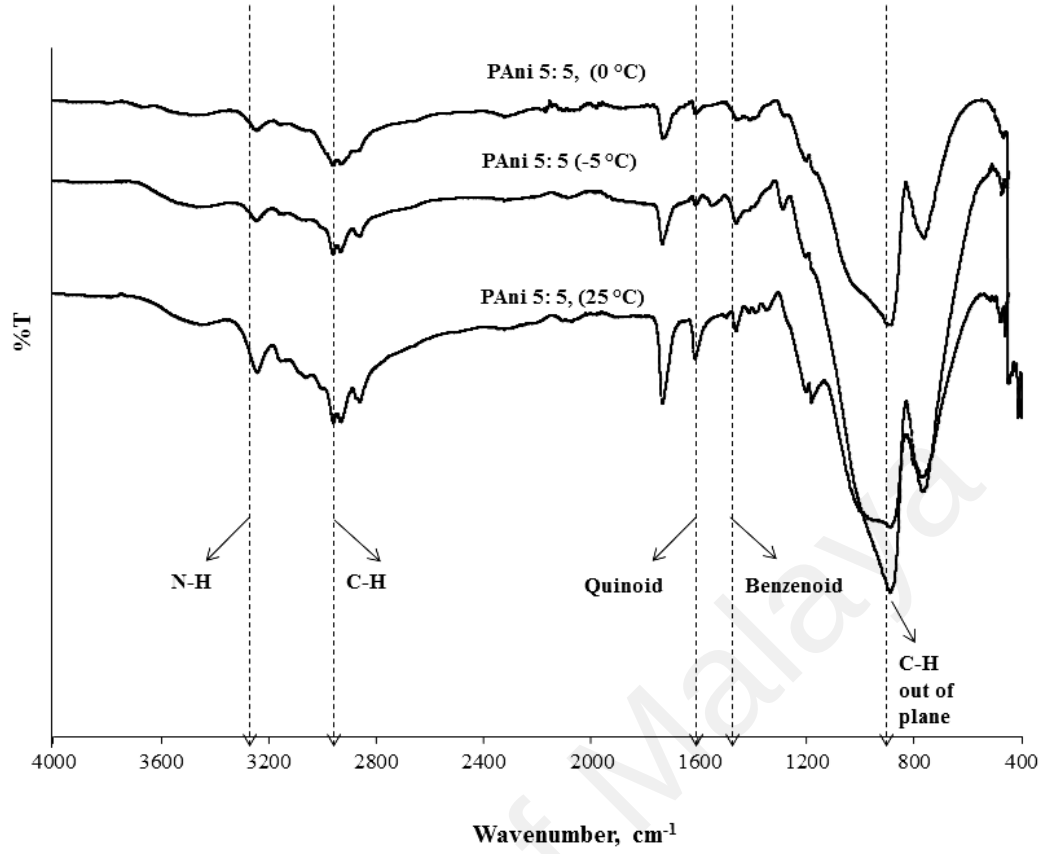

Figure 4.20: FTIR spectra of PAni 5: 5 (different polymerization temperatures).

4.3.1.2 UV-Vis Analysis

Figure 4.21 shows the UV-Vis absorption spectra of PAni 5:5 synthesized at different polymerization temperatures (-5°C, 0 °C and 25 °C). All PAni 5:5 synthesized at different polymerization temperatures exhibited similar absorption peaks at ~350 nm, ~420 nm and ~765 nm. As discussed previously, the absorption peak at ~350nm referred to π-π* transition of benzenoid rings, while the peak at ~420 nm indicated the polaron to π* transition and localized polaron bands of protonated imines C=N. The strong absorption peak at 765 nm indicated that all of the PAni are present in the ES form (Sambasevam, 2015). Among all PAni, PAni 5: 5, 0 °C possess the highest absorption of polaron peak (~750 nm) due to the highest doping level compared with

University of Malaya

those synthesized at -5 °C and 25 °C. Both characterizations were carried out by FTIR and UV-Vis analysis that have significantly confirmed the chemical structure of PAni.

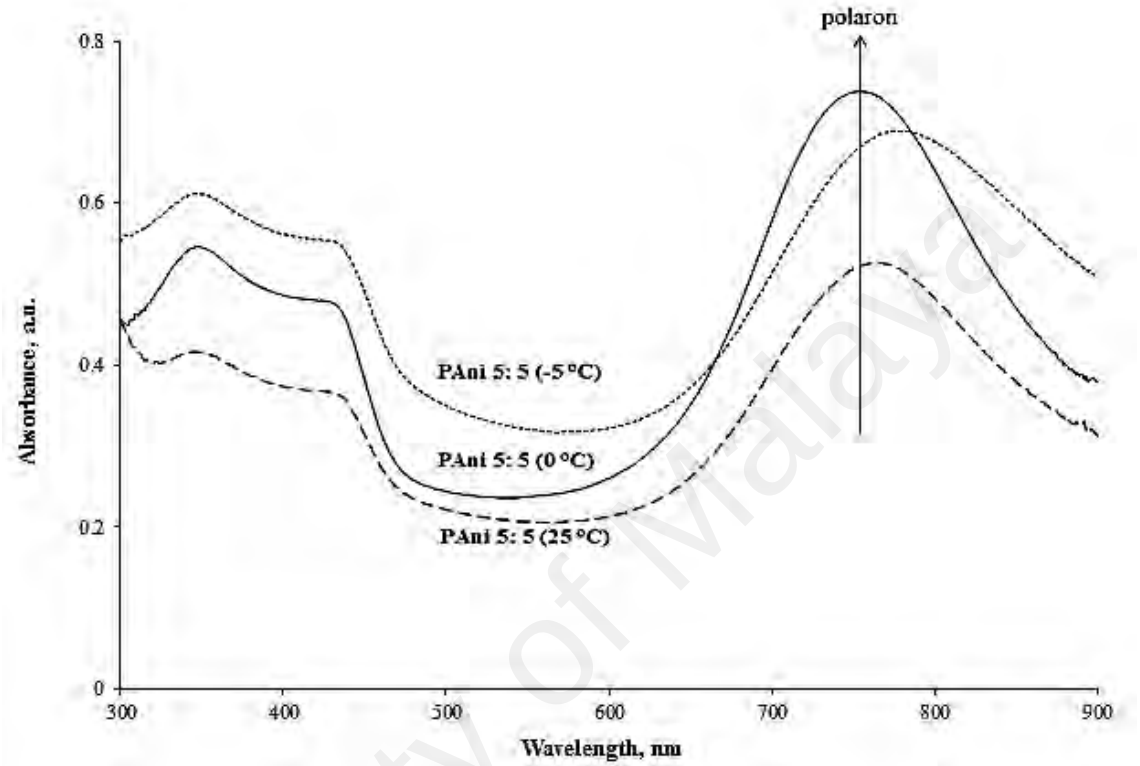

Figure 4.21: UV-Vis spectra of PAni 5:5 (different polymerization temperatures).

4.3.1.3 Conductivity Measurement

The conductivity of PAni 5: 5 synthesized at different polymerization temperatures (-5 °C, 0 °C and 25 °C) are shown in Figure 4.22. In this study, PAni 5: 5, 0 °C shows the highest conductivity ($1.627 \times 10^{-2} \pm 0.001$ S/cm) followed by PAni 5: 5, -5 °C and 25 °C with conductivities of $1.544 \times 10^{-2} \pm 0.001$ S/cm and $0.684 \times 10^{-2} \pm 0.001$ S/cm, respectively. This has clearly demonstrated that the polymerization temperature play an important role in affecting the doping and conductivity level of

University of Malaya

PAni. PAni that synthesized at lower polymerization temperature (PAni 5: 5, 0°C) may produce longer polymer chains which able to extend the conjugation of polaron. Similarly, the longer polymer chains will also allow more free charge carriers to propagate along the PAni chain, thus increased the conductivity (Kapil et al., 2010).

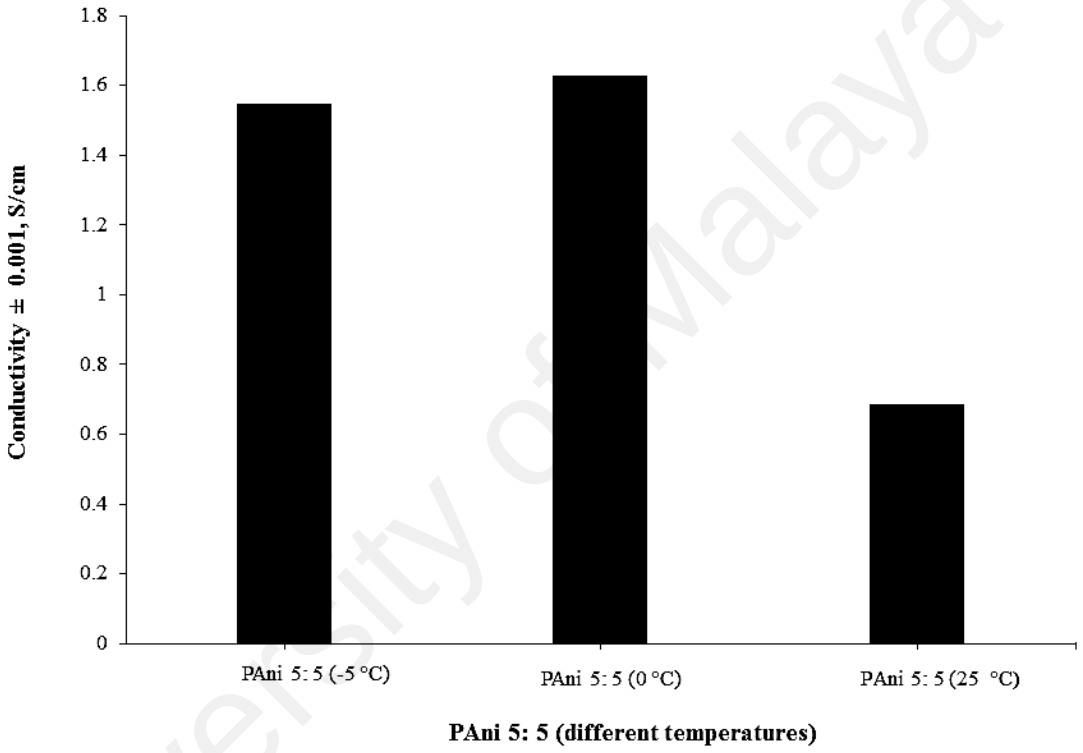

Figure 4.22: Conductivity of PAni 5: 5 (different polymerization temperatures).

However, further decreased on polymerization temperature to -5 °C would significantly decrease the conductivity of PAni 5: 5. This is because the addition of LiCl at sub-zero temperature (to avoid the freezing of solution) would cause the ring chlorination that disturbs the movement of charge carrier along the PAni chain, thus decreased the conductivity (Adams et al., 1996). Besides, increasing in polymerization

University of Malaya

temperature up to 25 °C will significantly decrease the conductivity of PAni 5: 5, 25 °C due to the shorter polymer chains with many defect sites that may block the movement of charge carriers, thus reduced the conductivity (Ansari & Keivani, 2006).

The conductivity trend of PAni (different polymerization temperatures) shows similar trend with UV-Vis analysis at polaron peak (Figure 4.21). PAni 5: 5, 0 °C possesses the highest absorbance at polaron peak (~750 nm) that indicates the highest doping level of PAni, hence possessed the highest conductivity ($1.627 \times 10^{-2} \pm 0.001$ S/cm) as shown in Figure 4.22. Thus, the conductivity result obtained in this part was strongly supported by UV-Vis analysis in Section 4.3.1.2.

University of Malaya

4.3.2 Application of PAni (Different Polymerization Temperatures) Coated FBG for Chloroform Detection

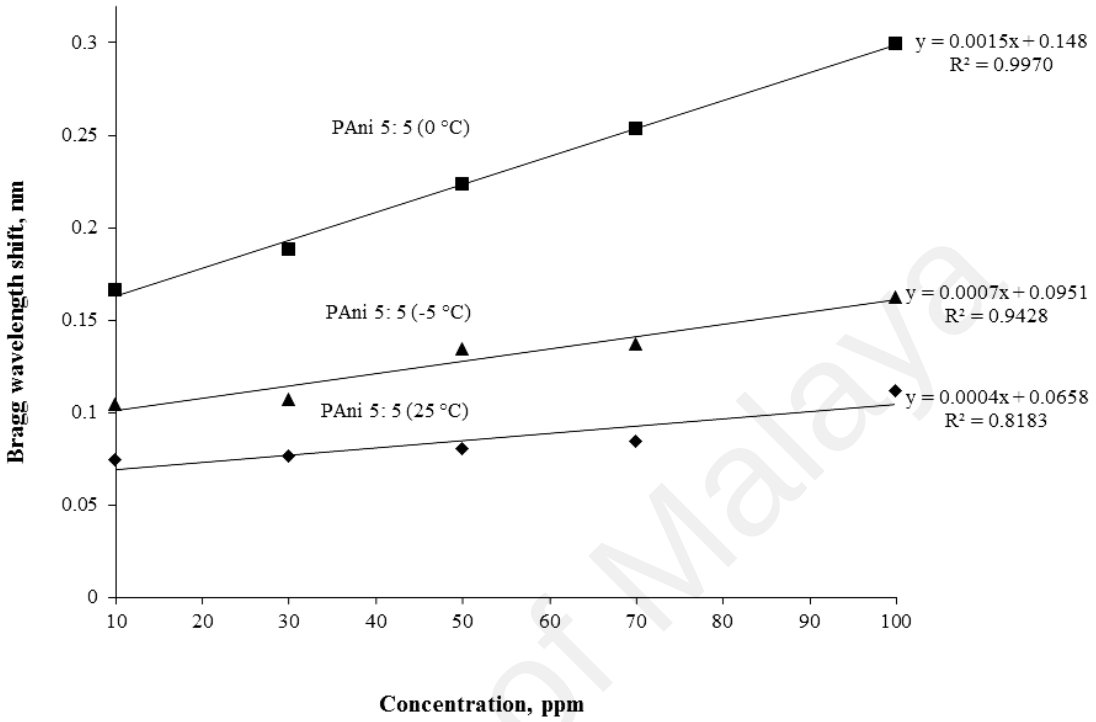

Figure 4.23: Bragg wavelength shift of PAni (different polymerization temperatures) coated FBG sensor in chloroform detection.

Figure 4.23 shows the optical sensor response of PAni 5: 5 (different polymerization temperatures) coated FBG toward different concentration of chloroform that was determined based on the Bragg wavelength shift at ~1557 nm. The response time of PAni 5: 5 (different polymerization temperatures) coated FBG in different concentration of chloroform was 7 s. The sensitivity of PAni coated FBG sensor was based on the gradient of the slope for the Bragg wavelength shift. Besides, the linear regression analyses as shown in Appendix D1- D5 have been calculated in order to check the accuracy of the data. In this study, PAni 5: 5 (0 °C) coated FBG sensor possessed the highest sensitivity (0.0015) because of the presence of longer PAni chains

University of Malaya

with more charge carriers and -NH^+ reactive sites that eventually enhanced the interaction between PAni and chloroform (Adams et al., 1997).

On the other hand, PAni 5: 5 (-5 °C) coated FBG sensor possesses the lowest sensitivity (0.0007) in chloroform detection. Theoretically, polymerization at lowest temperature (-5 °C) will produce the longest PAni chain with the highest sensitivity. However, the addition of LiCl at sub-zero temperature has adversely affected the PAni structure by formation of more barriers between the charge carriers and reactive sites, finally block the interaction between PAni with chloroform, hence reduced the sensitivity (Adams et al., 1996).

In contrast, increasing of polymerization temperature to 25 °C possessed lower sensitivity (0.0004) in chloroform detection due to the formation of shorter PAni chains with branching that provide less charge carriers and reactive sites (more defect sites) that disturb the interaction between PAni with chloroform (Bhala et al., 2013). Similarly, the proposed mechanism between PAni (different polymerization temperatures) and chloroform during sensor detection has been investigated using UV-Vis, FTIR and conductivity analysis as the supporting data.

University of Malaya

4.3.3 Supporting Data

4.3.3.1 UV-Vis Analysis

The polaron shift (~750 nm) of PAni 5: 5 (different polymerization temperatures) before and after immersion in 50 ppm of chloroform solution possessed similar UV-Vis pattern as shown in Appendix E1-E3. The P_f/P_i ratios of PAni (different polymerization temperatures) after immersion in chloroform solution (50 ppm) that was determined based on Equation 4.1 are shown in Figure 4.23.

Based on the result obtained, the polaron peak of all PAni (different polymerization temperatures) was shifted to higher wavelength from ~750 nm (before immersion) to ~780 nm (after immersion) that represented a red shift because the dipole moment of chloroform in the excited state was greater than the dipole moment in the ground state after interaction with PAni (Sharma & Kumar, 2010). As discussed earlier, it will lead to higher stabilization of the excited state of chloroform and causing a red shift in the spectra.

As showed in Figure 4.23, PAni 5: 5 (0 °C) showed the highest P_f / P_i ratio compared to PAni 5: 5 (-5 °C) and PAni 5: 5 (25 °C) due to the formation of longer PAni chains with more charge carriers and more reactive sites that significantly enhances the interaction between chloroform and PAni (Adams et al., 1997). However, PAni 5: 5 (25 °C) showed the lowest P_f / P_i ratio because the shorter PAni chains with branching have significantly reduced the charge carriers and reactive sites (more defect sites), thus block the movement of charge carriers, finally reduce the interaction between chloroform and PAni. (Bhala et al., 2013).

University of Malaya

On the other hand, the P_f / P_i ratio of all PAni are also affected by the concentration of chloroform. Increasing concentration of chloroform (0-100 ppm) will significantly increase the P_f / P_i ratio of all PAni. It is because the increasing of concentration of chloroform has remarkably provided more chloroform molecules to interact with PAni, thus increased the wavelength shift at polaron peak (higher P_f / P_i ratio) (Yin & Ruckenstein, 2000).

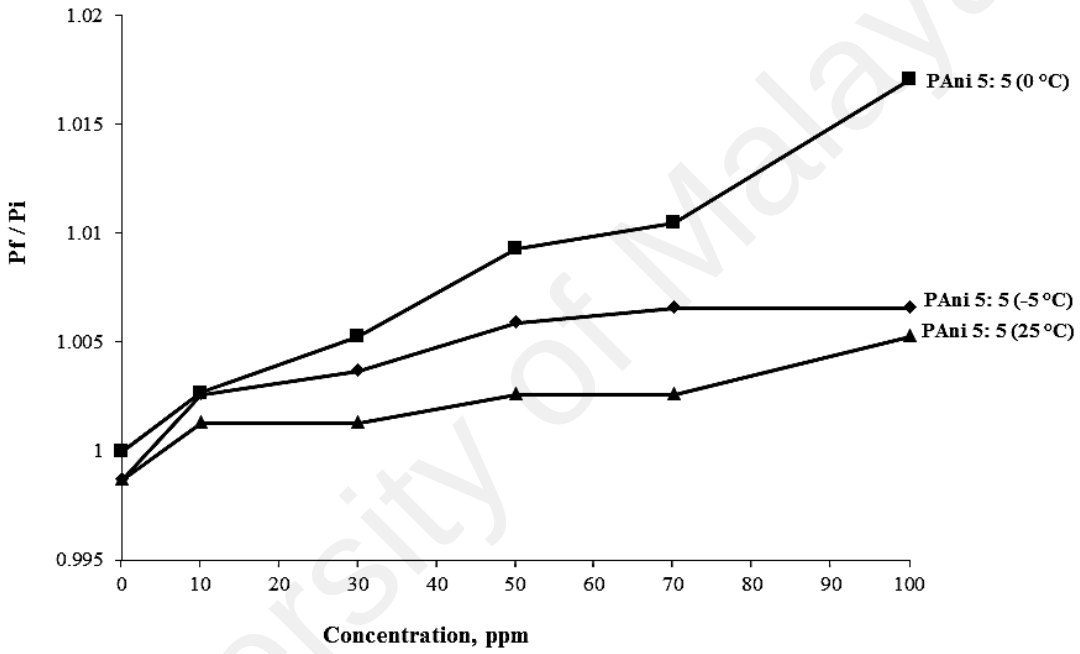

Figure 4.24: P_f/ P_i ratio for PAni 5: 5 (different polymerization temperatures) after immersion in different concentration of chloroform.

4.3.3.2 FTIR Analysis

The FTIR responses of PAni 5: 5 (different polymerization temperatures) before and after immersion in (50 ppm) chloroform solutions showed similar trend as depicted in Appendix E4-E6. Besides, the I_Q/ I_B ratio of PAni 5: 5 (-5 °C, 0 °C and 25 °C) before

University of Malaya

and after immersion in chloroform solution (50 ppm) are tabulated in Table 4.4. (Shao et al., 2012).

Same as in Section 4.2.3.2, all PAni (different polymerization temperatures) showed almost similar I_Q/ I_B ratio (1.0020- 1.0084) before and after immersion in chloroform solution (Table 4.4). Besides, increasing concentration of chloroform from 0 ppm to 100 ppm also did not affect the I_Q/ I_B ratio for all PAni (different polymerization temperatures) during sensor detection. The amount of benzenoid and quinoid structures along the PAni chain (different polymerization temperatures) are remain unchanged before and after immersion in chloroform due to no electron shifting between both quinoid and benzenoid structures. Thus, it significantly proved that the Bragg wavelength shift of PAni coated FBG sensor is contributed by the physical interaction between PAni and chloroform (without any chemical interaction). The physical interaction during sensor detection is caused by the interaction between $Cl^{\delta-}$ of chloroform and $NH^{\delta+}$ of PAni which called dipole-dipole interaction. (Li et al., 2009).

Table 4.4: The I_Q/I_B ratio of PAni 5: 5 (different polymerization temperatures) in different concentration of chloroform.

Concentration (ppm)	I_Q/I_B ratio					
	PAni -5 °C		PAni 0 °C		PAni 25 °C	
	Before	After	Before	After	Before	After
0	1.0036	1.0036	1.0048	1.0049	1.0023	1.0023
10	1.0035	1.0036	1.0053	1.0053	1.0027	1.0027
30	1.0036	1.0037	1.0062	1.0062	1.0028	1.0028
50	1.0037	1.0038	1.0062	1.0062	1.0028	1.0029
70	1.0040	1.0041	1.0078	1.0078	1.0029	1.0029
100	1.0042	1.0042	1.0084	1.0084	1.0029	1.0029

University of Malaya

4.3.3.3 Conductivity Measurement

As discussed earlier, the σ_f/σ_i of PAni 5: 5 (different polymerization temperatures) after immersion in chloroform solution that determined by using Equation 4.3 are shown in Figure 4.25. Theoretically, the σ_f/σ_i ratio of PAni would be increased by further increasing in the concentration of chloroform. However, in this study, the σ_f/σ_i ratio of PAni is contradicted with the FTIR and UV-Vis analysis in Figure 4.23 and Figure 4.24.

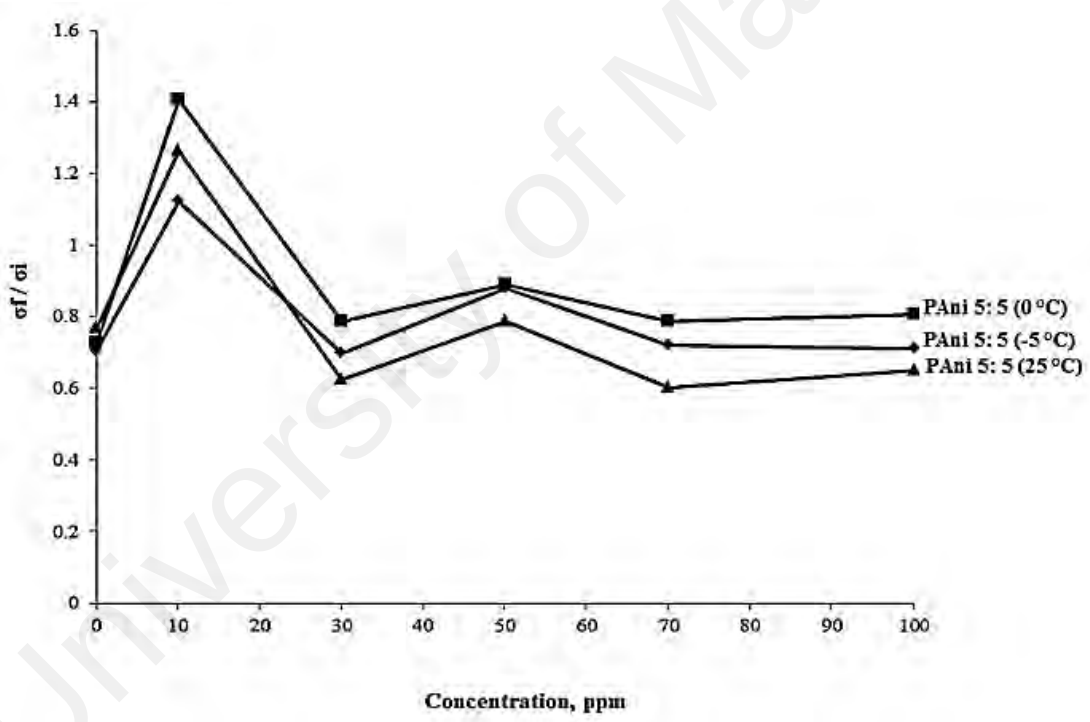

Figure 4.25: The σ_f/σ_i ratio of PAni 5: 5 (different polymerization temperatures) after immersion in different concentration of chloroform.

The σ_f/σ_i ratio of PAni (different polymerization temperatures) significantly increased at the initial state (0-10 ppm) because the acidity of chloroform (weak acid) significantly increased the acidity of PAni in ES state and achieved a maximum σ_f/σ_i

University of Malaya

ratio at 10 ppm due to the saturation of chloroform at the NH^+ reactive sites on PAni. However, the σ_f/σ_i ratio was significantly decreased above 10 ppm of chloroform due to the overlapping layer of chloroform (above the NH^+ reactive sites and first layer of chloroform) that would increase the hopping distance of the charge carrier, thus significantly reduced the $\sigma_f/\ \sigma_i$ ratio (Arenas et al., 2012).

Based on the result obtained, PAni 5: 5 (0 °C) showed the highest $\sigma_f/\ \sigma_i$ ratio compared to PAni 5: 5 (-5 °C) and PAni 5: 5 (25 °C) because the formation of longer polymer chain with more charge carrier and reactive site significantly enhances the interaction between the chloroform and PAni, thus increase the $\sigma_f/\ \sigma_i$ ratio (Adams et al., 1997). Meanwhile, PAni 5: 5 (25 °C) showed the lowest $\sigma_f/\ \sigma_i$ ratio due to the formation of shorter polymer chain with branching that would significantly reduce the charge carrier and reactive sites (more defect sites that disturb the movement of charge carrier), finally reduced the interaction between chloroform and PAni. (Bhala et al, 2013). The UV-Vis, FTIR and conductivity analysis obtained in this part strongly support the Bragg wavelength shift in the optical sensor response (Section 4.3.2).

4.3.3.4 Proposed Mechanism for the Interaction between Chloroform and PAni (Different Polymerization Temperatures)

The results obtained from the UV-Vis, FTIR and conductivity measurements (Section 4.3.3.1, Section 4.3.3.2 and Section 4.3.3.3) significantly proved the ability of PAni coated FBG sensor in chloroform detection. In this study, the polymerization temperatures strongly affect the sensing properties of PAni coated FBG sensor.

University of Malaya

At low polymerization temperature (0 °C), PAni 5: 5 tends to produce longer polymer chain which able to extend the conjugation of polaron. Similarly, it will also provide more free charge carriers and NH^+ reactive sites along the PAni chains. This condition significantly enhanced the interaction between the $Cl^{\delta-}$ of chloroform and $NH^{\delta+}$ on PAni, hence improve the sensitivity of PAni 5: 5 (0 °C) coated FBG sensor in chloroform detection (Adams et al., 1997).

Further decrease on polymerization temperature to sub-zero temperature (-5 °C) produced the longest PAni chain with more charge carriers and NH^+ reactive sites. However, the addition of LiCl during polymerization has adversely affected the PAni structure due to the formation of barriers that block the interaction between the $NH^{\delta+}$ on PAni and $Cl^{\delta-}$ of chloroform, thus decreased the sensitivity of of PAni 5: 5 (-5 °C) coated FBG sensor in chloroform detection (Adams et al., 1996).

Oppositely, at high polymerization temperatures (25 °C), PAni 5: 5 produced shorter PAni chain with many defect sites and less polaron that may block the movement of charge carrier and reduce the interaction between the $Cl^{\delta-}$ of chloroform molecules and $NH^{\delta+}$ on PAni chains. This condition leads decreasing in the sensitivity of of PAni 5: 5 (25 °C) coated FBG sensor in chloroform detection (Bhala et al., 2013). The proposed mechanisms for the interaction between chloroform and PAni (different polymerization temperatures) are shown in Figure 4.26.

University of Malaya

a) PAni 5: 5 (0 °C)

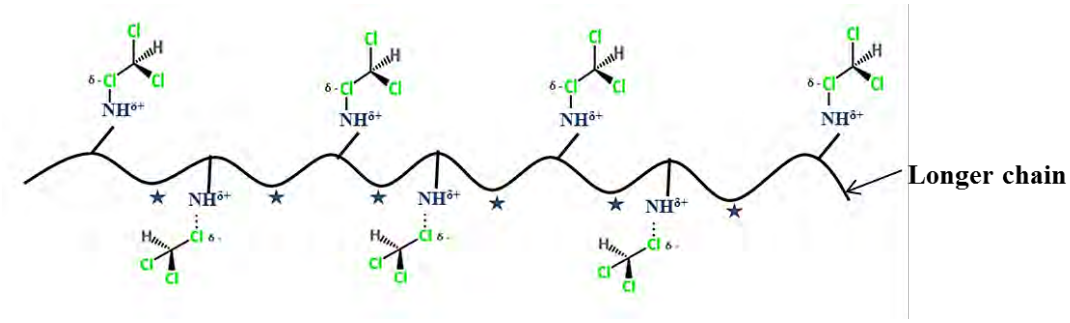

b) PAni 5: 5 (-5 °C)

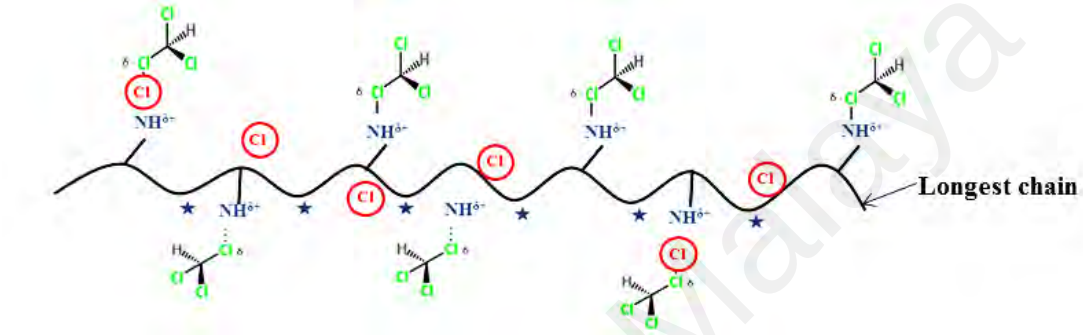

c) PAni 5: 5 (25 °C)

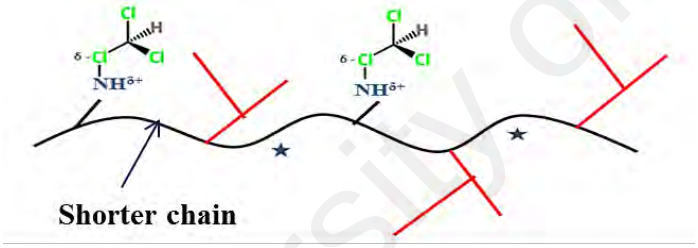

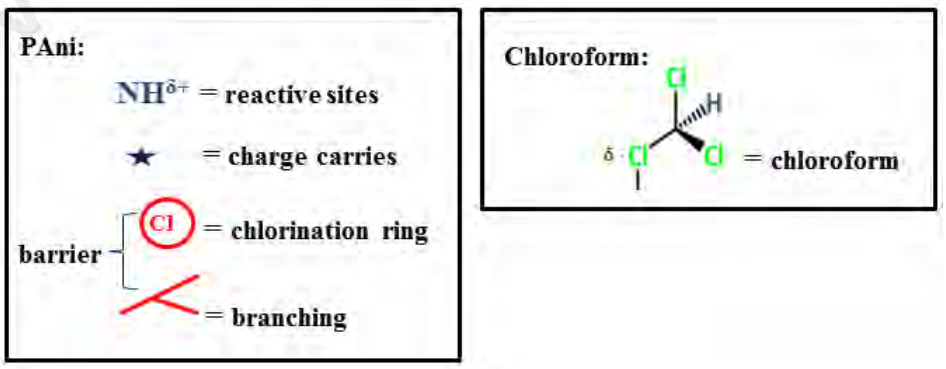

Figure 4.26: Proposed mechanisms for the interaction between chloroform and PAni (different polymerization temperatures) during sensor detection.

University of Malaya

4.4 Sensor performance for PAni 5: 5 (0 °C) coated FBG for Chloroform Detection

In this research study, different types of PAni were synthesized using different synthesis parameters such as different dopant ratios (ratio Ani: AOT= 5: 3, 5: 5 and 5: 7) and different polymerization temperatures (-5 °C, 0 °C and 25 °C). All these PAni were then coated onto FBG and applied as an optical sensor for chloroform detection.

Among all PAni obtained, PAni 5: 5 (0°C) coated FBG sensor possessed the highest sensitivity (0.0015) in chloroform detection from 10 ppm to 100 ppm. Hence, the sensor performance of PAni 5: 5 (0 °C) in chloroform detection will be studied in more details in terms of the recyclability, selectivity, accuracy, limit of detection (LOD) and limit of quantitation (LOQ) in the following part.

4.4.1 Recyclability Study

As shown in Figure 4.27, recyclability test has been carried out on sensor detection of PAni 5: 5 (0 °C) coated FBG in 50 ppm of chloroform solution (Figure 4.27 (i)), followed by removal of chloroform using distilled water and dried before reuse the sensor (Figure 4.27 (ii)). Application of 50 ppm of chloroform solution on PAni 5: 5 (0 °C) coated FBG sensor, followed by removal of chloroform using distilled water is considered as “one cycle”. The application of PAni coated FBG sensor towards 50 ppm of chloroform solution was repeated up to 10 cycles.

Based on the result obtained, the Bragg wavelength shift of PAni 5: 5 (0 °C) coated FBG sensor before and after immersion in chloroform solution (50 ppm) showed similar trends from 1st to 10th cycle. During 1st cycle, the Bragg wavelength shift of

University of Malaya

PAni 5: 5 (0 °C) coated FBG sensor before and after immersion in chloroform solution possessed a value of 1557.2 nm and 1557.4 nm, respectively. Before reimmersed in chloroform solution, the virgin PAni (after washed with distilled water) was shifted back to 1557.2 nm (initial wavelength) due to the dissociation of chloroform from the PAni surface. After reimmersed in chloroform solution, the Bragg wavelength of PAni 5: 5 (0 °C) was shifted to 1557.5 nm again. Since the Bragg wavelength shift for each cycle is small and almost similar, thus the recyclability result in this study is reliable.

As shown in Figure 4.27, PAni 5: 5 (0 °C) coated FBG sensor showed good recyclability up to at least 10 cycles in chloroform detection. Based on the proposed mechanism, the interaction between PAni and chloroform is the weak dipole-dipole interaction between the partial negative charge ($Cl^{\delta-}$) of chloroform and the partial positive charge ($NH^{\delta+}$) of PAni. During the recyclability test, chloroform is easily removed by using distilled water due to the weak physical interaction between $Cl^{\delta-}$ of chloroform and $NH^{\delta+}$ of PAni.

University of Malaya

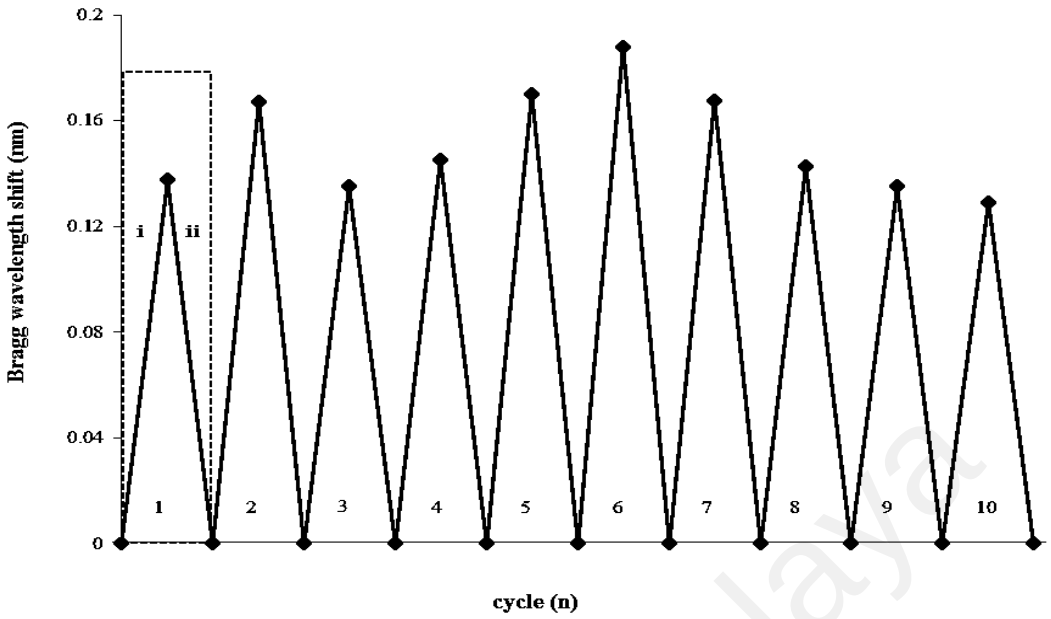

Figure 4.27: Recyclability of PAni 5: 5 (0 °C) coated FBG sensor in chloroform (50 ppm) detection. [(i) Chloroform detection (ii) Remove chloroform with distilled water and dried].

4.4.2 Selectivity Study

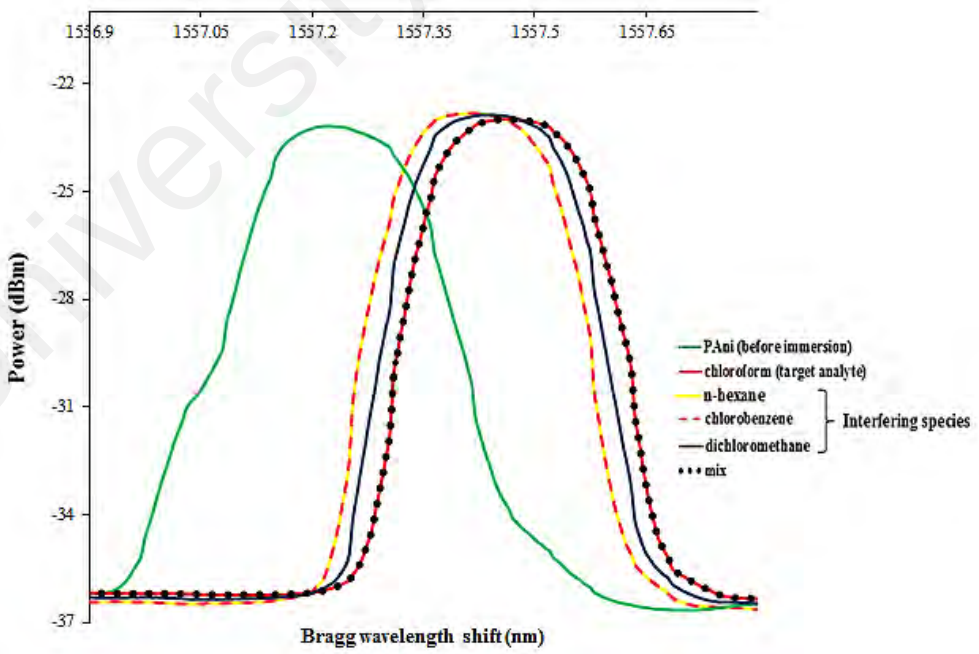

Figure 4.28: Bragg wavelength shift (~1557 nm) of PAni 5:5 (0 °C) coated FBG sensor in different analyte solutions.

University of Malaya

Another important study of method validation in sensor performance is the selectivity study (or interference study). In principal, the interference study is focused on the ability of optical sensor to distinguish the target analyte from the presence of other analytes in the sensor system. In this part, the interference study of PAni 5: 5 (0 °C) coated FBG sensor (as optical sensor) in chloroform (as target analyte) detection was carried out in the presence of n-hexane (n-C_6H_{14}), chlorobenzene and dichloromethane (CH_2Cl_2) as interference species. As mentioned previously, chloroform is a weak acid and weak reducing agent, thus these properties have been used as guideline to choose the interfering species used in this study.

Figure 4.28 shows the Bragg wavelength shift of PAni coated FBG sensor before and after immersion in chloroform, dichloromethane, chlorobenzene, n-hexane and the combination all interfering species with chloroform. In general, PAni 5: 5 (0 °C) coated FBG sensor showed similar Bragg wavelength shift pattern to a higher wavelength (red shift) in all interfering species and target analyte. Compare to other interfering species, the Bragg wavelength of PAni 5: 5 (0°C) coated FBG sensor was shifted from ~1557.2 nm to the highest wavelength (~1557.5 nm) after immersion in chloroform solution due to the physical interaction between $Cl^{\delta-}$ of chloroform and $NH^{\delta+}$ of PAni.

Among all interfering species, n-C_6H_{14} and chlorobenzene possessed the lowest Bragg wavelength shift due to their weak reducing agent property. Meanwhile, CH_2Cl_2 showed a lower Bragg wavelength shift (near to wavelength shift of target analyte) due to its similar weak reducing agent and weak acid properties with chloroform. Finally, immersion of PAni 5: 5 (0 °C) coated FBG sensor in all analytes (mixture of interfering species and target analyte) in sensing environment exhibited a similar Bragg wavelength shift to chloroform detection (target analyte). Therefore, PAni 5: 5 (0 °C) coated FBG

University of Malaya

sensor showed good selectivity in chloroform detection in the present of other interfering species.

4.4.3 Method of Validation

Figure 4.29 shows the calibration curve for PAni 5: 5 (0 °C) coated FBG sensor in different concentration of chloroform solution (10-100 ppm). Based on the calibration curve obtained, the Bragg wavelength shift of PAni 5: 5 (0 °C) coated FBG sensor increased significantly with the increasing of chloroform concentration. The sensitivity of PAni coated FBG sensor is 0.0015 (gradient of the slope) with correlation coefficient (R^2) of 0.9988. The accuracy of this sensor is about 104 ± 6 that was calculated based on Equation 4.4.

The limit of detection (LOD) and limit of quantitation (LOQ) of chloroform is calculated based on Equation 4.6 and Equation 4.7. This sensor possesses a LOD of 9.22 ppm which is lower than the LOD of chloroform set by the Occupational Safety and Health Administration (50 ppm) (Pradip & Arup, 2013). Besides, the LOQ of this sensor is about 27.9 ppm. Based the calibration curve obtained, PAni 5: 5 (0 °C) showed good optical sensor performance in chloroform detection with linear range (LR) from 10 ppm to 100 ppm of chloroform.

Accuracy = mean ± SD Equation 4.4

$$\text{Standard deviation (SD)} = \sqrt{\frac{\sum(X-X'')^2}{N}} \quad \text{Equation 4.5}$$

University of Malaya

$$\text{Limit of detection} = 3.3 \text{ x } \frac{SD}{S} \quad \text{Equation 4.6}$$

$$\text{Limit of quantitation} = 10 \text{ x } \frac{SD}{S} \quad \text{Equation 4.7}$$

where; SD = standard deviation

S = the slope of calibration curve

$\sum$ = the sum of

X = each value in the data set

N = number of values in the data set

X" = mean of all values in the data set

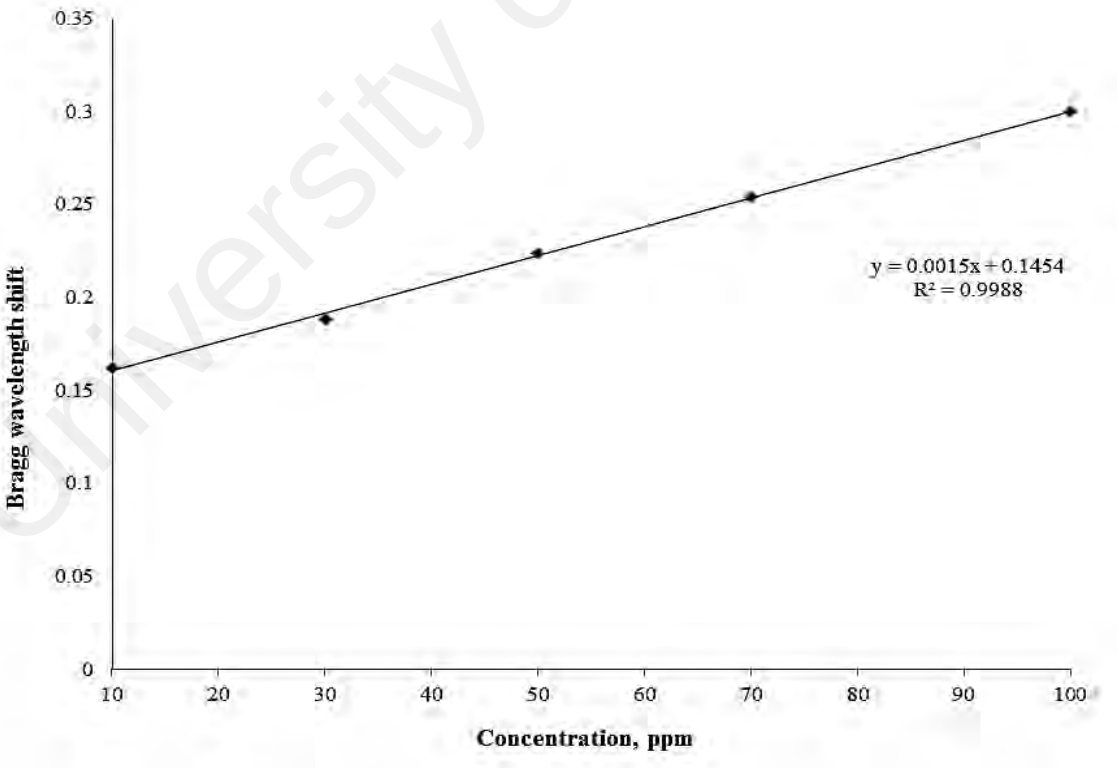

Figure 4.29: Calibration curve for PAni 5: 5 (0 °C) coated FBG sensor with LR of 10 ppm to 100 ppm.

University of Malaya

The comparison between PAni 5: 5 (0 °C) coated FBG sensor and other conventional methods (from previous research studies) for chloroform detection are notable in Table 4.5. PAni coated FBG sensor showed the lowest LOD of 9.22 ppm compared to other research studies that give a higher LOD of 95.7–100 ppm. Besides, PAni coated FBG sensor also possessed a lower and broader LR from 10–100 ppm compared to DPPTP sensor (100–800 ppm) and MWCNT/PAni sensor (50–250 ppm). As summary, PAni coated FBG sensor with a lower and broader LR will significantly broaden the application of this optical sensor in various field.

Table 4.5: Comparison of LR and LOD for different conventional method in chloroform detection.

Method for chloroform detection	LR (ppm)	LOD (ppm)	References
1,2,4,5- tetraphenyl-1, 4-dihydropyrrolo[3,2-b] pyrrole (DPPTP)	100- 800	95.7	Peng et al., 2016
Carboxylic acid functionalized multi-walled carbon nanotube doped PAni (MWCNT/ PAni)	50- 250	-	Kar and Choudhury, 2013.
Copper/ PAni	10- 100	<100	Sharma et al., 2002
PAni coated FBG sensor	10- 100	9.22	Present work

LR = Linear range

LOD = Limit of detection

University of Malaya

4.4.4 Real Sample Analysis

In this study, the application of the proposed PAni 5: 5 (0 °C) coated FBG sensor has been tested on the real samples using the optical sensor setup. The real samples were collected from three sources. The first real sample is the tap water (Water 1) that collected from a Chemistry Laboratory at Department of Chemistry, University of Malaya. The second real sample (Water 2) was collected from the residential area (Vista Angkasa Apartment, Kuala Lumpur) and the last real sample (Water 3) is the drinking water obtained from reverse osmosis treatment (model; Jantzen). All types of water sample were filtered in order to remove any large trash before experiment.

First, the known concentration of chloroform was spiked into the different types of water sample (Water 1, Water 2 and Water 3) separately. The optical sensor response of PAni 5: 5 (0 °C) coated FBG sensor on the different types of water sample are repeated for three times (A1 – A3) in different concentrations of chloroform (30 ppm, 50 ppm and 70 ppm). The concentration of the chloroform in the different types of water sample (Water 1, Water 2, Water 3) were determined based on the Bragg wavelength shift of PAni 5: 5 (0 °C) coated FBG sensor (calibration curve) as shown in Figure 4.29. The recovery and relative standard deviation (RSD) of PAni 5: 5 (0 °C) coated FBG sensor were calculated using Equation 4.8 and Equation 4.9 and tabulated in Table 4.6, Table 4.7 and Table 4.8.

$$\text{Recovery} = \frac{\text{Amount of chloroform determined}}{\text{Amount of chloroform spiked}} \times 100\% \qquad \text{Equation 4.8}$$

$$\text{RSD} = \left(\frac{\text{SD}}{\text{means}}\right) \times 100\% \qquad \text{Equation 4.9}$$

University of Malaya

According to Fuentes and Simmons, the percentage of RSD value is ≤ 20% indicates the acceptable precision data, while the percentage of RSD value is ≤ 10% represents the excellent precision data (Fuentes & Simmons, 1991). The excellent precision is generally shows the percent recovery in the range of 86 – 107% (Pellizzari & Clayton, 2005). In this study, PAni 5: 5 (0 °C) coated FBG sensor showed high recovery range of 96 – 103.9% and good RSD range of 0.70 – 7.26% in real samples (Water 1, Water 2 and Water 3).

Table 4.6: Spiked, determined concentration, recovery and RSD values of PAni 5: 5 (0 °C) coated FBG sensor in Water 1 during chloroform detection.

Spiked (ppm)	Determined concentration (ppm)			Means	Recovery (%)	RSD (%)
	A1	A2	A3			
30	31	33	29.5	31.2	103.9	7.26
50	50	52	49.5	50.5	101	2.89
70	71.5	70	69.9	70.5	100.7	1.51

Table 4.7: Spiked, determined concentration, recovery and RSD values of PAni 5: 5 (0 °C) coated FBG sensor in Water 2 during chloroform detection.

Spiked (ppm)	Determined concentration (ppm)			Means	Recovery (%)	RSD (%)
	A1	A2	A3			
30	31	33	29.5	31.2	103.9	7.26
50	49	48	47.3	48.1	96.2	5.15
70	68	70	67.4	68.5	97.8	3.37

University of Malaya

Table 4.8: Spiked, determined concentration, recovery and RSD values of PAni 5: 5 (0 °C) coated FBG sensor in Water 3 during chloroform detection.

Spiked (ppm)	Determined concentration (ppm)			Means	Recovery (%)	RSD (%)
	A1	A2	A3			
30	29	27.5	30	28.8	96	4.37
50	49	48	47.3	48.1	96.2	5.15
70	68	70	67.4	68.5	97.8	3.37

4.5 Summary of PAni Coated FBG Sensors

In the initial part, PAni was used as the modified cladding on the FBG sensor for organic compounds detection. The summary of PAni coated FBG sensors in organic compounds detection (1-propanol, 2-propanol, ethylenediamine, chloroform, dichloromethane, dimethyl sulphide and dimethyl disulphide) are tabulated in Table 4.9. The most sensitive analyte that possessed the highest Bragg wavelength shift (0.095 nm) on the PAni coated FBG sensor is chloroform. Thus, further studies in the application of PAni coated FBG sensor is focusing on chloroform detection.

University of Malaya

Table 4.9: Bragg wavelength shift (~1557 nm) of PAni 5:5 coated FBG sensor in different organic compounds solution.

Organic compounds	Bragg wavelength shift, nm
1- propanol	0.005
2- propanol	0.003
Chloroform	0.095
Dichloromethane	0.087
Dimethyl sulfide	0.084
Dimethyl disulfide	0.085
Ethylenediamine	0.002

In general, the sensitivity of PAni coated FBG sensor is significantly affected by the synthesis parameter of PAni. Table 4.10 shows the summary of PAni (different dopant ratios) coated FBG sensor in chloroform detection. Among all PAnis, PAni 5: 5 performed the best sensitivity in chloroform detection (0.0015) due to the formation of more NH^+ reactive sites along the PAni chains eventually enhances the interaction between chloroform and PAni.

Table 4.10: PAni (different dopant ratios) coated FBG sensor for chloroform detection.

PAni	Sensitivity	Sensor performance	Description
5: 3	0.0009	Moderate	Moderate NH^+ reactive sites
5: 5	0.0015	Best	High NH^+ reactive sites
5: 7	0.0008	Poor	Less NH^+ reactive sites

University of Malaya

PAni 5: 5 has been chosen for the next synthesis parameter with different polymerization temperatures as shown in Table 4.11. Among all PAnis, PAni 5: 5 (0 °C) coated FBG sensor possessed the higher sensitivity (0.0015) in chloroform detection due to the formation of longer PAni chains with more charge carriers and -NH^+ reactive sites that eventually enhanced the interaction between PAni and chloroform. Although, PAni 5: 5 (-5 °C) coated FBG sensor produce the longest PAni chains but addition of LiCl significantly created ring chlorination and barriers that block interaction between chloroform and PAni, thus reduced the sensitivity (0.0007).

Table 4.11: PAni 5: 5 (different polymerization temperatures) coated FBG sensor for chloroform detection.

PAni	Sensitivity	Sensor performance	Description
-5 °C	0.0007	Moderate	Longest polymer chain with the presence of ring chlorination
0 °C	0.0015	Best	Longer polymer chain with more reactive sites and charge carrier
25 °C	0.0004	Poor	Short polymer chain with barrier and defect sites

Among all PAnis, PAni 5: 5 (0°C) coated FBG sensor possessed the highest sensitivity (0.0015) in chloroform detection, hence, the sensor performance of PAni 5: 5 (0 °C) will be studied in more details. This sensor showed good recyclability up to 10 cycle with fast response time (7 s) and recovery time (8 s). In addition, this sensor possessed a lower LOD of 9.22 ppm and LOQ of 27.9. Based on the interference study,

University of Malaya

this sensor significantly showed good selectivity in chloroform detection in the present of other interfering species. Furthermore, this sensor showed high recovery range of 96 – 103.9% and good RSD range of 0.70 – 7.26% in real samples analysis (Water 1, Water 2 and Water 3).

Besides, FTIR, UV-Vis and conductivity analysis (supporting data) significantly suggested that the proposed mechanism for the interaction between PAni and chloroform is the dipole-dipole interaction (physical interaction) between $Cl^{\delta-}$ of chloroform and $NH^{\delta+}$ of PAni.

University of Malaya

CHAPTER 5: CONCLUSION AND SUGGESTIONS FOR FUTURE WORKS

5.1 Conclusion

In this study, PAni has been used as a coating material on FBG sensor for organic compounds detection. PAni was successfully synthesized through chemical oxidation by different synthesis parameter such as different dopant ratios (Ani: AOT= 5: 3, 5: 5 and 5: 7) and different polymerization temperatures (-5 °C, 0 °C and 25 °C). FTIR and UV-Vis spectra have confirmed the chemical structures of PAni, while the conductivity study showed all PAnis obtained are in ES state (conducting state).

At the initial stage, PAni 5: 5 (0°C) coated FBG sensor has been applied in different organic compounds detection (1-propanol, 2-propanol, ethylenediamine, chloroform, dichloromethane, dimethyl sulphide and dimethyl disulphide). Since the highest Bragg wavelength shift (0.095 nm) for PAni 5: 5 (0°C) coated FBG sensor is chloroform, hence, the application of PAni (different synthesis parameters) coated on FBG sensor is focused on the chloroform detection.

PAni 5: 5 (0°C) coated FBG sensor possessed the highest sensitivity (0.0015) in chloroform detection due to the longer polymer chain length with more NH^+ reactive sites and charge carriers that enhances the interaction between $Cl^{\delta-}$ of chloroform and $NH^{\delta+}$ of PAni. The sensor performance of PAni 5: 5 (0°C) coated FBG sensor in chloroform detection has been studied in more details includes the recyclability, selectivity and real sample analysis.

PAni 5: 5 (0°C) coated FBG sensor shows good recyclability up to at least 10 cycle with short respond time (7 s) and recovery time (8 s) in chloroform detection. This

University of Malaya

sensor also showed good selectivity in chloroform detection in the present of other interfering analytes. The accuracy of this sensor is about 104 ± 6 with a linear range of 10 ppm to 100 ppm. This sensor possessed a lower LOD of 9.22 ppm (lower than Occupational Safety and Health Administration; 50 ppm) and a lower LOQ of 27.9 ppm.

Besides, PAni 5: 5 (0°C) coated FBG sensor was successfully applied in different types of water sample (water from the chemistry laboratory, the residential area and the drinking water from the reverse osmosis treatment) for chloroform detection with high recovery range of 96 – 103.9% and good RSD of 0.70 – 7.26%.

In conclusion, PAni 5: 5 (0 °C) coated FBG sensor is strongly recommended as a new optical sensor with a simple, inexpensive and effective set-up for chloroform detection due to its good recyclability (up to 10 cycle), fast response time (7 s), good sensitivity (0.0015) and lower LOD (9.22 ppm).

University of Malaya

5.2 Suggestion for Future Works

As discussed earlier, the synthesis parameter of PAni plays an important role in affecting the polymer structure and sensor performance. Therefore, this study can be further improve by modifying the chemical structure of PAni using other synthesis parameter such as different types of oxidant, different types of dopant, different oxidant and dopant ratio, different polymerization reaction times and etc.

According to Santiago and co-worker (2004), the thickness of polymer coating on the sensor can significantly improve the sensitivity, reproducibility and response times of the sensor. However, in this study, the thickness of PAni coated on FBG sensor for chloroform detection is fixed (~30 μm). Thus, for future investigation, manipulation of the thickness of PAni coating on FBG sensor might be a good parameter to be focused in order to improve the sensor performances.

As conclusion, modification of others synthesis parameters and modification of thickness for PAni coating that mentioned in this part are highly recommended to further improve the sensitivity of sensor in chloroform detection from ppm to ppb in order to broaden their application in various field.

University of Malaya

REFERENCES

Abd Razak, S. I., Wahab, I. F., Fadil, F., Dahli, F. N., Md Khudzari, A. Z. & Adeli, H. (2015). A Review of Electrospun Conductive Polyaniline Based Nanofiber Composites and Blends: Processing Features, Applications, and Future Directions. *Advances in Materials Science and Engineering,* 2015(35628), 1-19.

Adams, P. M., Abell, L., Middleton, A. & Monkman, A. P. (1997). Low Temperature Synthesis of High Molecular Weight Polyaniline using Dichromate Oxidant. *Synthetic Metals,* 84 (1–3), 61-62.

Adams, P.N., Laughlin, P.J. & Monkman, A. P. (1996). Synthesis of High Molecular Weight Polyaniline at Low Temperatures. *Synthetic Metals,* 76, 157-160.

Ahuja, D. & Parande, D. (2012). Optical Sensor and Their Applications. *Journal of Scientific Research and Reviews,* 1 (5), 60-68.

Ansari, R. & Keivani, M. B. (2006). Polyaniline Conducting Electroactive Polymers: Thermal and Environmental Stability Studies. *E-Journal of Chemistry,* 3 (4), 202-217.

Arasi, A.Y., Jeyakumari, J. J., Sundaresan, B., Dhanalakshmi, V. & Anbarasan, R. (2009). The Structural Properties of Poly(Aniline)--Analysis via FTIRSpectroscopy. *Spectrochimica Acta Part A: Molecular and Biomolecular Spectroscopy*, 74(5), 1229-34.

Arenas, M. C., Sánchez, G., Nicho, M. E., Elizalde- Torres, J. & Castáno, V. M. (2012). Engineered Doped and Codoped Polyaniline Gas Sensor Synthesized in N, N, Dimethylformamide Media. *Applied Physics A,* 106, 901-908.

Arsat, R., Yu, X. F., Li, Y. X., Wlodarski, W. & Kalantar-Zadeh, K. (2009). Hydrogen Gas Sensor Based on Highly Ordered Polyaniline Nanofibers. *Sensors and Actuators B: Chemical,* 137 (2), 529-532.

University of Malaya

Ashish, K., Arushi, S. & Jyoti, R. (2015). Fiber-Optical Sensing Communication. *International Journal of Innovative Research in Technology*, 1 (12), 2349-6002.

Atesa, M., Karazehira, T., & Sarac, A. S. (2012). Conducting Polymers and Their Applications. *Current Physical Chemistry,* 2, 224-240.

Ayad, M. M., El-Hefnawey, G. & Torad, N. L. (2008). Quartz Crystal Microbalance Sensor Coated with Polyaniline Emeraldine Base for Determination of Chlorinated Aliphatic Hydrocarbons. *Sensors and Actuators B: Chemical,* 134, 887.

Bai, H. & Shi, G. (2007). Gas Sensors Based on Conducting Polymers. *Sensors,* 7(3), 267-307.

Behera, S., Ghanty, S., Ahmad. F., Santra. S. & Banerjee, S. (2012). UV-Visible Spectrophotometric Method Development and Validation of Assay of Paracetamol Tablet Formulation. *Journal of Analytical and Bioanalytical Techniques,* 3 (151), 1-6.

Bhawani, A. S., Fong, S. S. & Mohamad Ibrahim, M. N. (2015). Review Article Spectrophotometric Analysis of Caffeine. *International Journal of Analytical Chemistry,* 2015 (170239), 1-7.

Bhadra, J., Al-Thani, N. J., Madi, N. K., & Al-Maadeed, M. A. (2017). Effects of Aniline Concentrations on the Electrical and Mechanical Properties of Polyaniline Polyvinyl Alcohol Blends. *Arabian Journal of Chemistry,* 10 (5), 664- 672.

Chiam, Y. S., Lim, K. S., Harun, S. W., Gan, S. N. & Phang, S. W. (2014). Conducting Polymer Coated Optical Microfiber Sensor for Alcohol Detection. *Sensors and Actuators A,* 205, 58–62.

Chen, J., Liu, B. & Zhang, H. (2011). Review of Fiber Bragg Grating Sensor Technology. *Frontiers of Optoelectronics in China,* 4(2), 204-212.

Chutia, P., Nath, C. & Kumar, A. (2014). Dopant Size Dependent Variable Range Hopping Conduction in Polyaniline Nanorods. *Applied Physics A,* 115, 943–951.

University of Malaya

Correia, S. F. H., Antunes, P., Pecoraro , E., Lima, P. P., Varum, H., Carlos, L. D., Ferreira , Rute A. S. & André, P. S. (2012). Optical Fiber Relative Humidity Sensor Based on a FBG with a Di-Ureasil Coating. *Sensors,* 12, 8847-8860.

Devi, M. R., Lawrence, B., Prithivikumaran, N. & Jeyakumaran, N. (2014). Synthesis and Characterization of Conducting Polymer Polyaniline Doped with Salicylic Acid. *International Journal of Chemtech Research,* 6 (13), 5400-5403.

Dubey, N. & Leclerc, M. (2011). Conducting Polymers: Efficient Thermoelectric Materials. *Journal of Polymer Science Part B: Polymer Physics*, 49 (7), 467-475.

El-Sherif, M., Bansal, L. & Yuan, J. (2007). Review Fiber Optic Sensors for Detection of Toxic and Biological Threats. *Sensors,* 7, 3100-3118.

Flory, P. J. (1974). Review the Challenge to Macromolecular Science. *Angewandte International Edition,* 13 (2), 97-98.

Focke, W.W., Wnek, G. E. & Wei, Y. (1987). Influence of Oxidation State, pH and Counterion on The Conductivity of Polyaniline. *The Journal of Physical Chemistry,* 91 (22), 5813–5818.

Fuentes, A. & Simmons, M. S. (1991). Sampling and Analysis of Hazardous Wastes to Toxic Pollutants. In: Simmons MS, (Ed.) *Hazardous waste measurements*. 17-34. Chelsea, Michigan: Lewis Publishers, Inc.

Ghetia, S., Gajjar, R. & Trivedi, P. (2013). Classification of Fiber Optical Sensors. *International Journal of Electronics Communication and Computer Technology,* 3 (4), 442-445.

Ghosh, C., Alfred, Q. M. & Ghosh, B. (2015). Analysis of Wavelength Shift in FBG on External Perturbation. *International Journal of Electronics and Communication Engineering*, 4(4), 1-8.

Gospodinova, N. & Terlemezyan, L. (1998). Conducting Polymers Prepared by Oxidative Polymerization: Polyaniline. *Progress Polymer Science,* 23, 1443–1484.

University of Malaya

Harun, S.W., Lim, K. S., Damanhuri, S. S. A. & Ahmad, H. (2011). Microfiber Loop Resonator Based Temperature Sensor. *Journal of the European Optical Society – Rapid Publications,* 6, 11026.

Hawaldar, R., Kulkarni, M., Jadkar, S., Pal, U. & Amalnerkar, D. (2009). Synthesis and Characterization of Polyaniline- Crooked Gold Nanocomposite with Reduced Conductivity. *Journal of Nano Research,* 5, 79-85.

Heeger, A. J. (2001). Semiconducting and Metallic Polymers: The Fourth Generation of Polymeric Materials (Nobel Lecture). *Angewandte International Edition,* 40 (14), 2591-2611.

Heeger, A. J., Macdiarmid, A. G. & Shirakawa, H. (2002). Macromolecules. *American Chemical Society,* 35 (4), 1137-1139.

Hill, K. O. & Meltz, G. (1997). Fiber Bragg Grating Technology Fundamentals and Overview. *Journal of Lightwave Technology,* 15 (8), 1263-1276.

Idumah, C. I. & Hassan, A. (2016). Emerging Trends in Graphene Carbon Based Polymer Nanocomposites and Applications. *Reviews in Chemical Engineering,* 32 (2), 223–264.

Jawad, I. A. M., Al-Hamdani, A. A. & Hasan, R. M. A. (2016). Fourier Transform Infrared (FT-IR) Spectroscopy of Modified Heat Cured Acrylic Resin Denture Base Material. *International Journal of Enhanced Research in Science, Technology & Engineering,* 5 (4), 130-140.

Kao, K. C. & Hockham, G. A. (1996). Dielectric-Fibre Surface Waveguides for Optical Frequencies. *1EE Proceeding Journal of Optoelectronic,* 113 (3), 1151-1158.

Kapil, A., Taunk, M. & Chand, S. (2010). Preparation and Charge Transport Studies of Chemically Synthesized Polyaniline. *Journal of Materials Science: Materials in Electronics,* 21, 399–404.

Kar, P. & Choudhury, A. (2013). Electrical and Dielectric Properties of Polyaniline Doped with Carboxyl-Functionalized Multiwalled Carbon Nanotube. *Advances in Polymer Technology,* 32(1), 760-770.

University of Malaya

Kawase, M. (1998). Simple Structure Optical Fiber Cables Manufactured Without Stranding Processes. *Journal of Lightwave Technology,* 6(8), 1280-1284.

Kim, S., Seong, J. & OH, K. (2002). Effect of Dopant Mixture on the Conductivity and Thermal Stability of Polyaniline/Nomex Conductive Fabric. *Applied Polymer,* 83 (10), 2245-2254

Kint, D. P. R. & Munoz-Guerra, S. (2003). Review Modification of Thermal Properties and Crystallization Behaviour of Poly (Ethylene Terephthalate) by Copolymerization. *Polymer International,* 52, 321-336.

Kinyanjui, J. M., Wijeratne, N. R., Hanks, J. & Hatchett, D. W. (2006). Chemical and Electrochemical Synthesis of Polyaniline/Platinum Composites. *Electrochimica Acta,* 51, 2825–2835.

Kotlarchyk, M., Huang, J. S. & Chen, S. H. (1985). Structure of AOT Reversed Micelles Determined by Small-Angle Neutron Scattering. *The Journal of Physical Chemistry,* 89 (20), 4382–4386.

Kumirska, J., Czerwicka, M., Kaczyński, Z., Bychowska, A., Brzozowski, K., Thöming, J. & Stepnowski, P. (2010). Application of Spectroscopic Methods for Structural Analysis of Chitin and Chitosan. *Marine Drugs,* 8(5), 1567–1636.

Li, M. & Nolan, D. A. (2008). Optical Transmission Fiber Design Evolution. *Journal of Lightwave Technology,* 26(9), 1079-1092.

Li, X., Kang, Y. & Huang, M. (2006). Optimization of Polymerization Conditions of Furan with Aniline for Variable Conducting Polymers. *Journal of Combinatorial Chemistry,* 8, 670-678.

Luo, J., Shen, P., Yao, W., Jiang, C. & Xu, J. (2016). Synthesis, Characterization, and Microwave Absorption Properties of Reduced Graphene Oxide/Strontium Ferrite/Polyaniline Nanocomposites. *Nanoscale Research Letters,* 11, 141.

Madejová, J. (2003). FTIR Techniques in Clay Mineral Studies. *Vibrational Spectroscopy,* 31 (1), 1-10.

University of Malaya

Magnuson, M., Guo, J. H., Butorin, S. M., Agui, A. & Såthe, C. (1999). The Electronic Structure of Polyaniline and Doped Phases Studied by Soft X-Ray Absorption and Emission Spectroscopies. *Journal of Chemical Physics,* 111, 4756.

Mekki, A., Mettai, B., Ihdene, Z., Mahmoud, R. & Mekhalif, Z. (2013). VOCs Vapour Sensor Based on Polyaniline Salts Films and Quartz Crystal Microbalance. *AMA Conferences 2013 - Sensor 2013,* 709-712.

Miccoli,B., Cauda, V., Bonanno, A., Sanginario, A., Bejtka, K., Bella, F., Fontana, M. & Demarchi, M. (2016). One-Dimensional Zno/Gold Junction for Simultaneous and Versatile Multisensing Measurements. *Scientific Reports,* 6 (26763), 1-10.

Molapo, K. M., Ndangili, P. M., Ajayi, R. F., Mbambisa, G., Mailu, S. M., Njomo, N., Masikini, M., Baker, P. & Iwuoha, E. I. (2012). Review Paper Electronics of Conjugated Polymers (I): Polyaniline. *International Journal of Electrochemical Science,* 7, 11859 – 1187.

Mukherjee, G. S. (2014). Staudinger's Concept on Polymer Science and the Impact of Ziegler-Natta Catalyst on Polymer Technology. *Defence Science Journal,* 64 (3), 191-192.

Nadagouda, M. N. & Varma, R. S. (2007). Green Approach to Bulk and Template-Free Synthesis of Thermally Stable Reduced Polyaniline Nanofibers for Capacitor Applications. *Green Chemistry,* 9, 632-637.

Okan, A. & Qinguo, F. (2009). Applications of Conducting Polymers in Electronic Textiles. *Research Journal of Textile and Apparel,* 13 (4), 51-68.

Omastova, M., Chodak, I. & Pionteck, J. (1999). Electrical and Mechanical Properties of Conducting Polymer Composites. *Synthetic Metal,* 102(1-3), 1251-1252.

Pellizzari, E. D. & Clayton, C. A. (2005). Assessing the Measurement Precision of Various Arsenic Forms and Arsenic Exposure in the National Human Exposure Assessment Survey (Nhexas). *Environmental Health Perspect,* 114(2), 220–227.

Peng, Z., Feng, X., Tong, B., Chen, D., Shi, J., Zhi, J. & Dong, Y. (2016). The Selective Detection of Chloroform using an Organic Molecule with Aggregation-Induced

University of Malaya

Emission Properties in the Solid State as a Fluorescent Sensor. *Sensors and Actuators B: Chemical,* 232, 246-268.

Purchase, K. G., Brady, B. J., Roh, S. D., Lammert, R. M., Osowski, M. L. & Coleman, J. J. (1999). The Distributed Bragg Pulse Shaper: Demonstration and Model. *Journal of Lightwave Technology,* 17 (4), 621 – 628.

Ramachandran, R., Mani ,V., Chen,S., Gnana Kumar, G.P., Gajendran, P., Devi,N. B. & Devasenathipathy, R. (2015). Review Recent Progress in Electrode Fabrication Materials and Various Insights in Solar Cells. *International Journal of Electrochemical Science,* 10, 3301 – 3318.

Rao, Y., Deng, M., Duan, D., Yang, X., Zhu, T. & Cheng, G. (2007). Micro Fabry-Perot Interferometers in Silica Fibers Machined by Femtosecond Laser. *Optics Express,* 15 (21), 14123-14128.

Sambasevam, K. P., Mohamad, S. & Phang, S-W. (2014). Enhancement of Polyaniline Properties by Different Polymerization Temperatures in Hydrazine Detection. *Journal of Applied Polymer Science,* 132 (13), 41746-41753.

Santiago, E. V., Lopez, H. S., Escobar, C. H., Contreras, A. Z. & Farias, J. R. (2014), Thickness Effect on the Solvent Sensing Parameter of Carbon Black-Polymer Composites. *Procedia Engineering,* 87, 184-187.

Sapurina, I. & Stejskal, J. (2008). The Mechanism of the Oxidative Polymerization of Aniline and the Formation of Supramolecular Polyaniline Structures. *Polymer International,* 57(12), 1295–1325.

Schmidt, A., Karas, M. & Dülcks, T. (2003). Effect of Different Solution Flow Rates on Analyte Ion Signals in Nano-ESI MS, or: When does ESI turn into nano-ESI? *Journal of the American Society for Mass Spectrometry,* 14 (5), 492-500.

Shao, W., Jamal, R., Xu, F., Ubul, A. & Abdiryim, T. (2012). The Effect of a Small Amount of Water on the Structure and Electrochemical Properties of Solid-State Synthesized Polyaniline. *Materials,* 5, 1811-1825.

University of Malaya

Sharma, S., Nirkhe, C., Pethkar, S. & Athawale, A. A. (2002). Chloroform Vapour Sensor Based On Copper/ Polyaniline Nanocomposites. *Sensors and Actuators B: Chemical,* 85, 131-136.

Singh, B., Kumar, S., Basu, B. & Gupta, R. (2015). Conductivity Studies of Silver-, Potassium-, and Magnesium-Doped Hydroxyapatite. *Applied Ceramis Tecnology,* 12 (2), 319-328.

Song, E & Choi, J-W. (2013). Conducting Polyaniline Nanowire and Its Applications in Chemiresistive Sensing. *Nanomaterials,* 3(3), 498-523.

Stejskal, J., Kratochvíl, P. & Radhakrishnan, N. (1993). Polyaniline Dispersions 2. UV-Vis Absorption Spectra. *Synthetic Metals,* 61 (3), 225-231.

Sun, W., Wang, L., Wu, T., Pan, Y. & Liu, G. (2014). Synthesis of Low-Electrical-Conductivity Graphene/Pernigraniline Composites and Their Application in Corrosion Protection. *Carbon,* 79, 605 – 614.

Teja, N.R., Babu, M. A., Prasad, T. R. S. & Ravi, T. (2012). Different Types of Dispersions in an Optical Fiber. *International Journal of Scientific and Research Publications,* 2 (12), 1-5.

Tran, H. D., D'Arcy, J. M., Wang, Y., Beltramo, P. J., Strong, V. A. & Kaner, R. B. (2011). The Oxidation of Aniline to Produce "Polyaniline": A Process Yielding Many Different Nanoscale Structures. *Journal of Materials Chemistry,* 21, 3534-3550.

Wolfrum, E. J., Meglen, R. M., Peterson, D. & Sluiter, J. (2006). Metal Oxide Sensor Arrays for the Detection Differentiation and Quantification of Volatile Organic Compounds at Sub-Parts-Per-Million Concentration Levels. *Sensors and Actuators B: Chemical,* 115 (1), 322-329.

Xiaolin, Z., Zongyi, Q., Xin, L., Banglei L., Na L., & Meifang Z. (2013). Flexible Sensing Fibers Based On Polyaniline-Coated Polyurethane For Chloroform Vapor Detection. *Journal of Materials Chemistry A,* 1, 10327-10333.

Yang, T., Qiao, X., Rong, Q. & Bao, W. (2016). Orientation-Dependent Displacement Sensor Using an Inner Cladding Fiber Bragg Grating. *Sensors,* 16, 1473-1479.

University of Malaya

Yin, W. & Ruckenstein, E.(2000). Water-soluble Self Doped Conducting Polyaniline Copolymer. *Macromolecules,* 33(4), 1129-1131.

Ying, Q. & Krishnan, A. (2010). Source Contributions of Volatile Organic Compounds to Ozone Formation in Southeast Texas. *Journal of Geophysical Research,* 115 (D17306), 1-14.

Zaarei, D., Sarabi, A. A., Sharif, F., Gudarzi, M. M. & Kassiriha, S. M. (2012). A New Approach to Using Submicron Emeraldine-Base Polyaniline in Corrosion-Resistant Epoxy Coatings. *Journal of Coatings Technology and Research,* 9 (1), 47–57.

Zamani, S. (2013). Measurement of Pesticides using Ultraviolet Visible Spectrometer. *European Journal of Experimental Biology,* 3(1), 608-616.

Zeghioud, H., Lamouri, S., Mahmoud, Y. & Hadj-Ali, T. (2015). Preparation and Characterization of a New Polyaniline Salt with Good Conductivity and Great Solubility in Dimethyl Sulphoxide. *Journal of the Serbian Chemical Society,* 80 (11), 1435–1448.

Zulkhairi, Z., Nurul F. A. H., Mubaraq H. V. S., Shafiqul Islam, A. K. M., Uda H. & Mohd N. A. (2015). Effect of Hydrochloric Acid Concentration on Morphology of Polyaniline Nanofibers Synthesized by Rapid Mixing Polymerization. *Journal of Nanomaterials,* 2015 (218204), 1-6.

University of Malaya

LIST OF PUBLICATIONS AND PAPERS PRESENTED

A. M. Aris, N. Irawati, H. A. Rahman, S. W. Harun and **I. Z. Mohamad Ahad**. (2015). Fiber Bragg grating sensor for humidity measurement. *2015 5th IEEE International Conference on System Engineering and Technology (ICSET), Shah Alam,* 55-59. doi: 10.1109/ICSEngT.2015.7412445

I. Z. Mohamad Ahad, S. Wadi Harun, S. N. Gan & S. W. Phang. (2017). Application of Fiber Bragg Grating Sensor Coated with Polyaniline as an Optical Sensor for Chloroform Detection. *Polymers & Polymer Composites,* 25(7), 555-562.

Y. S. Chiam**, I. Z. Mohamad Ahad, S.** Wadi Harun, S. N. Gan & S. W. Phang. (2016). Effects of the Dopant Ratio on Polyaniline Coated Fiber Bragg Grating for pH detection. *Synthetic Metals,* 211, 132-141.

Preparation of Polyaniline (PAni) as optical sensor for chloroform detection.

Irma Zulayka Mohamad Ahad, Sulaiman Wadi Harun, Seng Neon Gan, Sook Wai Phang. 4th FAPS-IPC 2015**,** October 5 – 8, 2015**,** PWTC, Kuala Lumpur, Malaysia.

Effect of Synthesis Parameters for Polyaniline (PAni) Optical Sensor in Chloroform Detection. **Irma Zulayka Mohamad Ahad,** Sulaiman Wadi Harun, Seng Neon Gan, Sook Wai Phang, ISCC 2016, May 16-18, 2016, PWTC, Kuala Lumpur, Malaysia.

University of Malaya

APPENDIX A –ORGANIC COMPOUNDS DETECTION

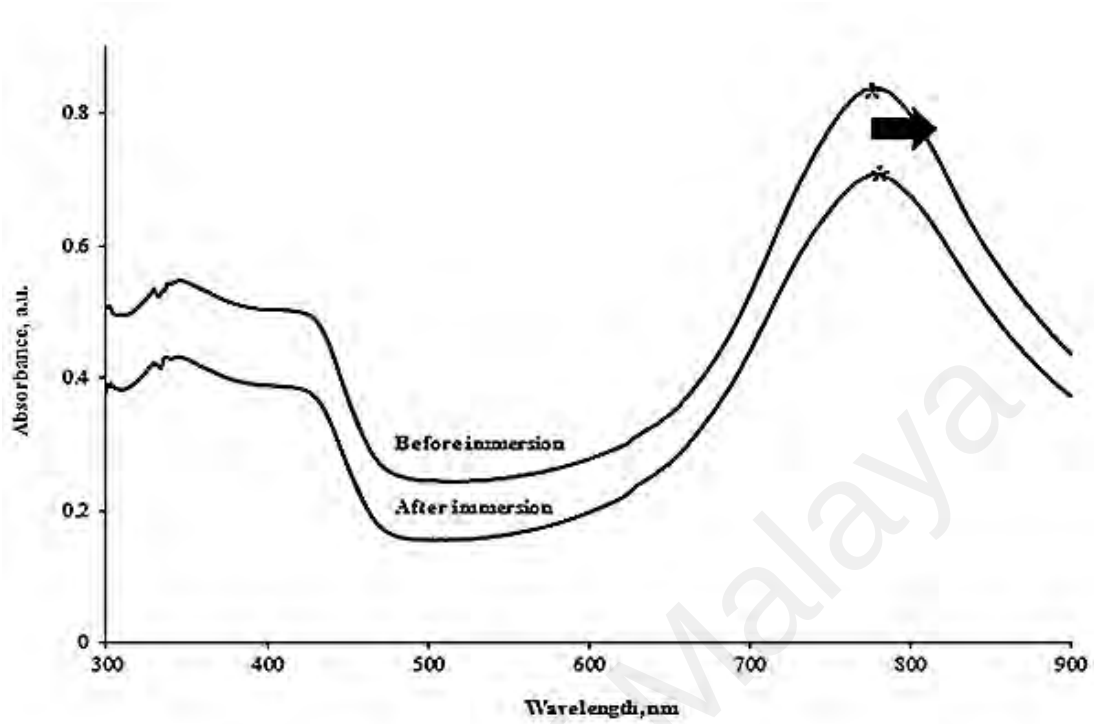

Appendix A1: UV-vis spectra that indicate the polaron shift of PAni 5: 5 before and after immersion in 2-propanol solution.

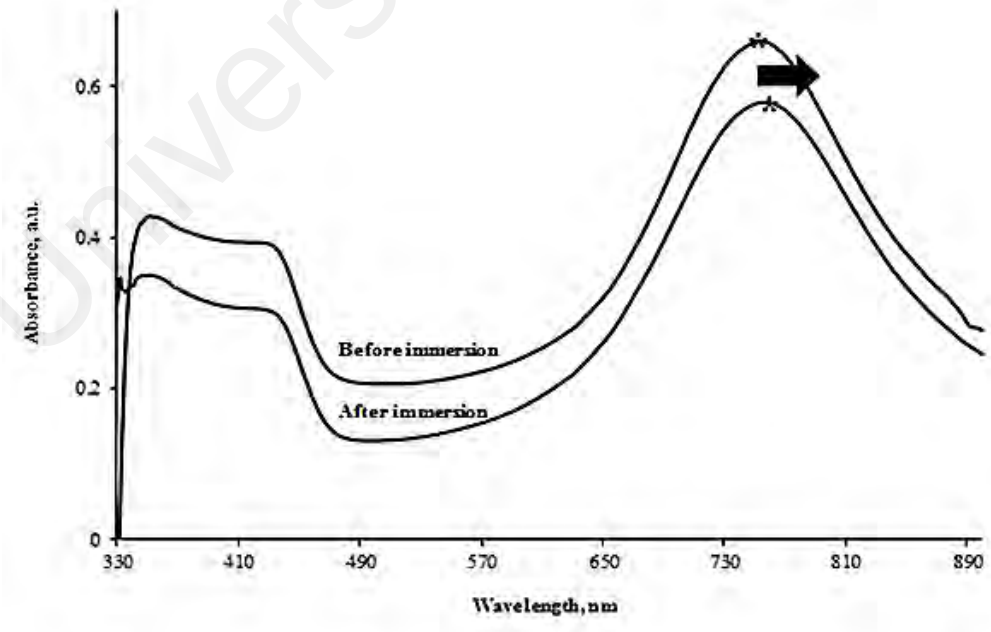

Appendix A2: UV-vis spectra that indicate the polaron shift of PAni 5: 5 before and after immersion in chloroform solution.

University of Malaya

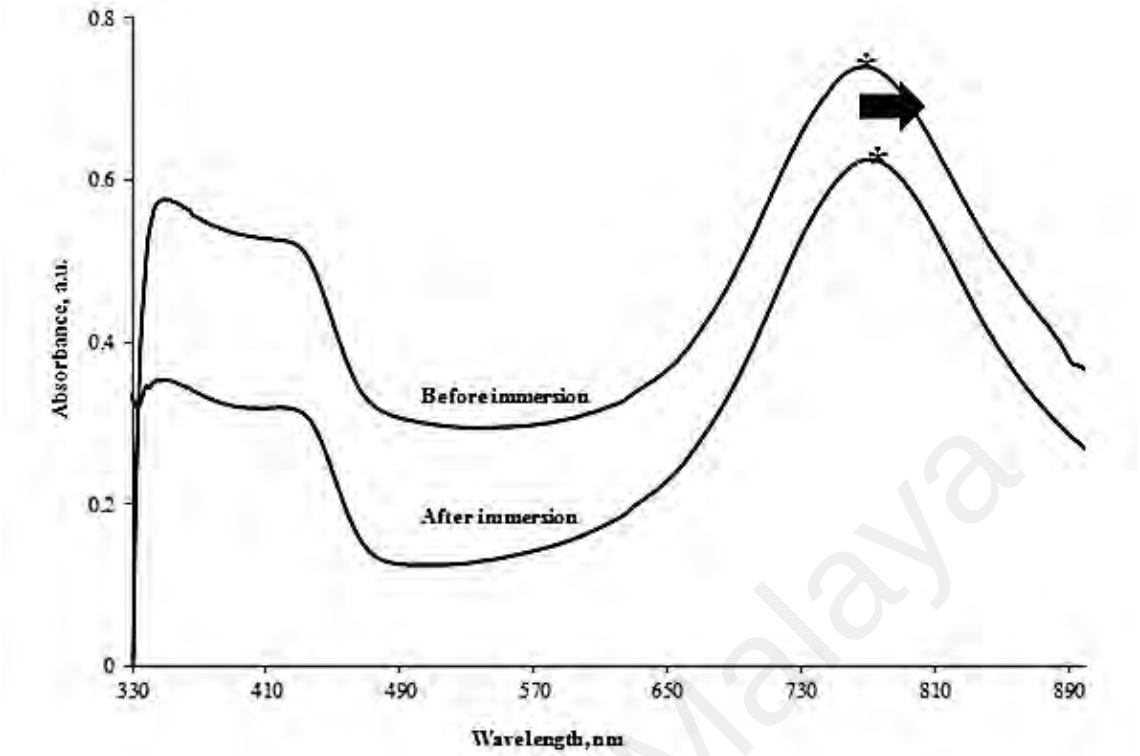

Appendix A3: UV-vis spectra that indicate the polaron shift of PAni 5: 5 before and after immersion in dichloromethane solution.

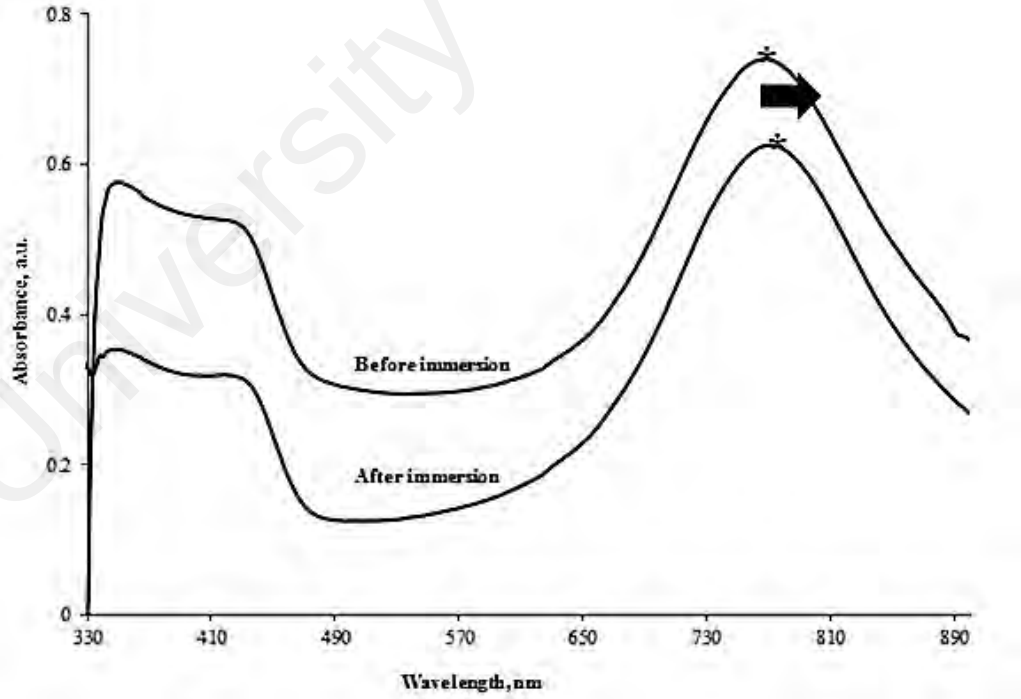

Appendix A4: UV-vis spectra that indicate the polaron shift of PAni 5: 5 before and after immersion in DMS solution.

University of Malaya

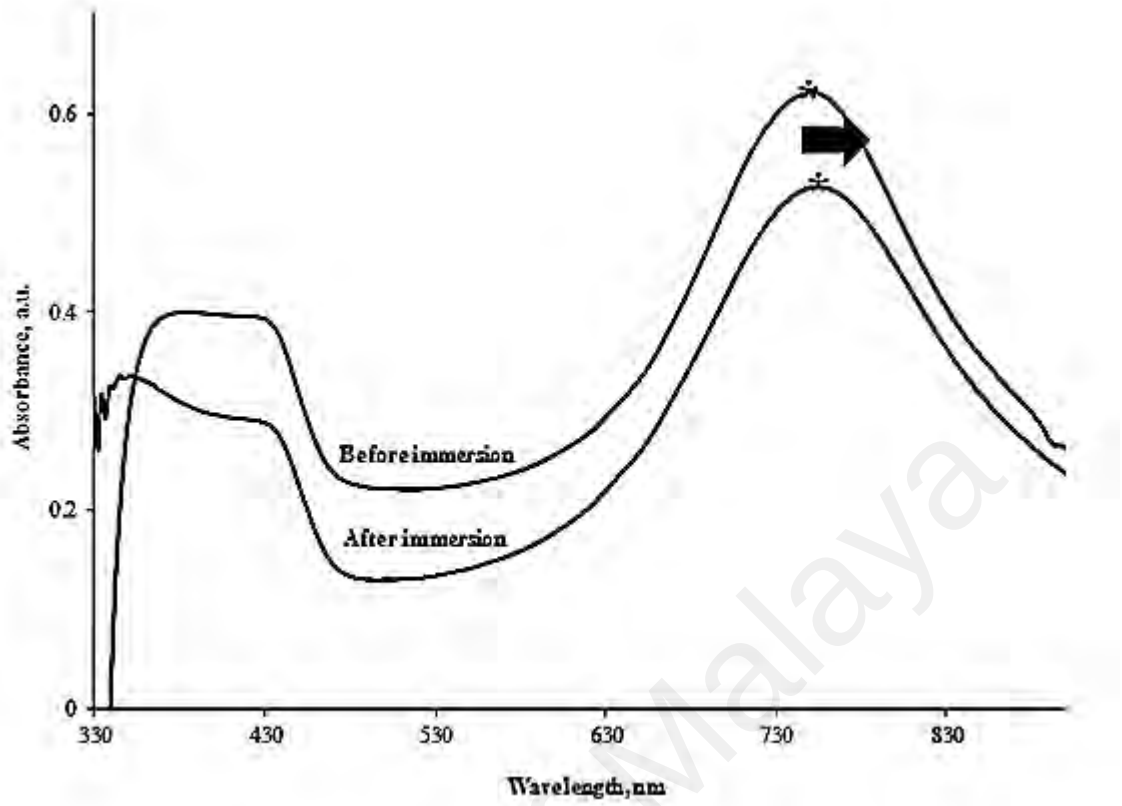

Appendix A5: UV-vis spectra that indicate the polaron shift of PAni 5: 5 before and after immersion in DMS solution.

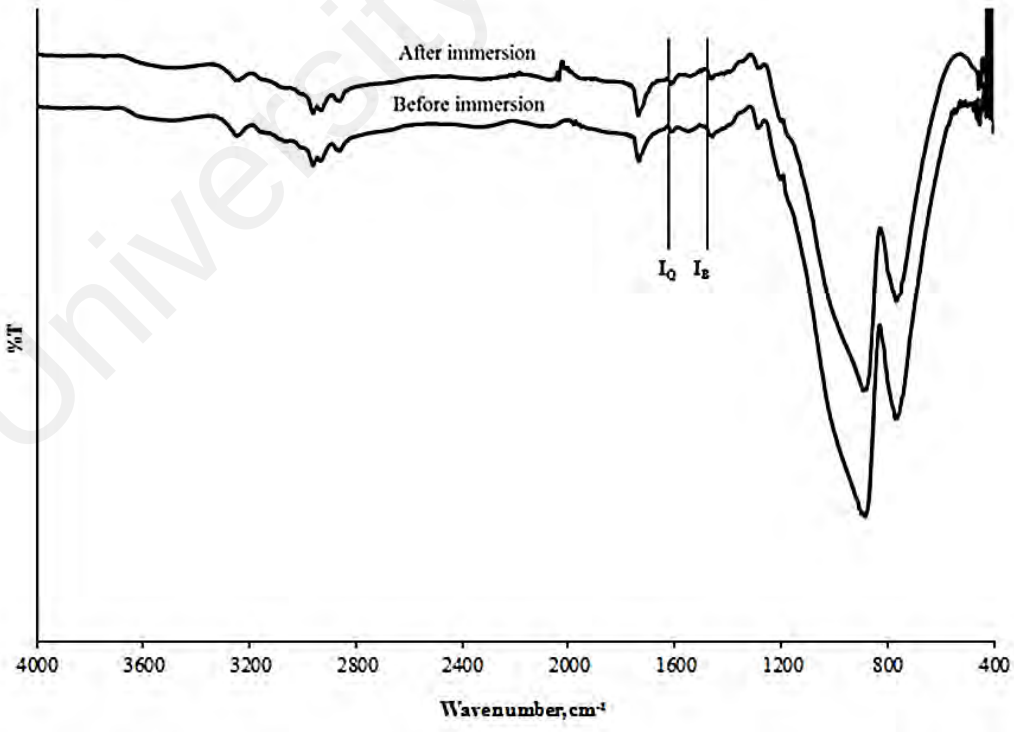

Appendix A6: FTIR spectra of PAni 5: 5 before and after immersion in 2-propanol solution.

University of Malaya

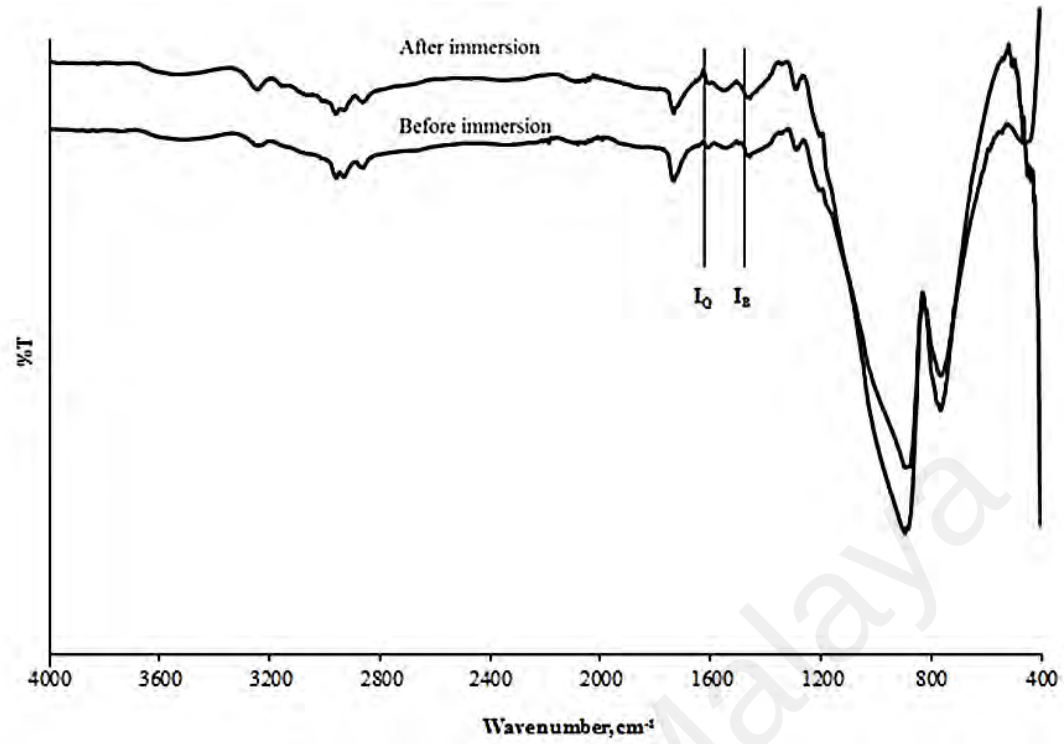

Appendix A7: FTIR spectra of PAni 5: 5 before and after immersion in chloroform solution.

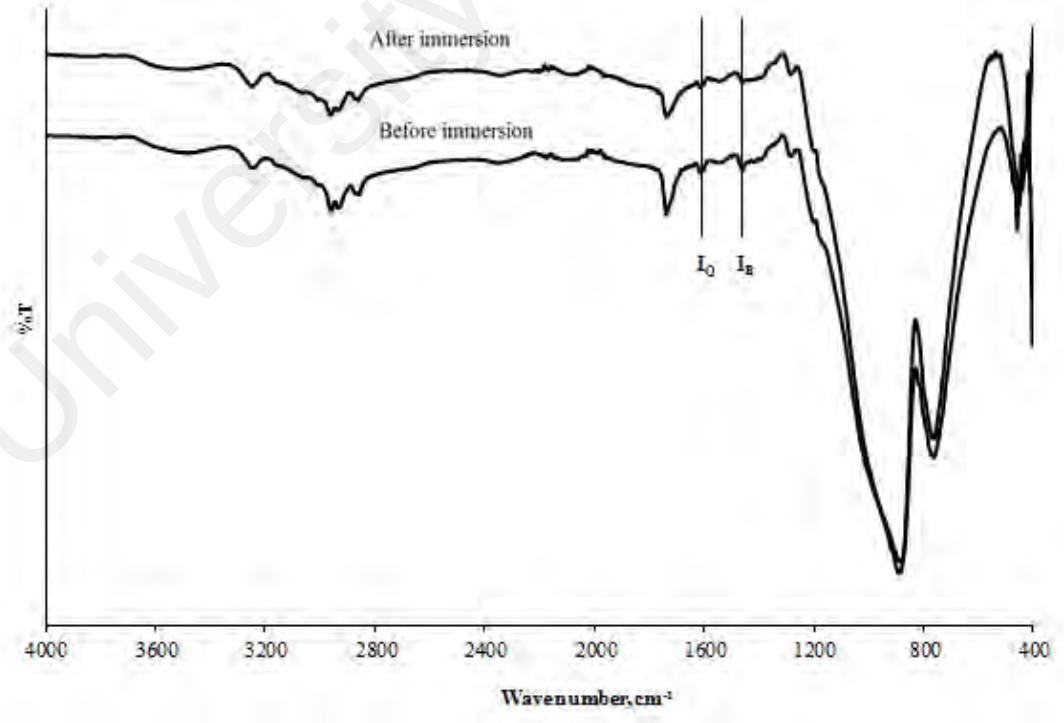

Appendix A8: FTIR spectra of PAni 5: 5 before and after immersion in dichloromethane solution.

University of Malaya

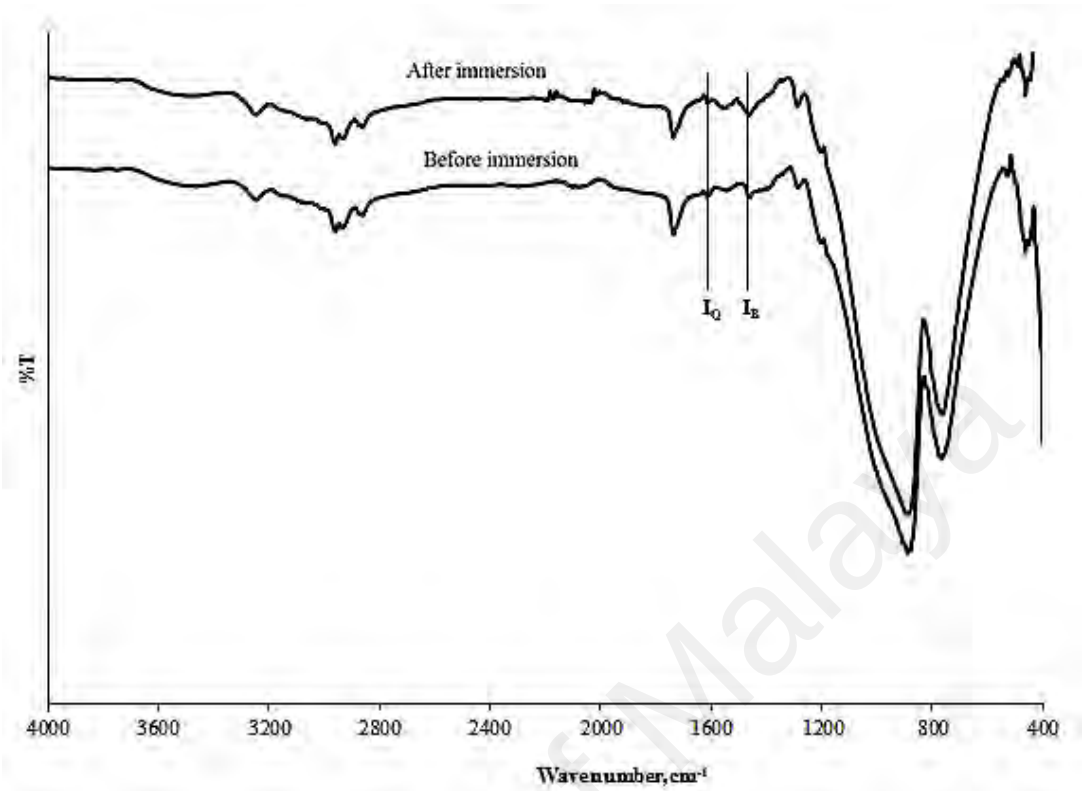

Appendix A9: FTIR spectra of PAni 5: 5 before and after immersion in DMDS solution.

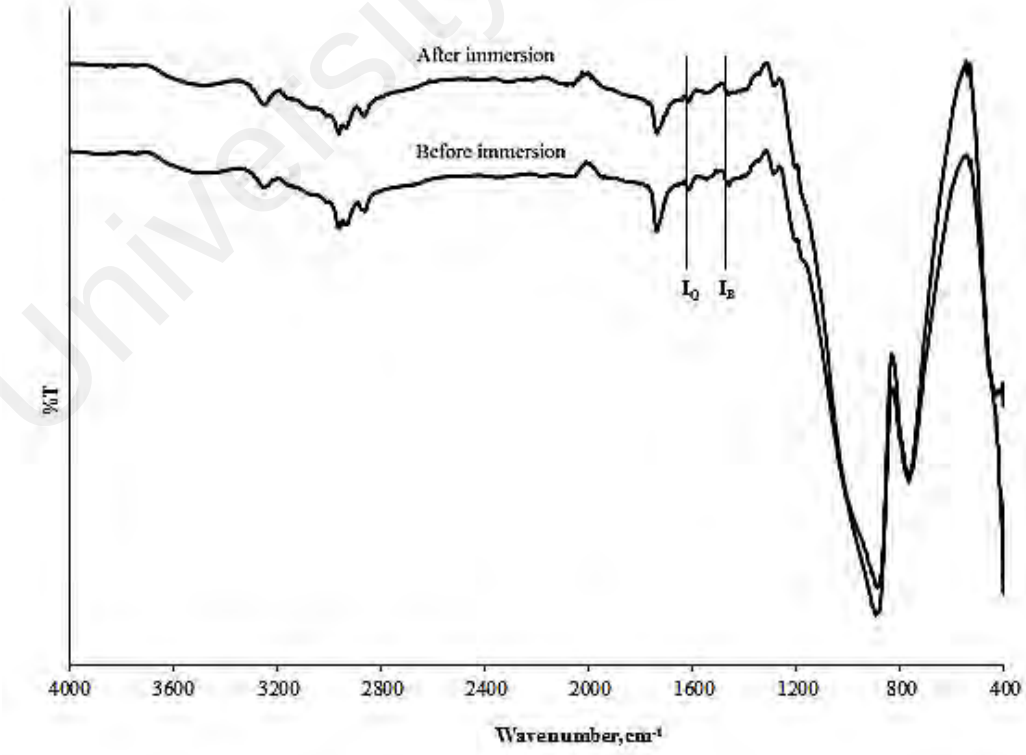

Appendix A10: FTIR spectra of PAni 5: 5 before and after immersion in DMS solution.

University of Malaya

APPENDIX B – CHLOROFORM DETECTION (DIFFERENT DOPANT RATIO)

Appendix B1: Summary of regression statistics of FBG without coated PAni.

Regression Statistics	
Multiple R	0.984205057
R Square	0.968659595
Adjusted R Square	0.958212793
Standard Error	0.001706625
Observations	5

	Coefficients	*Standard Error*	*t Stat*	*P-value*	*Lower 95%*	*Upper 95%*
Interaction	0.034967	0.001482	23.59440	0.00016682	0.0303	0.0397
X Variable	0.000235	2.4430E-05	9.629282	0.00237727	0.0002	0.0003

Appendix B2: Summary of regression statistics of PAni 5: 3 coated FBG sensor.

Regression Statistics	
Multiple R	0.998353573
R Square	0.996709856
Adjusted R Square	0.995613141
Standard Error	0.002166246
Observations	5

	Coefficients	*Standard Error*	*t Stat*	*P-value*	*Lower 95%*	*Upper 95%*
Interaction.	0.2231885	0.0018811	118.6452	1.3201E-06	0.2172	0.2292
X Variable	0.0009348	3.1010E-05	30.1465	8.0175E-05	0.0008	0.0010

University of Malaya

Appendix B3: Summary of regression statistics of PAni 5: 5 coated FBG sensor.

Regression Statistics	
Multiple R	0.999403369
R Square	0.998807094
Adjusted R Square	0.998409459
Standard Error	0.002158789
Observations	5

	Coefficients	*Standard Error*	*t Stat*	*P-value*	*Lower 95%*	*Upper 95%*
Interaction	0.145442	0.00187467	77.582739	4.7197E-06	0.1395	0.1514
X variable	0.001549	3.0903E-05	50.118530	1.7493E-05	0.0015	0.0016

Appendix B4: Summary of regression statistics of PAni 5: 7 coated FBG sensor.

Regression Statistics	
Multiple R	0.974178983
R Square	0.949024692
Adjusted R Square	0.932032922
Standard Error	0.007331573
Observations	5

	Coefficients	*Standard Error*	*t Stat*	*P-value*	*Lower 95%*	*Upper 95%*
Interaction	0.340554	0.006367	53.490287	1.43913E-05	0.3203	0.3608
X Variable	0.000784	0.000105	7.473421	0.0050	0.0005	0.0011

University of Malaya

Appendix B5: t-Test for two-sample assuming unequal variances of FBG without coated PAni and PAni 5: 3 coated FBG sensor.

	FBG without coated PAni	*FBG caoted PAni 5: 3*
Mean	0.0472	0.2718
Variance	6.97E-05	0.0010697
Observations	5	5
Hypothesized Mean Difference	0	
df	5	
t Stat	-14.87841426	
P(T<=t) one-tail	1.24079E-05	
t Critical one-tail	2.015048373	
P(T<=t) two-tail	2.48157E-05	
t Critical two-tail	2.570581836	

Appendix B6: t-Test for two-sample assuming unequal variances of FBG without coated PAni and PAni 5: 5 coated FBG sensor.

	FBG without coated PAni	*FBG coated PAni 5: 5*
Mean	0.0472	0.22598
Variance	6.97E-05	0.002930052
Observations	5	5
Hypothesized Mean Difference	0	
df	4	
t Stat	-7.298964634	
P(T<=t) one-tail	0.000936686	
t Critical one-tail	2.131846786	
P(T<=t) two-tail	0.001873372	
t Critical two-tail	2.776445105	

University of Malaya

Appendix B7: t-Test for two-sample assuming unequal variances of FBG without coated PAni and PAni 5: 7 coated FBG sensor.

	FBG without coated PAni	*FBG coated PAni 5: 7*
Mean	0.0472	0.38134
Variance	6.97E-05	0.000790853
Observations	5	5
Hypothesized Mean Difference	0	
df	5	
t Stat	-25.46974864	
P(T<=t) one-tail	8.70972E-07	
t Critical one-tail	2.015048373	
P(T<=t) two-tail	1.74194E-06	
t Critical two-tail	2.570581836	

University of Malaya

APPENDIX C – SUPPORTING DATA OF PANI (DIFFERENT DOPANT RATIO) IN CHLOROFORM DETECTION

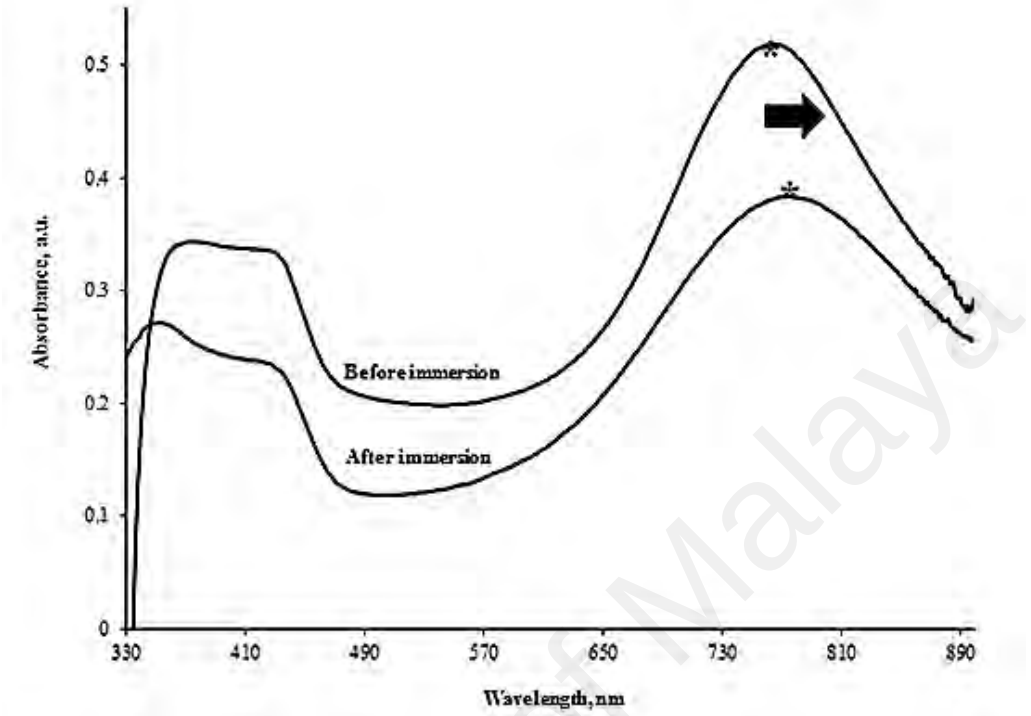

Appendix C1: UV-vis spectra that indicate polaron shift of PAni 5: 3 before and after immersion in chloroform (50 ppm) solution.

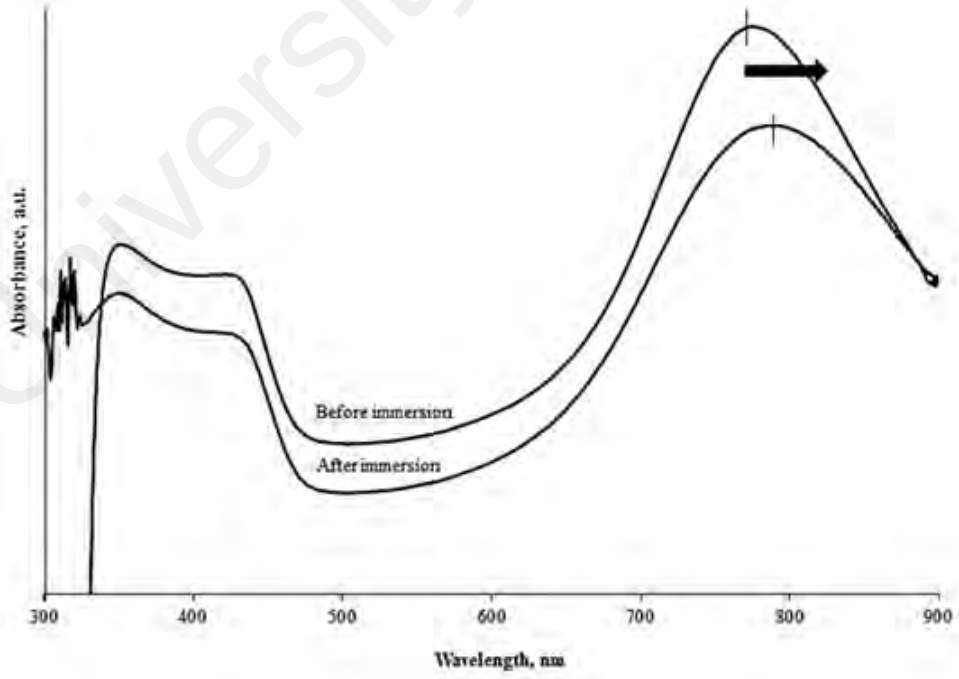

C2. UV-vis spectra that indicate polaron shift of PAni 5: 7 before and after immersion in chloroform (50 ppm) solution.

University of Malaya

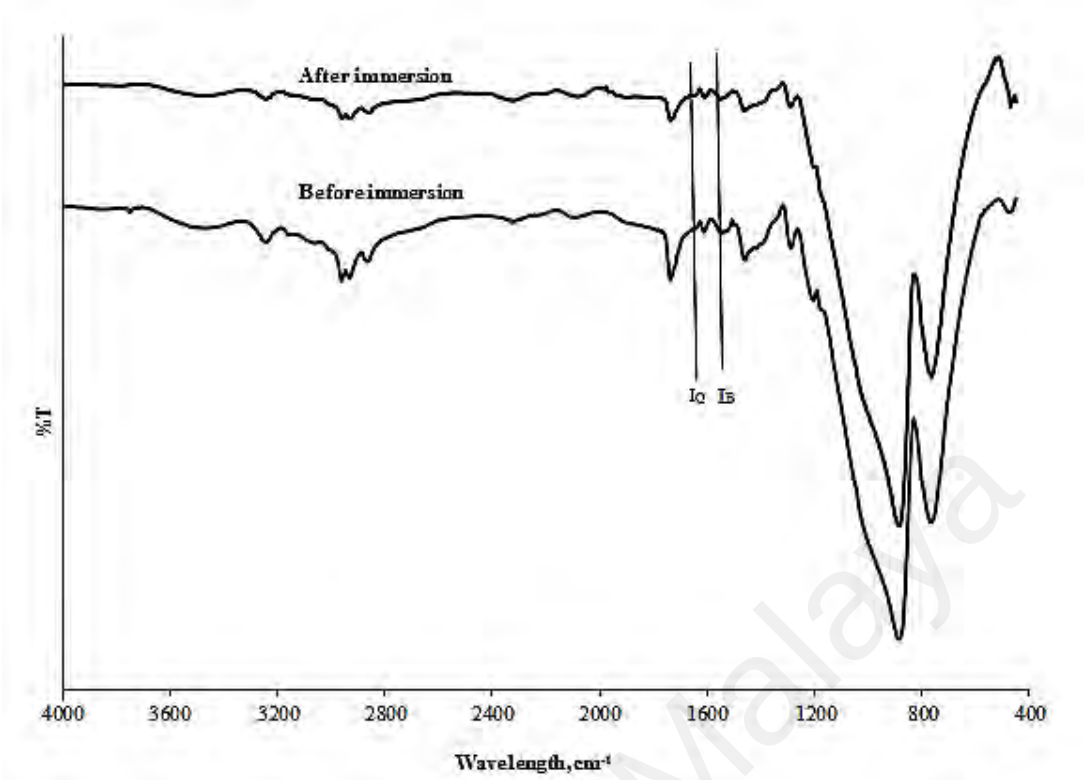

Appendix C3: FTIR spectra of PAni 5: 3 before and after immersion in 50 ppm of chloroform solution.

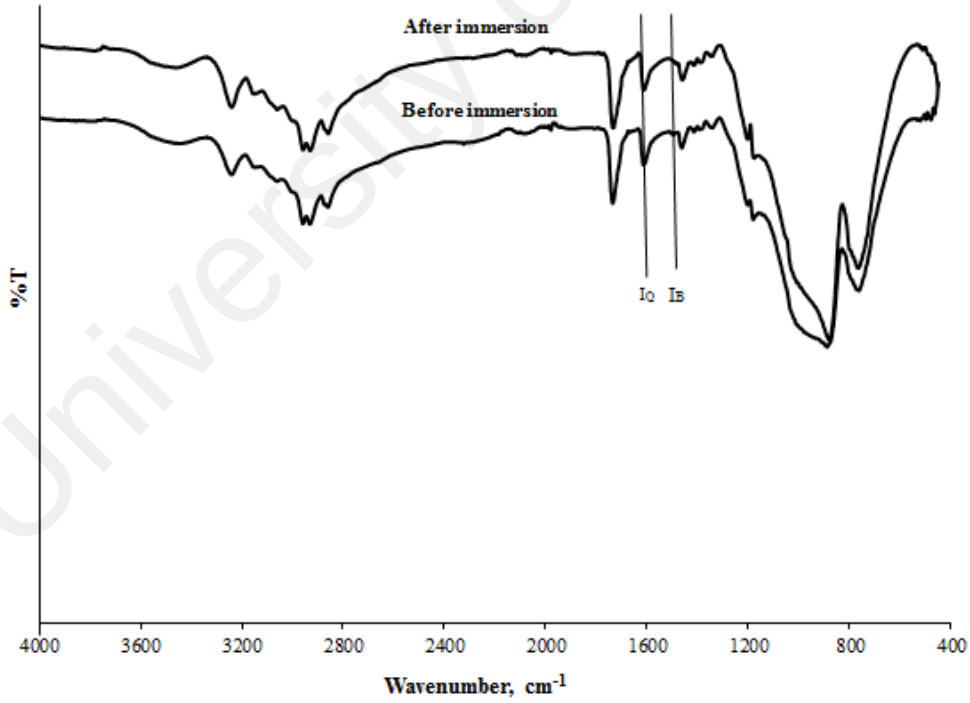

Appendix C4: FTIR spectra of PAni 5: 7 before and after immersion in 50 ppm of chloroform solution.

University of Malaya

APPENDIX D- CHLOROFORM DETECTION (DIFFERENT POLYMERIZATION TEMPERATURES)

Appendix D1: Summary of regression statistics of PAni 5: 5 (-5 °C) coated FBG sensor.

Regression Statistics	
Multiple R	0.9709994
R Square	0.94283984
Adjusted R Square	0.92378646
Standard Error	0.00657294
Observations	5

	Coefficients	*Standard Error*	*t Stat*	*P-value*	*Lower 95%*	*Upper 95%*
Interaction	0.095082	0.0057079	16.65806	0.00047	0.0769	0.1132
X Variable	0.000662	9.40914E-05	7.03449	0.00590	0.0004	0.0010

Appendix D2: Summary of regression statistics of PAni 5: 5 (0 °C) coated FBG sensor.

Regression Statistics	
Multiple R	0.999403369
R Square	0.998807094
Adjusted R Square	0.998409459
Standard Error	0.002158789
Observations	5

	Coefficients	*Standard Error*	*t Stat*	*P-value*	*Lower 95%*	*Upper 95%*
Interaction	0.145442	0.00187467	77.582739	4.7197E-06	0.1395	0.1514
X variable	0.001549	3.0903E-05	50.118530	1.7493E-05	0.0015	0.0016

University of Malaya

Appendix D3: Summary of regression statistics of PAni 5: 5 (25 °C) coated FBG sensor.

Regression Statistics	
Multiple R	0.904606022
R Square	0.818312056
Adjusted R Square	0.757749408
Standard Error	0.007399232
Observations	5

	Coefficients	*Standard Error*	*t Stat*	*P-value*	*Lower 95%*	*Upper 95%*
Interaction	0.0657541	0.0064254	10.233453	0.0020	0.0453	0.0862
X Variable	0.0003893	0.0001059	3.675844	0.0349	5.226E-05	0.0007

Appendix D4: t-Test for two-sample assuming unequal variances of PAni 5: 5 (-5 °C) coated FBG sensor and PAni 5: 5 (0 °C) coated FBG sensor.

	PAni 5: 5 (0 °C)	*PAni 5: 5 (-5 °C)*
Mean	0.22598	0.1295
Variance	0.00293	0.000567
Observations	5	5
Hypothesized Mean Difference	0	
df	5	
t Stat	3.648203	
P(T<=t) one-tail	0.007388	
t Critical one-tail	2.015048	
P(T<=t) two-tail	0.014776	
t Critical two-tail	2.570582	

University of Malaya

Appendix D5: t-Test for two-sample assuming unequal variances of PAni 5: 5 (25 °C) coated FBG sensor and PAni 5: 5 (0 °C) coated FBG sensor.

	PAni 5: 5 (0 °C)	*PAni 5: 5 (25 °C)*
Mean	0.22598	0.086
Variance	0.00293	0.000226
Observations	5	5
Hypothesized Mean Difference	0	
df	5	
t Stat	5.571587	
P(T<=t) one-tail	0.001283	
t Critical one-tail	2.015048	
P(T<=t) two-tail	0.002565	
t Critical two-tail	2.570582	

University of Malaya

APPENDIX E – SUPPORTING DATA OF PANI (DIFFERENT POLYMERIZATION TEMPERATURES) IN CHLOROFORM DETECTION

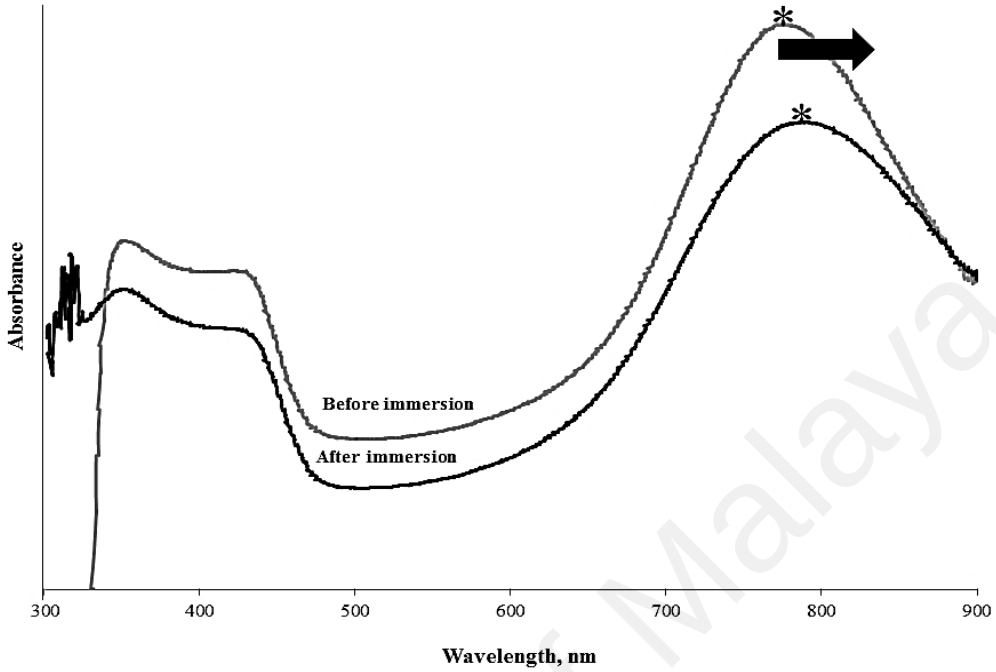

Appendix E1: UV-vis spectra that indicate polaron shift of PAni 5: 5 (0 °C) before and after immersion in chloroform (50 ppm) solution.

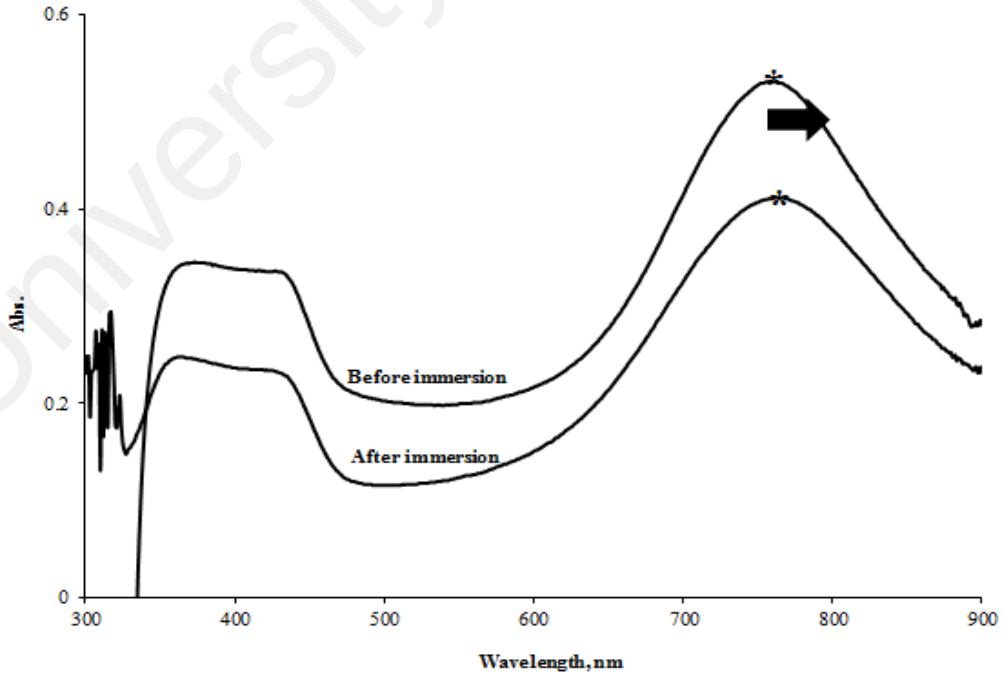

Appendix E2: UV-vis spectra that indicate polaron shift of PAni 5: 5 (-5 °C) before and after immersion in chloroform (50 ppm) solution.

University of Malaya

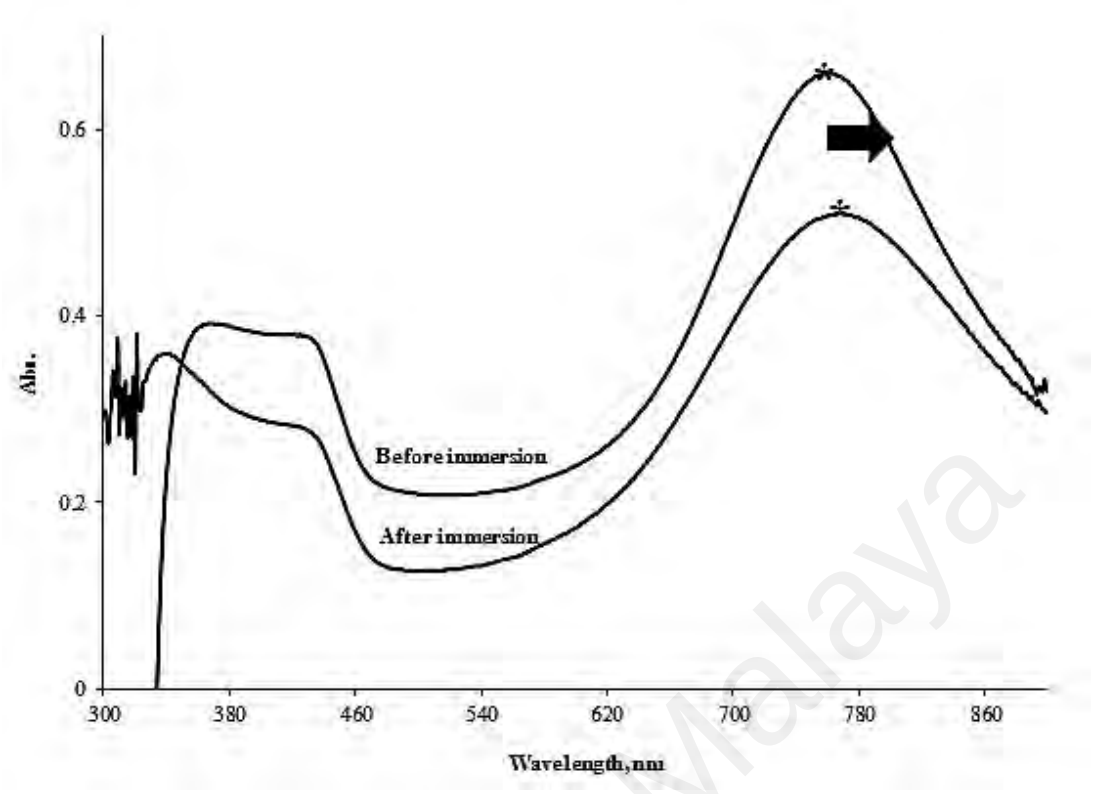

Appendix E3: UV-vis spectra that indicate polaron shift of PAni 5: 5 (25 °C) before and after immersion in chloroform (50 ppm) solution.

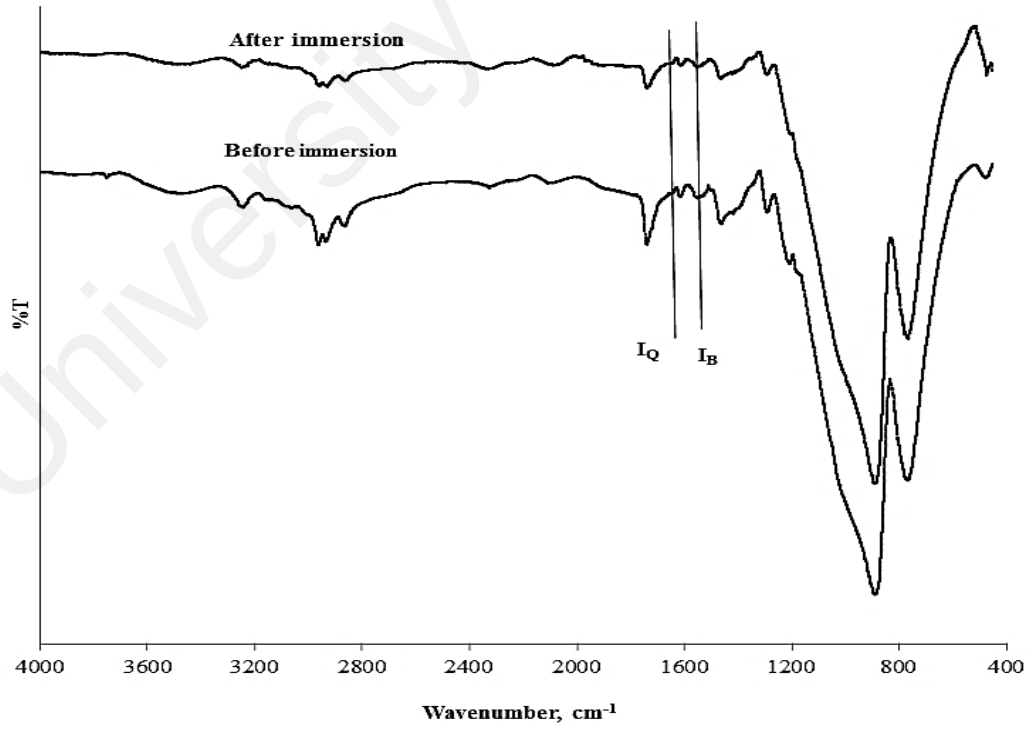

Appendix E4: FTIR spectra of PAni 5: 5 (0 °C) before and after immersion in 50 ppm of chloroform solution.

University of Malaya

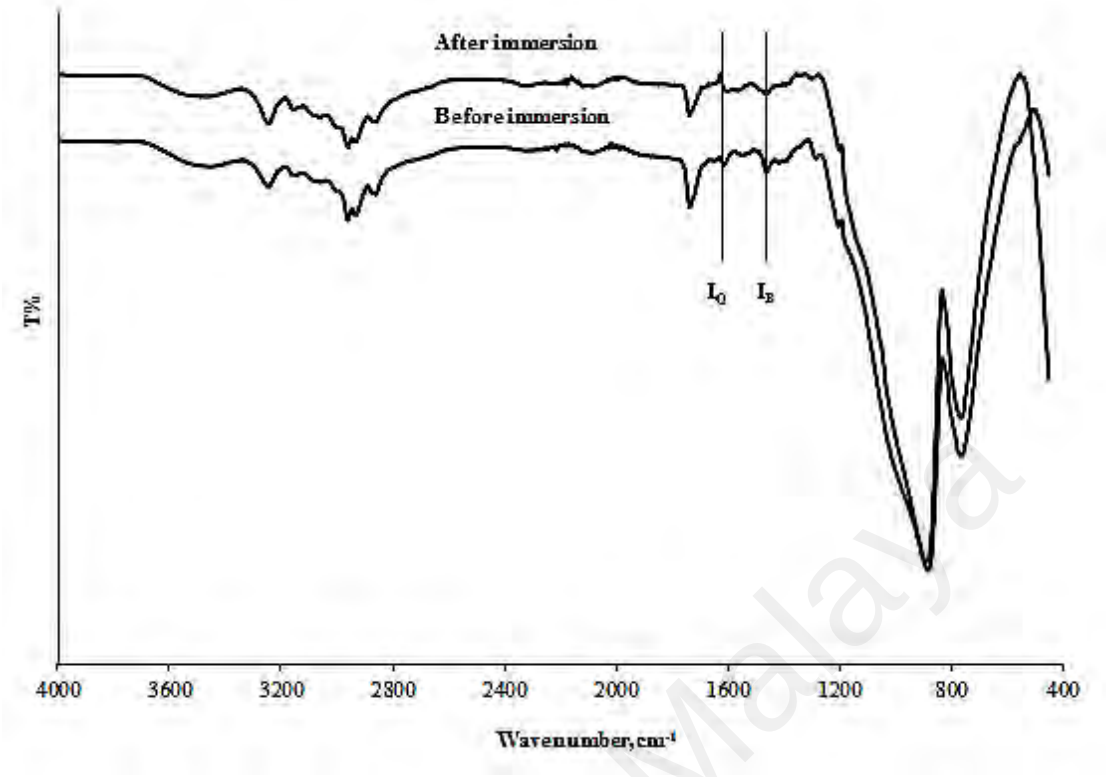

Appendix E5: FTIR spectra of PAni 5: 5 (-5 °C) before and after immersion in 50 ppm of chloroform solution.

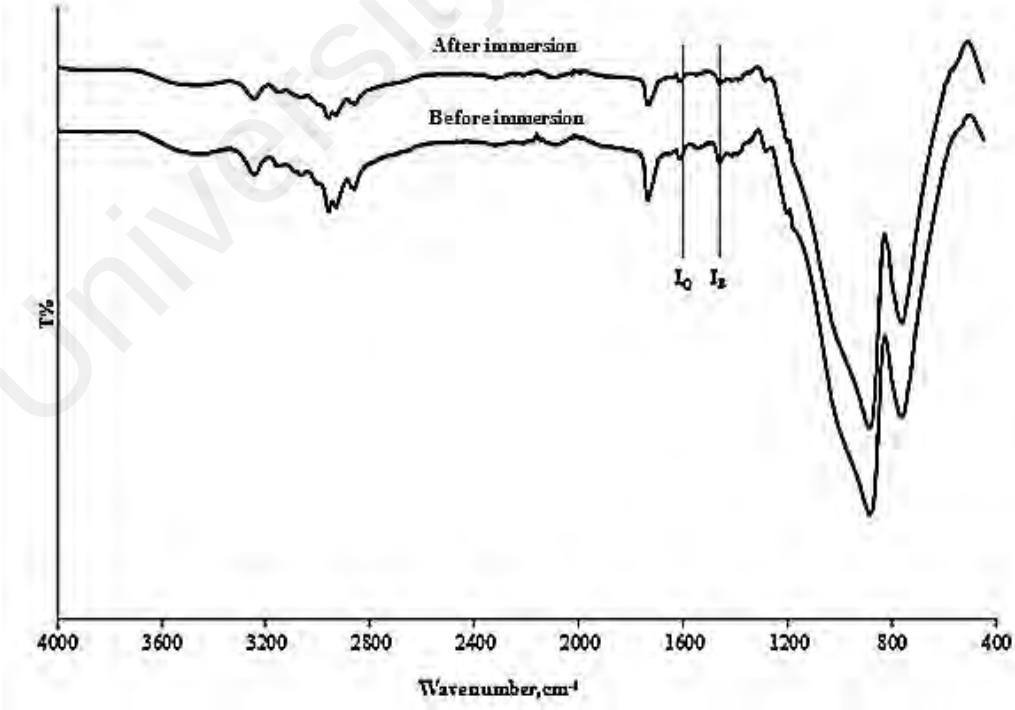

Appendix E6: FTIR spectra of PAni 5: 5 (25 °C) before and after immersion in 50 ppm of chloroform solution.

APPENDIX F – PAPER PUBLICATIONS

Application of Fiber Bragg Grating Sensor Coated with Polyaniline as an Optical Sensor for Chloroform Detection

Irma Zulayka Mohamad Ahad[1,a], Sulaiman Wadi Harun[2,b], Seng Neon Gan[1,c], and Sook Wai Phang[3,d,*]

[1] Department of Chemistry, Faculty of Science, University of Malaya, 50603 Kuala Lumpur, Malaysia
[2] Department of Electrical Engineering, Faculty of Engineering, University of Malaya, 50603 Kuala Lumpur, Malaysia
[3] Department of Physical Science, Faculty of Applied Sciences and Computing, Tunku Abdul Rahman University College, Setapak, 53300 Kuala Lumpur, Malaysia

SUMMARY

Fiber Bragg Grating (FBG) sensor coated with PAni was designed as a sensing device in chloroform detection. PAni thin film was synthesized through chemical oxidation method by using aniline (Ani) as a monomer, ammonium persulphate (APS) as an initiator and dioctyl sodium sulfosuccinate (AOT) as a dopant. The chemical structure of PAni thin film was confirmed by using Fourier transform infrared (FTIR) and ultraviolet-visible (UV-Vis) spectrometer. The conducting behaviour of PAni thin film (1.157×10^{-2} S/cm) was determined by using four-point probe measurement. In the optical sensor part, FBG was etched in hydrofluoric acid solution (48% HF) to remove the cladding layer on fiber before coated with PAni. The response of this sensor was monitored based on the different of Bragg wavelength shift at ~1557 nm in an optical spectrum analyzer (OSA) detector. PAni-coated FBG significantly increased in the Bragg wavelength shift (sensitivity = 0.0009) compared with uncoated FBG (sensitivity = 0.0002). The interaction between PAni and chloroform was significantly confirmed by the "polaron peak ratio" (P_f/ P_i) and "quinoid and benzenoid peak ratio" (I_Q/ I_B) through UV-vis and FTIR spectroscopy analysis. In this study, FBG sensor coated with PAni thin film had been found as an efficient sensor in chloroform detection with fast response time (7 s).

Keywords: Polyaniline, FBG, Chloroform, Bragg wavelength shift

1. INTRODUCTION

Nowadays, many industries released toxic compounds that can be harmful to our environment. Chloroform was released into the environment through several anthropogenic sources such as transportation industry, solvent in paint industries, cleansing agent in waste water treatment and so on. According to the Occupational Safety and Health Administration (OSHA), the permissible exposure limit for chloroform is 50 ppm[1]. Continuous exposure towards chloroform can cause several health effects such as irritation, digestive disorder, headache, lung congestion, kidney damage, liver damage, and most seriously can cause cancer and death[2]. In fact, chloroform becomes the biggest challenges for analytical detection due to its weak interaction with others chemical compounds[3]. Thus, the effective device for chloroform detection is needed to maintain the environment cleanliness as well to decrease the risk of health problems cause by this pollutant.

During the last decades, the most widely use techniques in chloroform detection involved the uses of spectrophotometer and metal oxide. These methods are not suitable for on-line monitoring because they are easily affected by the environmental factors such as surrounding temperature and air humidity[4,5]. FBG has recently become the most popular optical material used in sensor application. There are many advantages of FBG such as inexpensive, light weight, immune to electromagnetic interference (EMI) etc.[6].

Nowadays, many researchers have devoted on conducting polymer due to its interesting properties such as low cost, lightweight, good flexibility, excellent ambient stability, and reversible absorption kinetics. Among all CPs, PAni commonly applied as optical and chemical sensor due to its excellent sensing properties such as good flexibility, excellent environmental stability and ability to make physical and chemical interaction during exposure to chemical solutions[7].

[a]zulkairma@gmail.com, [b]swharun@um.edu.my, [c]sngan@um.edu.my, [d]pinkyphang@gmail.com

©Smithers Information Ltd., 2017

Appendix F1: Mohamad Ahad, I. Z., Wadi Harun, S., Gan, S. N. & Phang, S. W. (2017). Application of Fiber Bragg Grating Sensor Coated with Polyaniline as an Optical Sensor for Chloroform Detection. *Polymers & Polymer Composites,* 25(7), 555-562.

Synthetic Metals 211 (2016) 132–141

Contents lists available at ScienceDirect

Synthetic Metals

journal homepage: www.elsevier.com/locate/synmet

Effects of the Dopant Ratio on Polyaniline Coated Fiber Bragg Grating for pH detection

Yeong Siang Chiam[a], Irma Zulayka Mohamad Ahad[a], Sulaiman Wadi Harun[b], Seng Neon Gan[a], Sook Wai Phang[c,*]

[a] Department of Chemistry, Faculty of Science, University of Malaya, 50603 Kuala Lumpur, Malaysia
[b] Department of Electrical Engineering, Faculty of Engineering, University of Malaya, 50603 Kuala Lumpur, Malaysia
[c] Department of Physical Science, Faculty of Applied Sciences and Computing, Tunku Abdul Rahman University College, Jalan Genting Kelang, Setapak, 53300 Kuala Lumpur, Malaysia

ARTICLE INFO

Article history:
Received 28 May 2015
Received in revised form 20 November 2015
Accepted 24 November 2015
Available online 7 December 2015

Keywords:
Polyaniline
AOT dopant ratio
FBG
pH solution
Bragg wavelength shift

ABSTRACT

Polyaniline (PAni) coated Fiber Bragg Grating (FBG) for pH detection is presented in this study. PAni was synthesized at low temperature through chemical oxidation by using aniline (Ani) as monomer, ammonium persulphate (APS) as oxidant and dioctyl sodium sulfosuccinate (AOT) as dopant. The immersion of PAni-coated FBG in different pH solutions could produce different Bragg wavelength shift (~1557 nm) in the optical spectrum analyzer (OSA). Fourier transformed infrared (FTIR) spectroscopy, ultraviolet–visible (UV–vis) spectroscopy and conductivity measurements were carried out to investigate the chemical interaction between protonated nitrogen atom of PAni backbone and pH analytes. The sensitivity of PAni-coated FBG was adjusted by changing the ratio of Ani:APS:AOT during the polymerization reaction. PAni-coated FBG with molar ratio of Ani:APS:AOT = 5:5:5 achieved the highest sensitivity with response time of 10 s. Besides, the PAni-coated FBG also showed good recyclability up to 10 times.

© 2015 Elsevier B.V. All rights reserved.

1. Introduction

Organic conducting polymer possesses both the mechanical property of a polymer and the electrical property of a conductor and has great potential in many technological applications. Polyaniline (PAni) is a well-known conducting polymer, which is relatively easy to prepare, shows excellent ambient stability and has rapid and reversible adsorption or desorption kinetics. It has attracted much attention in various sensor applications, such as gas detection by using Langmuir–Blodgett thin films [1,2], multielectrode sensor array [3], as coatings for quartz crystal microbalance sensors [4,5,6], microcantilever sensors [7], chemiresistor using single walled carbon nanotube (SWNT) [8,9] and as modified cladding in the optical fiber sensors [10–13].

Sensor is a device capable of detecting and converting physical and chemical changes to a measureable signal. Sensor becomes a very important device in our daily life, for example it can be used to detect pollutant and toxic chemical in our surrounding, and play a role in the maintainance of the environmental cleanness to reduce the risk of health problems. During the last decade, traditional sensor that has been widely used is prepared from metal oxide. However, this traditional sensor is costly due to the complicated fabrication process. Besides, metal oxides are easily affected by the environmental factors such as surrounding temperature and air humidity [14]. Recently, sensor using hydrogel coating is introduced as smart coating material due to its properties such as good gel strength, long service lifetime, and has excellent water absorption. Although, hydrogel is effective but it still involves complicated preparation method [15].

Fiber optic is a new sensor system that can overcome the disadvantages of the traditional sensor. Its numerous advantages include immunity to the electromagnetic interference, small and compact in size, high sensitivity, possible remote sensing, ability to be multiplexed, and most importantly is the ability to be embedded into textile structure [16]. PAni can be potentially applied as an efficient optical sensor with low cost of production, easy to synthesis and independent environmental.

This research work combines the advantages of Fiber Bragg Grating (FBG) and PAni in the construction of a new optical sensor for the detection of pH changes. The sensor works on the principle of wavelength shift modulation induced by the FBG. The passive glass cladding of the FBG is replaced by the PAni (sensitive

* Corresponding author. Fax: +60 3 41423166.
E-mail address: pinkyphang@gmail.com (S.W. Phang).

http://dx.doi.org/10.1016/j.synthmet.2015.11.026
0379-6779/© 2015 Elsevier B.V. All rights reserved.

Appendix F2: Chiam, Y. S., Mohamad Ahad, I. Z., Wadi Harun, S., Gan, S. N. & Phang, S. W. (2016). Effects of the Dopant Ratio on Polyaniline Coated Fiber Bragg Grating for pH detection. *Synthetic Metals,* 211, 132-141.

2015 IEEE 5th International Conference on System Engineering and Technology, Aug. 10 - 11, UiTM, Shah Alam, Malaysia

Fiber Bragg Grating Sensor for Humidity Measurement

A. M. Aris[1,2], N. Irawati [2,3], H. A. Rahman[1], S. W. Harun[2,4], I. Z. M. Ahad[5]

[1] Faculty of Electrical Engineering, Universiti Teknologi MARA (UiTM), 40450 Shah Alam, Malaysia
[2] Photonics Research Centre, University of Malaya, 50603 Kuala Lumpur, Malaysia
[3] Institute of Postgraduate Studies, University of Malaya, 50603 Kuala Lumpur, Malaysia
[4] Department of Electrical Engineering, University of Malaya, 50603 Kuala Lumpur, Malaysia
[5] Department of Chemistry, University of Malaya, 50603 Kuala Lumpur, Malaysia

Abstract **– A new approach to measure relative humidity changes by using fiber Bragg grating (FBG) is presented. Etching method is used to fabricate an FBG taper. The sensitivity of the FBG sensor for relative humidity change is 0.0014 dB/% and the linearity value which is the measure of the goodness of fit is 98%. The wavelength shift with respect to relative humidity is measured to be 0.00268 nm/%.**

Keywords **— fiber Bragg grating (FBG), FBG sensor, relative humidity**

I. INTRODUCTION

Humidity acts as an indication of the moisture levels in the environment and affects industrial and biological elements of life. Detecting, monitoring and controlling of humidity level is crucial in many industrial and domestic applications in order to attain desirable surrounding atmosphere for industrial processes and ensuring human comfort [1]. In semiconductor industries, humidity control is required during wafer processing while in medical applications, it is vital for respiratory equipment, sterilizers, incubators and pharmaceutical processing [2].

Growing studies on humidity sensing over the years presented numerous methods of measuring relative humidity (RH). The easiest method is accomplished through the use of a simple instrument called psychrometer [3]. Another method is by using hygrometric sensors which detect changes in physical and electrical properties of sensitive elements exposed to different humidity conditions [4]. The principle behind this type of RH sensing is the physical and chemical adsorption of water molecules which contribute to the changes [5].

Additionally, fiber optic sensor is another possible method for the implementation of humidity sensing. Extensive research has been done on fiber optic sensing as it offers advantages such as electrically passive operation, immunity to electromagnetic interference (EMI), lightweight, small size, high sensitivity and multiplexing capabilities [6]. Diverse methods in applying fiber optic for humidity sensing as either extrinsic or intrinsic sensor types [7] include direct spectroscopic, evanescent wave and in-fiber grating [8].

In direct spectroscopic, tip of the sensing fiber is affixed with a moisture sensitive reagent such as cobalt chloride ($CoCl_2$) [9] and cobalt oxide (Co_3O_4) [10]. Monitoring is done on the optical absorption properties of the reagent due to the interaction between the reagent and moisture. Employing evanescent wave (EW) method for optical fiber sensing entitled it to be used as an intrinsic sensor. Data on optical absorption, refractive index (RI) change or scattering can be obtained from the interaction between the field generated at the interface and the target analyte surrounding the fiber [11]. The principle behind RI change is that the fiber core is coated with a polymer of different refractive index, forming a humidity-sensitive cladding layer that reduces the intensity of propagating light through the fiber when the layer hydrates [12].

Recent years had seen in-fiber grating becoming a favorable option for intrinsic fiber optic sensors. It can be categorized into two main classes according to its grating period, namely the fiber Bragg grating (FBG) and long period grating (LPG). Increasing interest in the development of FBG as a viable sensing approach is driven by the fact that FBG is corrosion resistant and durable [13]. Gratings on FBG is inscribed through exposure of the core using ultraviolet light and a phase mask [14]. FBG sensor emerged as a useful sensing element for various applications and is commonly used for measuring parameters such as strain, temperature [15], or electromagnetic field [16].

In contrast, applying FBG for RH sensing is yet much developed. Humidity sensor demonstrated by Tao et al. [17] cascaded an FBG with a multimode fiber (MMF) taper coated with polyvinyl alcohol (PVA). The sensitivity of the humidity sensor is enhanced as the optical power is modulated twice by the multimode fiber taper (MFT). However, the addition of MFT and PVA coating further complicates the fabrication process. Other works also experimented with a different

978-1-4673-6713-4/15/$31.00 ©2015 IEEE

University of Malaya

Appendix F3: Aris, A. M., Irawati, N., Rahman, H. A., Wadi Harun, S. & Mohamad Ahad, I. Z. (2015). Fiber Bragg grating sensor for humidity measurement. *2015 5th IEEE International Conference on System Engineering and Technology (ICSET), Shah Alam,* 55-59. doi: 10.1109/ICSEngT.2015.7412445